NTNU

Norwegian University of
Science and Technology

State of art spatial data measurements methods for civil engineering structures

Lukasz Andrzej Pieczonka

Civil and Environmental Engineering
Submission date: June 2017
Supervisor: Terje Skogseth, IBM

Norwegian University of Science and Technology
Department of Civil and Environmental Engineering

NORGES TEKNISK-
NATURVITENSKAPELIGE UNIVERSITET
INSTITUTT FOR BYGG OG MILJØTEKNIKK

Report Title: State of art spatial data measurements methods for civil engineering structures	**Date:** 11.06.2017 **Number of pages (including appendices):** 103	
	Master Thesis	x
Name: Lukasz Andrzej Pieczonka		
Professor in charge/supervisor: Terje Skogseth (NTNU)		
Other external professional contacts/supervisors: Tomasz Owerko (AGH UST)		

Abstract:

There are many spatial data collection methods, but their characteristics favour ones over another when it comes to engineering structures inspections.

Recently, with rapid growth of Unmanned Aerial System technology, their application starts to be appreciated in many scientific fields. In the thesis classical methods of obtaining spatial data: total station positioning and terrestrial laser scanning are presented, and compared with UAS-based photogrammetry. The thesis presents whole process of obtaining data, quality assessment and results comparison. Moreover, Pix4Dmapper Pro, Agisoft Photoscan and Bentley ContextCapture photogrammetry software are tested and analysed with regards of use for spatial engineering structures.

For the analysis Tyholt tower was chosen. It is a concrete cylinder-shaped tower with a number of balconies. It is simple, yet distinct engineering structure, providing good testing field for the study.

Obtained results corresponds with initial assumptions when it comes to accuracy, efficiency and workload. The most noticeable contrast while processing was performance of analysed software.

Keywords:

1. Spatial data
2. UAS-based Photogrammetry
3. Laser scanning
4. Engineering structures surveying

_____

NTNU
Norwegian University of Science and Technology
Faculty of Engineering
Department of Civil and Environmental Engineering

Date
15.01.2017

MASTER DEGREE THESIS

Course TBA4925 Geomatics, master thesis
Spring 2017
Student:
Lukasz Andrzej Pieczonka

State of art spatial data measurements methods for civil engineering structures

BACKGROUND

The ca. 120 m high Tyholt tower in Trondheim, Norway, is well suitable for testing methods and software that can be used to determine the geometry of large objects and structures in civil engineering. The quality of the final products can be checked with use of various methods and software, to be better able to choose an optimal way to obtain a 3D model of a structure in future.

TASK

The main objective of this thesis is to look into and compare the accuracy of spatial data collected with use of various measuring methods (for instance using low-cost unmanned aerial systems (UAS), laser scanner, and total station) and processing the data by various processing software. See the task description below.

Theoretical part

The candidate shall describe and discuss the equipment, software and methods used in the thesis concerning: Aerial photogrammetry with low-cost UAS based imagery, laser scanning, total station measurements, and software packages.

Data capture and processing of the captured data

The fieldwork will be done at Tyholt, where the student shall establish the study field.

The following instruments and software packages can be used: UAV (DJI Phantom 3 Professional), laser scanner (Topcon GLS1000), total station (Leica TCRP 1201), GNSS (Leica Viva GS15), the software packages Pix4Dmapper Pro, Agisoft PhotoScan Professional, Bentley ContextCapture, and CloudCompare.

Results of the processing of the captured data should be: The accuracy of photogrammetric products from unmanned aerial vehicles (UAV) and a model acquired from laser scanning, by comparing different parameters and software. Comparison of a model acquired from a laser scanner with a model from an UAV flight. Comparisons of photogrammetric products from UAV, and a model acquired from laser scanning, with the shape of the object obtained from distinct points on the structure measured by using a total station.

Results and conclusions

Interpretation, discussion and conclusions of the results achieved, and suggestions of improvements.

STARTUP AND SUBMISSION DEADLINES

Startup: January 15th 2017. Submission date: Digitally in DAIM at the latest June 11th 2017.

SUPERVISORS

Supervisor at NTNU: Terje Skogseth.
Co-supervisor: Tomasz Owerko, AGH University of Science and Technology, Krakow, Poland

Department of Civil and Environmental Engineering, NTNU. Date 15.01.2017 (revised May 2017).

Terje Skogseth (signature)

Acknowledgments

I would like to thank my supervisor Terje Skogseth at Norwegian University of Science and Technology, NTNU, Trondheim for support and engagement throughout my thesis. He consistently allowed this paper to be my own work, but gave me precious guidance whenever he thought I needed it.

I would also like to thank my friend Rafał Szymanowski for inspiration for the thesis and guidance for measuring process.

Finally, I would like to express my very profound gratitude to my family and friends for providing me with unfailing support and continuous encouragement throughout my years of study and through the process of researching and writing this thesis. This accomplishment would not have been possible without them.

Thank you.

Abstract

There are many spatial data collection methods, but their characteristics favour ones over another when it comes to engineering structures inspections.

Recently, with rapid growth of Unmanned Aerial System technology, their application starts to be appreciated in many scientific fields. In the thesis classical methods of obtaining spatial data: total station positioning and terrestrial laser scanning are presented, and compared with UAS-based photogrammetry. The thesis presents whole process of obtaining data, quality assessment and results comparison. Moreover, Pix4Dmapper Pro, Agisoft Photoscan and Bentley ContextCapture photogrammetry software are tested and analysed with regards of use for spatial engineering structures.

For the analysis, Tyholt tower was chosen. It is a concrete cylinder-shaped tower with a number of balconies. It is simple, yet distinct engineering structure, providing good testing field for the study.

Obtained results corresponds with initial assumptions when it comes to accuracy, efficiency and workload. The most noticeable contrast while processing was performance of analysed software.

Table of Contents

List of appendices

List of figures

List of tables

1. Introduction

Spatial data is information about physical object represented by coordinates and relations between them in set coordinate system. It provides extensive knowledge about represented object and allows it to be visualized, analysed and manipulated. It significantly improves analysing abilities possibilities and gives better perspective view over the object. Three-dimensional (3D) models fully represent shape of worlds, physical objects and thus deliver comprehensive data for miscellaneous space analyses.

Object can be represented as point-clouds or mathematical-based surfaces such as cylinders, cones, quadrics, mesh etc. Models are used for documentation, structures monitoring, deformation monitoring, structures life service, simulations, designing.

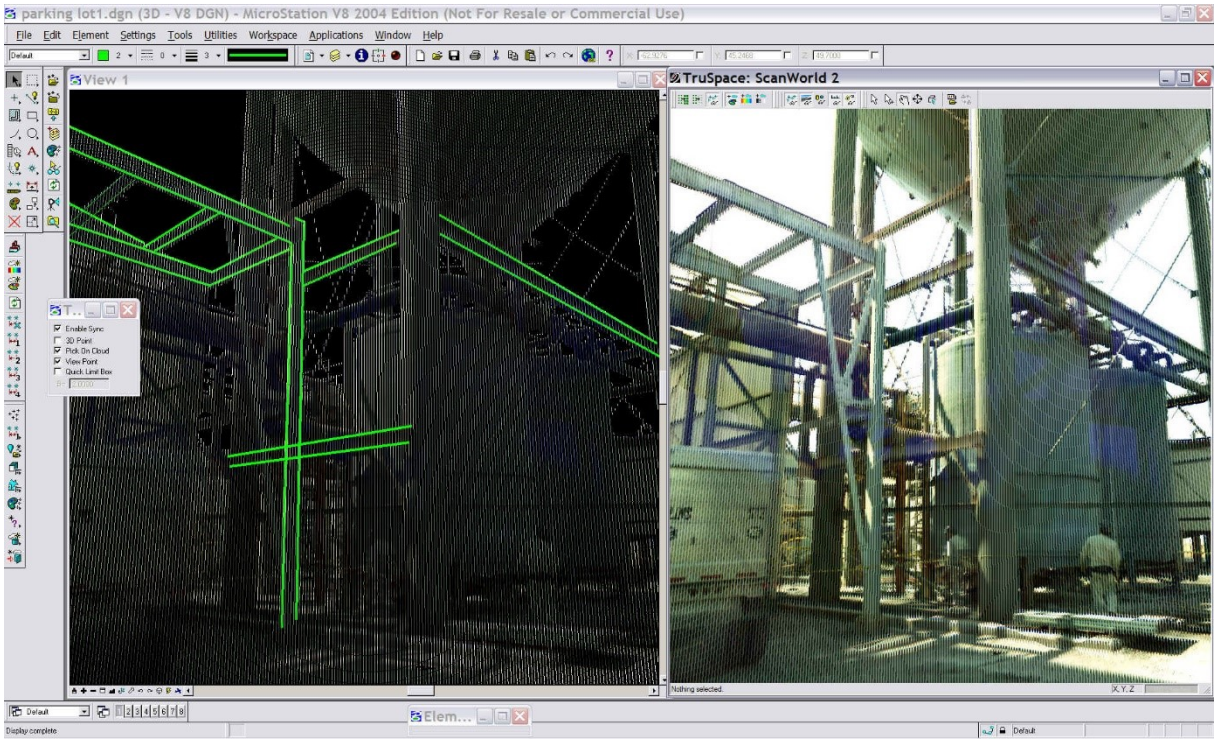

Figure 1.1 Extraction of analysed objects from point cloud [http://hds.leica-geosystems.com]

Through the years, technology of spatial acquisition has been significantly developed meeting higher and higher industry demands regarding accuracy, efficiency, flexibility and profitability. Higher demands on that kind of data have entailed to measuring technologies development and improvement. There are many ways of obtaining spatial data but theirs specification makes

ones superior over another considering vertical height engineering constructions. Nowadays Unmanned Aerial Systems (UAS) find favour with use in geodesy thanks to its versatility.

UAS give capability of carrying various measuring sensors e.g. photo-video cameras, scanners, thermo-vision cameras etc. and thanks to its manoeuvrability, it is possible to place sensor in desired location and perform essential data collection from different perspectives unapproachable for other measuring systems. UAS platforms have overcome inconveniences of aerial photography: its high cos and low flexibility. This way collected photos serve for 3D point cloud generation in photogrammetry software.

1.1. Objectives of the thesis

This paper presents acquiring, processing and presenting spatial data of an object in particular with use of UAS- based photogrammetry, laser scanning and total station measurements. Focus of the thesis is comparison of available UAS-obtained data processing software. Obtained results are compared in reference to classical land surveying methods. Differences between them concerning usability for the engineering object type are indicated.

1.2. Outline of the thesis

The papers layout follows all processing stages of spatial data acquisition, starting from measurement design, through measurements stage, ending up with post processing and results comparison. Chapters of the thesis presents workflow of a project. In chapter one, the main object is presented and analysed with regard to measurement layout. Chapters two and three refers to used instruments and performed measurements. Post processing stage is presented with explanation of used functions and parameters in chapter four. Finally, chapter five presents comparison of obtained results, thoughts and suggestion for improvements for this kind of projects.

1.3. Object of interest

Tower is a tall, self-supporting structure with significantly greater vertical than horizontal size. It can serve supporting bridges, aerials, giving visibility e.g. viewpoints, direct aviation traffic.

Figure 1.2 Tyholt tower [Wikipedia]

Tyholt tower (norw: *Tyholttårnet*) is a television and radio transmission tower located in Tyholt – district of Trondheim, Norway. It is 76,6 m reinforced concrete tower with 43,4 m steel mast on the top.

It is one of the most significant landmarks in Trondheim and its main gallery located atop, 72m above ground, offers panoramic view of the city and the fjord performing full revolution per hour. The object is located in technological area. Surroundings consist of low buildings that are location of NRK Trøndelag - Radio broadcaster, SINTEF - Ocean Research Foundation, and Telenor - Telecommunications Equipment supplier.

The object has been chosen to perform spatial data acquisition for its accessibility and simple yet distinct shape, which causes problems in obtaining full model using classical measurements.

The object outline consist of five maintenance galleries and top main gallery that is a place of a viewpoint. Due to its function, the tower is location of many satellite dishes, aerials and transmitters, which causes problems in obtaining entire cover of the model.

1.4. Control network

For the purpose of comparing obtained results and referencing models in geodetic reference system, control network was established. Whole project was realized in NMT zone 10 coordinate system with vertical datum NN2000. NMT is modified UTM system recommended by the Norwegian Mapping Authority for engineering surveys, in particular construction projects. Its utility in that kind of projects is caused mainly because of scale factor along the north axis, and high number of zones with main axis located in 1º spread, and therefore not causes additional distance distortion. The projected coordinate system is marked as ESPG: 5110. EPSG is international coordinate systems database that catalogues and standardizes parameters of Coordinate Systems and Transformations.

In order to orientate the control in geodetic datum GPS-RTN measurements were performed.

During designing phase, attention was paid on accuracy and possibility of using marked control points as observation stations for laser scanning and total station measurements. Field inspection unveiled that the terrain is uneven and highly developed which urged to modify initial draft and create connecting points.

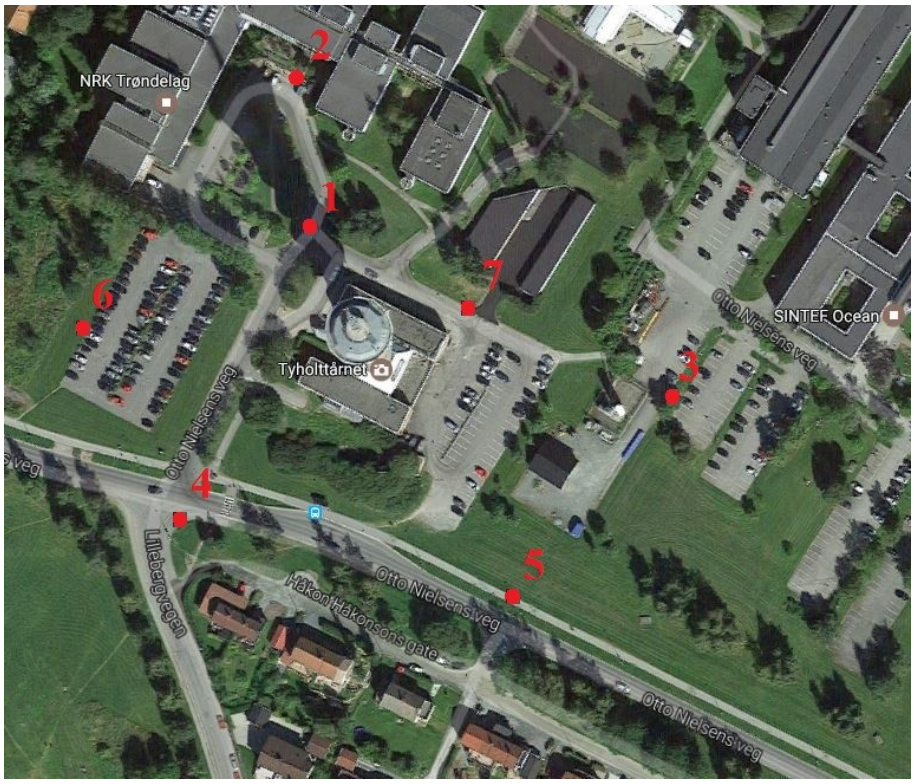

Figure 1.3 Established control network around the object

After establishing exact position of each point, they were marked firmly in the ground. It was made by engraving signs on firm kerbstones or with use of special, intended to that purpose nails.

Figure 1.4 Kerbstone control point marking

Figure 1.5 Control point nail

2. Methods of data acquisition

There are many ways of obtaining 3D spatial data: total station positioning, laser scanning, and photogrammetry. Basis of them are angular and distance measurements or taking photos. Those methods require vision between measuring device and object. This condition implies necessity of proper measuring station setting and measurement circumstances. Proper method is chosen according to desired accuracy, coverage, object-surrounding conditions and cost. For the purposes of object shape reproduction, four measuring methods were used: Classical point positioning, GNSS, laser scanning, Unmanned Aerial System-based photogrammetry.

2.1. Classical point positioning

Classical point positioning is based on manual manipulation of measuring device in order to obtain single points position. The method is based on angular and distance measurement to determining mutual relation between points. For that kind of measurements, total station is used. The device's basic function is to measure distance and record direction to a certain point. It is realized by built in optoelectronic distance meter and electronic scanner of limbus (coded

circular scale). The method requires suitable station, sufficient quantity and proper placement of measured points for adequate representation of surveyed object. The method is one of the most accurate and versatile regarding object type, but is the most time-consuming and demanding. Technique of obtaining desired structure's properties depends on the requirements and structure properties, its surrounding and desired accuracy. Properly prepared measurements provide accuracy meeting highest standards for engineering structures inspection.

Figure 2.1 High precision, bridge hooks total station measurements

For the task, classical measurements were performed with use of Leica TCRP1201 total station and Leica 360 prism (GRZ4). Along with the total station, Leica CS10 controller to control the total station remotely. The device is high precision, firm measuring instrument with highly developed software allowing easy measurements. Thanks to Automatic Target Recognition and Tracking, one-man survey was possible.

Figure 2.2 Used Total Station (Leica TCRP1201), Controller (Leica CS15) and 360 prism (Leica GRZ4).

Angle measurement		
Accuracy [1]	Hz, V	1” (0.3 mgon)
	Display resolution	0.1” (0.1 mgon)
Method	Absolute, continuous, diametrical	
Compensator	Working range:	4’ (0.07 gon)
	Setting accuracy:	0.5’’ (0.2 mgon)
Distance measurement (IR-Mode)		
Range [2]	Round prism (GPR1):	3000 m
	360° reflector (GRZ4):	1500 m
	Reflective tape (60 mm x 60mm):	250 m
	Shortest measurable distance:	1.5 m

Accuracy / Measurement time [3]	Standard mode:	1 mm + 1.5 ppm / typ. 2.4 s
	Fast mode:	3 mm + 1.5 ppm / typ. 0.8 s
	Tracking mode:	3 mm + 1.5 ppm / typ. <0.15 s
PinPoint R1000 reflectorless distance measurement (RL-Mode)		
Range [2]		1000 m
Accuracy / Measurement time [3,4]	Reflectorless < 500 m:	2 mm + 2 ppm / typ. 3 – 6 s, max. 12 s
	Reflectorless > 500 m:	4 mm + 2 ppm / typ. 3 – 6 s, max. 12 s
	Long Range:	5 mm + 2 ppm / typ. 2.5 s, max. 12 s
Laser-dot size	At 30 m:	approx. 7 mm x 10mm
	At 50 m:	approx. 8 mm x 20 mm

Table 1 Leica TCRP1201 Total Station specification table

1 - (standard deviation, ISO 17123-3);

2 - (average atmospheric conditions); 3- (standard deviation, ISO 17123-4) ; 4 - (object in shade, sky overcast)

With use of the total station control network, GCPs and cross-sections were measured.

First step was measuring control network. The task was done by performing angular and distance measurements in two faces of an instrument.

After completing measurements to neighbouring control points from a station, cross-sections and Ground Control Points (GCP) were measured. They were measured using reflectorless method.

GCPs were established as corners of red maintenance doors as easily distinguishable points with flat, steady surface and texture what matters when performing distance measurement in RL mode.

Figure 2.3 GCP placing

Cross-sections points were established little lower than balconies, because of its possible negative influence on measured distance. Due to significant laser-dot size, aiming on edge of structures causes fault measurement.

Figure 2.4 Total station cross-sections measurements placement

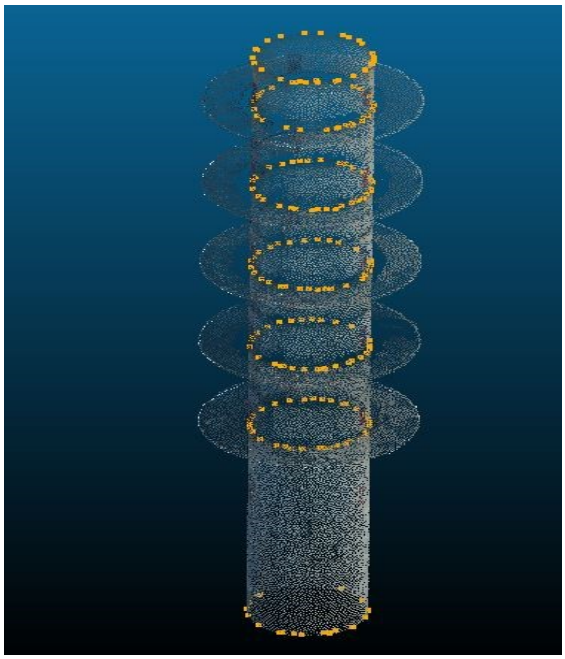

Figure 2.5 Cross-sections, CloudCompare

Each cross-section consist of ~30 evenly spread points. Total of 210 points were collected.

2.2. GNSS measurement

After the classical measurement, two of the control points were measured using GNSS. For the task Real Time Network (RTN), relative positioning method was used. Generally relative positioning consist of two (or more) receivers with one set as know position, base station and

another considered as rover. Thanks to know coordinates of base station and ones calculated with use of satellite ranging for the same point, correction for observations can be calculated. The correction can be applied for rover receiver. The difference in network method is that corrections are calculated for network of stations located across the country, and interpolated for position of the receiver. The system establish a Virtual Reference Station (VRS) in the project area and provides GNSS measurements corrections.

Norwegian Mapping Authority takes responsibility for corrections spreading, it is called SATREF CPOS system. It contains ca. 180 stations

Figure 2.6 Norway CPOS RTK network stations

In the measurements, geodetic Carrier Phase receiver Leica GS15 Carrier Phase Method receiver and Leica CS15 controller were used.

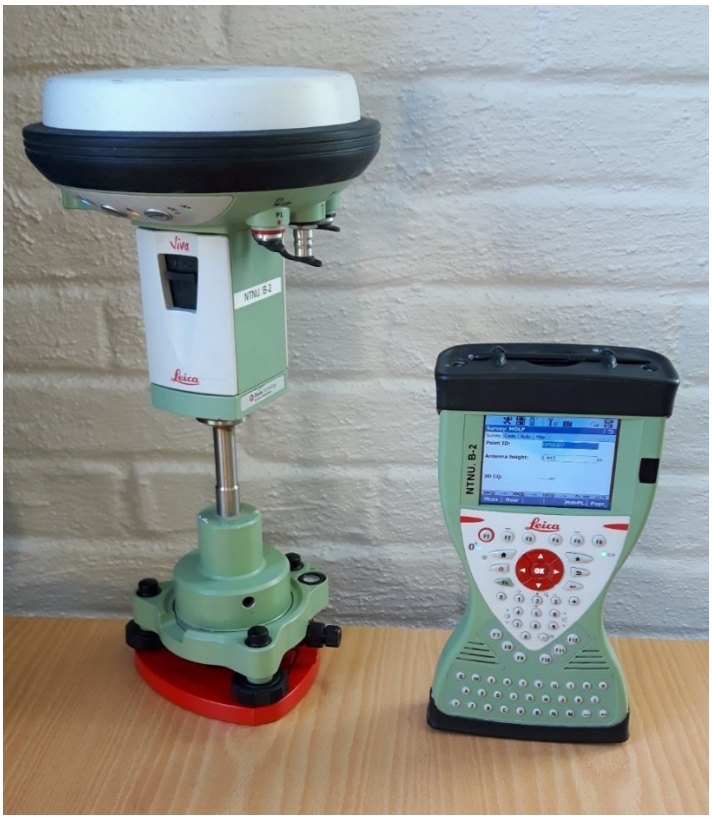

Figure 2.7 Used GNSS Receiver (Leica GS15) and Controller (Leica CS15)

GNSS Performance		
No. of channels	120	
Max. simultaneous tracked satellites	Up to 60 Satellites simultaneously on two frequencies	
Satellite signals tracking	GPS:	L1, L2, L2C, L5
	GLONASS:	L1, L2
GNSS measurements (Fully independent code and phase measurements of all frequencies)	GPS	carrier phase full wave length, Code (C/A, P, C Code)
	GLONASS	carrier phase full wave length, Code (C/A, P narrow Code)
	Reacquisition time	< 1 sec
Measurement Performance and Accuracy		
Accuracy (rms) Code differential with DGPS / RTCM[1]	DGPS / RTCM	Typically 25 cm (rms)

Accuracy (rms) with Real-Time-Kinematic (RTK)[1]	Single Baseline (<30 km)	Horizontal: 8 mm + 1 ppm (rms) Vertical: 15 mm + 1 ppm (rms)
	Network RTK	Horizontal: 8 mm + 0.5 ppm (rms) Vertical: 15 mm + 0.5 ppm (rms)
Accuracy (rms) with Post Processing[1]	Static (phase) with long observations	Horizontal: 3 mm + 0.1 ppm (rms) Vertical: 3.5 mm + 0.4 ppm (rms)
	Static and rapid static (phase)	Horizontal: 3 mm + 0.5 ppm (rms) Vertical: 5 mm + 0.5 ppm (rms)
	Kinematic (phase)	Horizontal: 8 mm + 1 ppm (rms) Vertical: 15 mm + 1 ppm (rms)
On the Fly (OTF) Initialization	RTK technology	Leica SmartCheck techo.
	Reliability of OTF initialization	Better than 99,99%[1]
	Time for initalization	Typically 4 sec[2]
	OTF range	up to 70 km[2]
Network RTK	Supported RTK network solutions	VRS, FKP, iMAX
	Supported RTK network standards	MAC (Master Auxiliary Concept) approved by RTCM SC 104

Table 2 Leica GS15 GNSS Receiver specification table

1 - Measurement precision, accuracy and reliability are dependent upon various factors including number of satellites, geometry, obstructions, observation time, ephemeris accuracy, ionospheric conditions, multipath etc. Figures quoted assume normal to favorable conditions. Times required are dependent upon various factors including number of satellites, geometry, ionospheric conditions, multipath etc. GPS and GLONASS can increase performance and accuracy by up to 30% relative to GPS only. A full Galileo and GPS L5 constellation will further increase measurement performance and accuracy.

2 - Might vary due to atmospheric conditions, signal multipath, obstructions, signal geometry and number of tracked signals.

Points 4 and 5 were chosen for orienting control network in coordinate system because these were measured most precisely and theirs surrounding granted steady results as opposed to others located near buildings, trees creating the possibility of signal obstructions and multi-pathing.

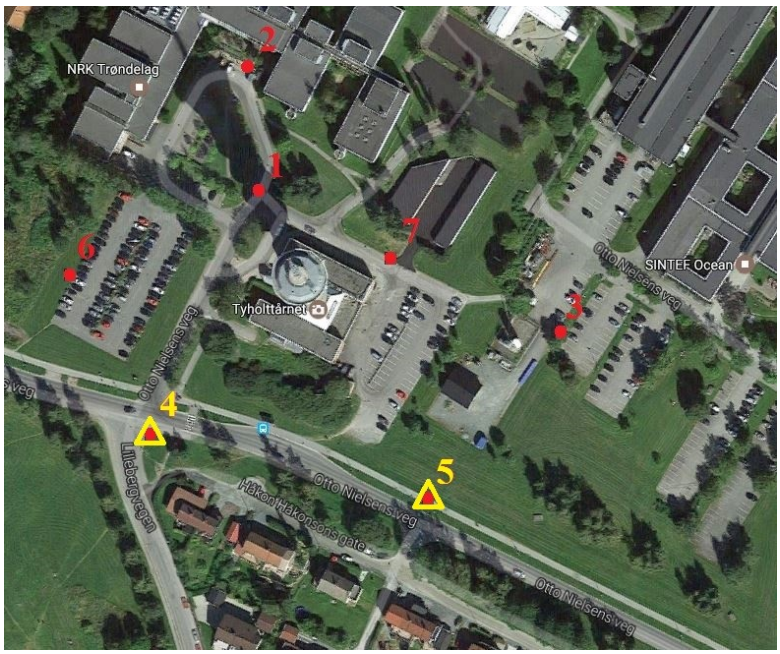

Figure 2.8 GNSS RTN measured points (yellow triangles)

Tripod use and long-time measurements provided precision of ~7mm. Norwegian mapping authority claim that accuracy of RTN measurements to be on a 10-20 mm accuracy level.

2.3. Laser scanning

Data acquisition using laser scanners is based on recording horizontal, vertical angle, and distance to certain point. Device performs the measurement by rotating objective lens (or mirror), which controls laser beam in vertical plane. After completing revolution, it rotates in horizontal plane and makes next vertical measurements. For every distance measurement angles are recorded simultaneously. As a result a point cloud is obtained, which density depends on angular interval of rotating objective lens. The method bases on total station, polar measurements, yet it is developed to be more effective in regards of point collection rate. Point clouds collected from multiple stations can be merged to obtain object's full point coverage. It can be performed with use of targets placed around scanned object, or distinct corresponding elements, included in scans obtained from following stations. The technology is applied in terrestrial scanning, mobile mapping, airborne and satellite scanning.

Figure 2.9 Leica C10 Laser scanner performing measurements [http://www.portusproject.org/technology/2012/10/laser-scanning-at-portus/]

Figure 2.10 Faro ScanArm scanner [http://www.faro.com]

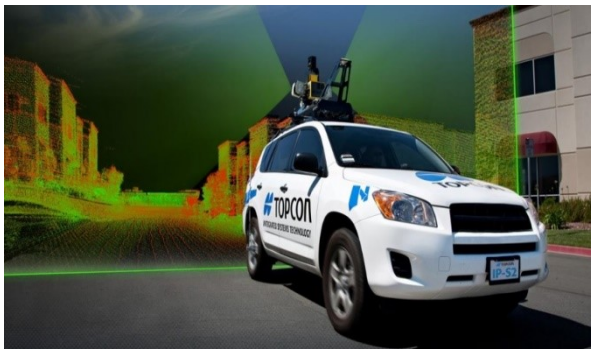

Figure 2.11 TOPCON Mobile LiDAR system [http://synergypositioning.co.nz]

Figure 2.12 RIEGL Airborne LiDAR system [http://www.riegl.com/]

3D object scanning finds application in many fields. It allows enhancing the inspection and design process by rapid capturing shapes of complex objects, structures and landscapes thus, making it more attractive and presentable form than classical data collection techniques.

Laser scanning was performed using Topcon GLS 1000 precise scanner, which integrates both the Time of Flight and the Phase Shift distance measurement methods. Time of flight method is based on accurate timing a light pulse to travel to the target and back. With the speed of light known, and an accurate measurement of the time taken, the distance can be calculated. Many pulses are fired sequentially and the average response is most commonly used. This technique requires very accurate sub-nanosecond timing circuitry. Phase Shift system is about measurement of the phase shift of the send pulse wave. It is impossible to calculate distance out of single survey, so device measures phase shift of multiple frequencies of reflection then solves some simultaneous equations to give a final measure. This method allows achieving very accurate and high quality data.

Figure 2.13 Topcon GLS 1000 terrestrial laser scanner

Scanning unit	
Maximum range	90% reflectivity Normal mode: 330m Long mode: 500m 18% reflectivity Normal mode: 150m Long mode: 230m
Minimum range	1.5 m
Distance accuracy (at 1 to 150m)	Normal mode: 4mm Long mode: 7mm
Angle accuracy	6” (1.8 mgon)
Surface accuracy (at 1 to 150m)	Normal mode: 2mm Long mode: 3mm
Target detection accuracy	3" at 50m
Scan rate (maximum)	30,000 points/second

Scan resolution	<6mm at 1 to 40m
Sample density (maximum)	1mm at 20m
Field of view (per scan)	Horizontal : 360 ° Vertical : ±35° (maximum)
Digital Camera	
Field of view	Approx. 22° (V) x 16.5° (H)
Number of pixels	2 megapixels
Tilt Compensator	
Type	Dual-axis tilt sensor
Compensation range	±6'

Table 3 Topcon GLS 1000 Terrestrial Laser Scanner specification table

Because of insufficient number of provided targets scanner station and orientating point were located on control network points. Procedure of orientating scans was performed with use of "Occupation and Backside" mode. After setting-up instrument above a desired point, target placed above another control point was scanned with the highest accuracy and density. Scan stations were distributed from available control points, in a way to provide complete and uniform object cover.

Figure 2.14 Scan stations localization (purple squares)

Density of scans was set to 20mm x 20mm. Along with scanning, device captured picture images simultaneously for photo-realistic point clouds.

While scanning some “backside” target scans had to be repeated due to sight obstructions or bad target recognition. Delay associated with that, and complex instrument levelling procedure extended measurement time to 4 hours.

Measurement was conducted in a partly clouded day what prevented shades and reduced noise, yet because long measurement, change in weather was noticeable especially in insolation on the last station (4).

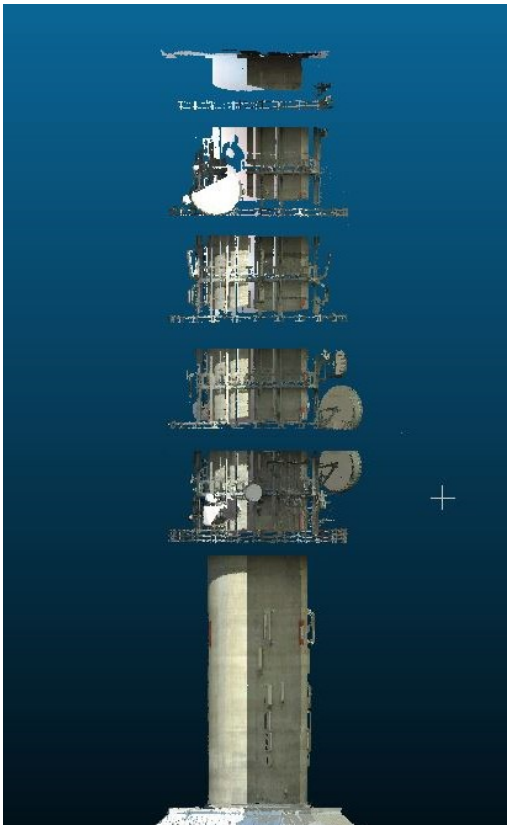

Figure 2.15 Laser scanning point cloud

As can be seen point cloud does not cover whole surface of the object. It lacks of data above the maintenance balconies and behind aerials. Any absence of data is caused by obstruction of measuring signal. There is no solution for the problem when concerning geodetic laser scanners. It is possible to avoid those holes by using sophisticated aerial LiDAR systems mounted on UAVs or helicopters.

2.4. UAS-based photogrammetry

Photogrammetry allows obtaining geometric properties of objects depicted on at least two photos taken from different positions. In order to obtain desired model of needed coverage and accuracy preparing flight plan is necessary. It is made by taking into consideration object

features, used hardware and desired model accuracy. To plan a mission we need to set area of interest and ground sample distance (size of a photo pixel in reality). Having those and knowing parameters of used camera: focal length and sensor size it is possible to calculate coordinates of camera perspective centres that serve as waypoints in planned mission.

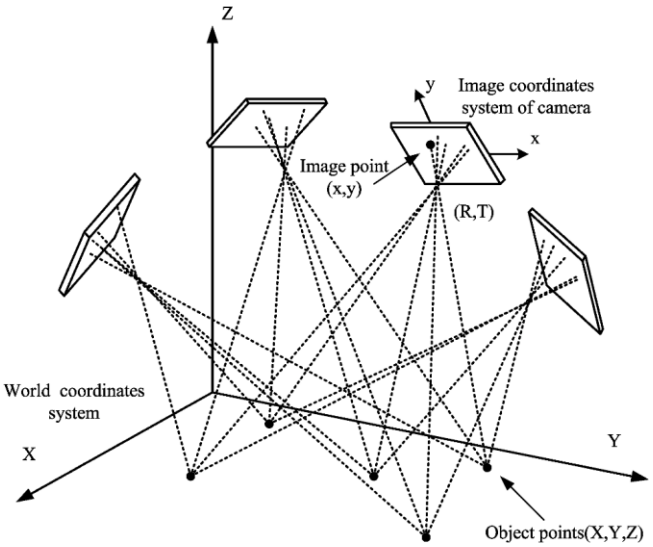

Figure 2.16 Photogrammetry creating rays

Close range photogrammetry can generate accurate, high-resolution 3D models of objects that provide accurate measurements as well as objective documentation of different perspectives. Through its abilities and versatility, this technology has many uses in broadly defined technology industry, e.g. biology/medicine, archaeology, architecture, production, engineering, etc.

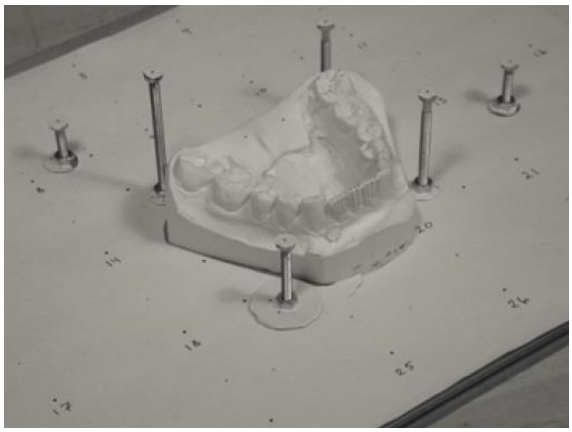

Figure 2.17 Photogrammetry measuring set for medical purposes

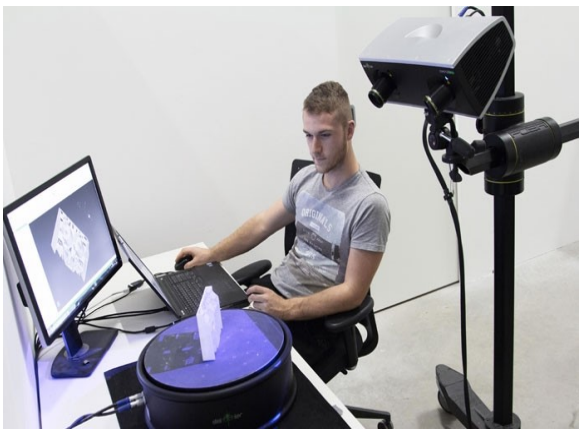

Figure 2.18 ZEISS COMET L3D - 5MP fringe projection scanner

When complex, inaccessible structures are to be measured and it is not possible to cover whole of it with required resolution, elevation of picturing device is necessary. It can be achieved by

ground structures as masts, scissor lifts, articulating booms, scaffoldings which employment depends on ground features and accessibility of the project area.

Figure 2.19 Taking photos on the roof. A shows scaffolding. B, C, D and E show capturing photos with use of tripod and telescopic lift (Martinez, Ortiz, Gil, Rego,2013)

Another, mode feasible and safe way of elevating camera is use of platform such as unmanned aircrafts – kites, balloons, glider and rotary or fixed wing UAVs.

Kites require specific weather conditions and highly experienced operator crew to maintain camera position and photo capturing.

Figure 2.20 Kite with attached photography camera [http://www.photoir.net/arial-photography/]

Unmanned Aerial Vehicles (UAV) also known as RPV (Remotely Piloted Aircraft) or drones are aircrafts without a human pilot aboard, led by human operator, or autonomously, by on-

board computers. These are component of a system, which depending on promoting community is named: UAS (Unmanned Aerial System) - adopted by US Department of Defence and UK Civil Aviation Authority, or RPAS (Remotely Piloted Aircraft System) adopted by International Civil Aviation Organization. Regardless of the name the system was originally developed for military use to perform missions to “dull, dirty or dangerous” for humans. In the text, UAS name is used when explaining use of whole platform as a system containing of: aircraft, controller and software; and UAV when treating about aircraft itself. Nonetheless, this highly developing technology rapidly expanded to scientific, commercial, agricultural and sport application.

Figure 2.21 Military use drone - MQ-1 "Predator" [Wikipedia]

Figure 2.22 Multirotor UAV - DJI S-1000 [www.dji.com]

Figure 2.23 Fixed wing UAV - senseFly eBee RTK [www.sensefly.com]

Figure 2.24 Airship UAV - RC Blimp [http://www.providentialsystems.com]

Hardware and software development increased flight-time, manoeuvrability and weight lifting abilities, which coordinated with advanced controlling system gave capability of steady, fully controlled even completely autonomously flights. This soaring use along with relative low-cost makes them valuable tool for professional data collection.

Selection of date and time of the measurement was guided mainly by weather conditions. Main factors were temperature, wind, sun activity and insolation.

Low temperature (below 0° C) can significantly reduce battery capacity causing serious danger while performing missions. Thanks to advanced stabilization and positioning systems, aircraft is able to maintain its position in air with wind up to 10 m/s but even lighter breeze might cause some troubles. Sun activity, its changing magnetic field and storms cause changes of Earth's magnetic field, what can cause abnormal measuring systems data, difficulties with connection and thus lead to flight failure. Proper insolation was taken into account for its influence on differences in picturing object. High insolation on southern side of the tower would cause poor picturing of northern side, causing problem with model generation and its accuracy therefore measurements were performed on a partly clouded morning.

In the project, DJI Phantom 3 Professional UAS was used.

Figure 2.25 Used DJI Phantom 3 Professional

Aircraft	
Weight (Battery and Propellers Included)	1280 g
Max Ascent Speed	5 m/s
Max Descent Speed	3 m/s
Hover Accuracy	Vertical: ± 0.1 m (VPS+ GPS) or ± 0.5 m (GPS) Horizontal: ± 1.5 m
Max Speed	16 m/s (ATTI mode, no wind)

Max Flight Altitude	6000 m
Max Flight Time	Approx. 23 minutes
Operating Temperature	0°C to 40°C
GPS Mode	GPS/GLONASS
Remote controller	
Operating Frequency	2.400 GHz-2.483 GHz
Transmitting Distance	2000m (Outdoor And Unobstructed)
Operating Temperature	0° to 40° C
Gimbal	
Controllable Range	Pitch: -90° to +30°
Stabilization	3-axis
Camera	
Sensor	Sony EXMOR 1/2.3" Effective pixels: 12.4 M (total pixels: 12.76 M)
Lens	FOV 94° 20 mm (35 mm format equivalent) f/2.8, focus at ∞
ISO Range	100-3200 (video), 100-1600 (photo)
Shutter Speed	8s -1/8000s
Image Max Size	4000 x 3000
Still Photography Modes	Single Shot Burst Shooting: 3/5/7 shots Auto Exposure Bracketing (AEB): 3/5 Bracketed frames at 0.7EV Bias Time-lapse
Photo/ Video Formats	JPEG, DNG / MP4, MOV (MPEG-4 AVC/H.264)

Table 4 DJI Phantom 3 Pro specification table

It is an X quadcopter with GPS, Vision Positioning System, barometer and compass that allows steady, controlled flights. Built-in 4K camera placed on 3-axis gimbal platform allows capturing stable, clear images and videos.

Because of the shape of the Tower flight mission was designed in such way that flight lines were parallel to main vertical axis of the tower, providing best photogrammetric reconstruction. Flight lines were performed in columns. That way photos were taken with main camera axis horizontal.

In order to provide best accuracy possible from UAV images forward and lateral overlaps had to be significantly increased compared with classical aerial photogrammetry because of consumer-grade quality of the camera and low quality of geolocation devices in the vehicle.

Task of providing small ground sample distance with provided camera and high overlaps required vertical flight-lines evenly spread around tower's centre point.

Figure 2.26 Designed light-lines in plan view

		Value	**Description**
Camera constant (ck)		3,61 mm	Taken from picture properties
Ground Sample Distance (GSD)		10 mm	Preliminary value
Pixel size (px)		0.001575 mm	Taken from properties of image sensor
Overlap	Forward	80%	Preliminary value
	Lateral	70%	Preliminary value

Table 5 Preliminary values for flight planning

Calculating scale of the projection

$$mz = \frac{GSD}{px} = \frac{12mm}{0.001575mm} = 6349$$

Calculating distance from object to sensor

$$H = ck * mz = 3.61mm * 6349.20 = 26.5m$$

Calculating actual lateral overlap

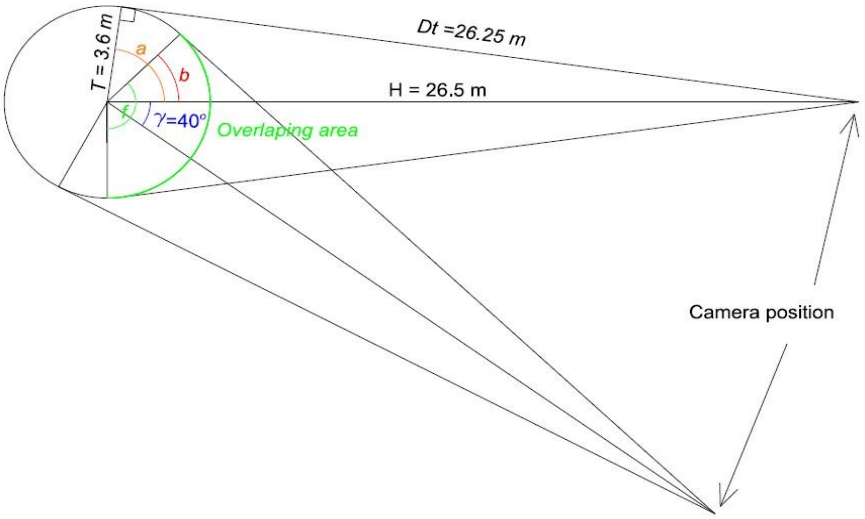

Figure 2.27 Lateral overlap calculation

$$a = \tan^{-1}(\frac{Dt}{T}) = \tan^{-1}(\frac{26.25\ m}{3.6\ m}) = 70.8\ g$$

$$b = a - \gamma = 70.8\ g - \ 40\ g = 30.8\ g$$

$$f = a + b = 101.6\ g$$

$$lat = \frac{f}{2 * a} * 100\% = \frac{101.6\ g}{141.6\ g} * 100\% = 72\%$$

Calculation of coordinates of flight-lines horizontal coordinates

	Bearing [g]	X [m]	Y [m]
Central Point		7033447,092	571477,050
1	0	7033473,592	571477,050
2	40	7033468,531	571492,626
3	80	7033455,281	571502,253
4	120	7033438,903	571502,253
5	160	7033425,653	571492,626
6	200	7033420,592	571477,050
7	240	7033425,653	571461,474
8	280	7033438,903	571451,847
9	320	7033455,281	571451,847
10	360	7033468,531	571461,474

Table 6 Horizontal coordinates of flight-lines

Calculating actual forward overlap (difference in elevation of taking photos in the flight-line)

$$for = fp * \left(1 - \frac{p0}{100}\right) = 36m * 0.20 = 7{,}20m$$

Because of performing free flight mission, photos were taken in 6m separation what provided 82, 5% forward overlap.

Figure 2.28 Photos location, Bentley ContextCapture

That high level of forward and lateral overlap was pursued because of its high influence in final model accuracy.

Lack of appropriate software for that kind of missions forced to perform free flight missions with manual placing of an aircraft in desired position based on telemetry data reading.

While performing mission, when UAV was placed in optimal position, waypoint, it was stabilized on desired altitude in order to perform steady photo capture. Photos were taken from 12m above ground level (AGL) in 6m separation, because of ground level maintenance buildings and aerials located around it. In one, vertical flight line, 15 photos were taken.

Whole process of calibrating the device and performing flights in which total of 150 photos were taken took an hour.

While performing UAV flights it is crucial to take precautions. The tower's structure and radio transmission function caused risk of on-board devices misreading and RC connection loss therefore it was necessary to pay attention to telemetry readings and RC connection.

3. Post processing

Post processing is a process of checking, adjusting, comparing and analysing obtained data. All data needed to be brought from instruments' internal local coordinate systems to global system established with use of the control points.

3.1. Control network adjustment

Adjustment was performed using Least Square Method in C-GEO software. The software consist of number of programs and applications useful for land surveyors and designers. The software was used for control network adjustments using Least Squares Method and presenting errors of each adjusted point.

Because main concept of the dissertation is to compare geometry of the object and its internal relations. Global accuracy – position in global reference system was not the main objective. GPS measured points has been used to orientate network in a way that does not influence internal relation between points. Two points were measured using GNSS RTN (4 and 5), one of them (5), was set as fixed and both were used for bearing calculation.

NR	X [m]	Y [m]	H [m]	mx [m]	my [m]	mp [m]	mh [m]
5	1604095.853	96659.154	108.828	0.000	0.000	0.000	0.000
4	1604130.218	96534.556	113.410	0.001	0.002	0.002	0.002
3	1604172.436	96696.703	109.163	0.002	0.002	0.003	0.002
2	1604273.699	96574.942	113.663	0.002	0.003	0.004	0.002
1	1604224.203	96573.409	113.789	0.002	0.003	0.003	0.002
7	1604200.363	96630.642	111.109	0.002	0.002	0.003	0.002
6	1604197.755	96508.734	113.958	0.002	0.003	0.004	0.002

Table 7 Control network points' coordinates and accuracy

Thanks to two-faced measurements performed with use of very accurate instrument and proper points stabilization results are satisfying.

Mean points adjustment accuracy value equals 0.0031m,

The software enables us also to see information about error ellipses and its' parameters.

Worse adjusted is point no. 2 with horizontal accuracy mp=0.004m, and vertical accuracy mh=0.002m, due to adverse network geometry – it is a corner point with acute angles arrangement. Arrangement of RTN measured points also have a major impact, as shown on a figure below, point no. 2 is located furthest from point no. 5 which was set as error-free

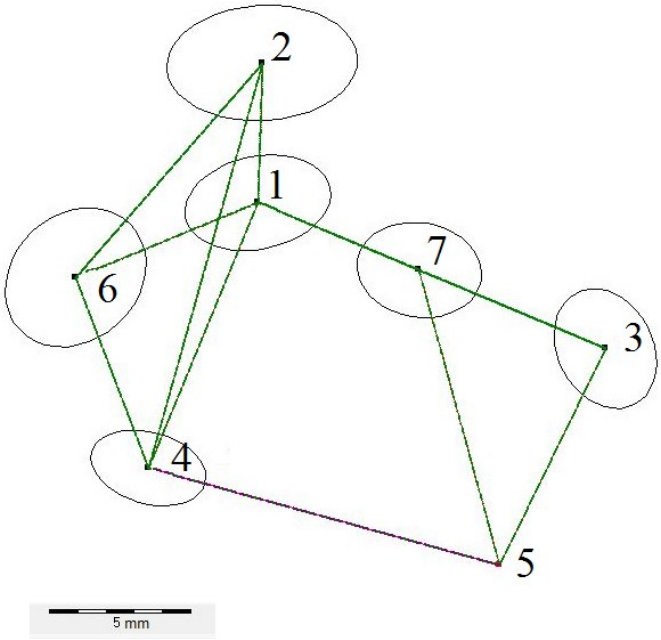

Figure 3.1 Adjustment error ellipses, C-Geo

Whole adjustment report from C-Geo in Appendix A

3.2. Cross-sections and GCPs coordinates calculation

Except occupation points for laser scanner control network, points were used to determine coordinates of Ground Control Points, which were distributed on the corners of maintenance doors, located on the structure of the object. Measurements were performed using total station.

Figure 3.2 Ground Control Point marked on a photo, Pix4Dmapper Pro

GCPs were distributed evenly around the object and through its height. Due to aerials or rods location, causing view obstruction, not every door had visible, distinguishable point. 16 GCPs were measured and their accuracy calculated for future accuracy assessment.

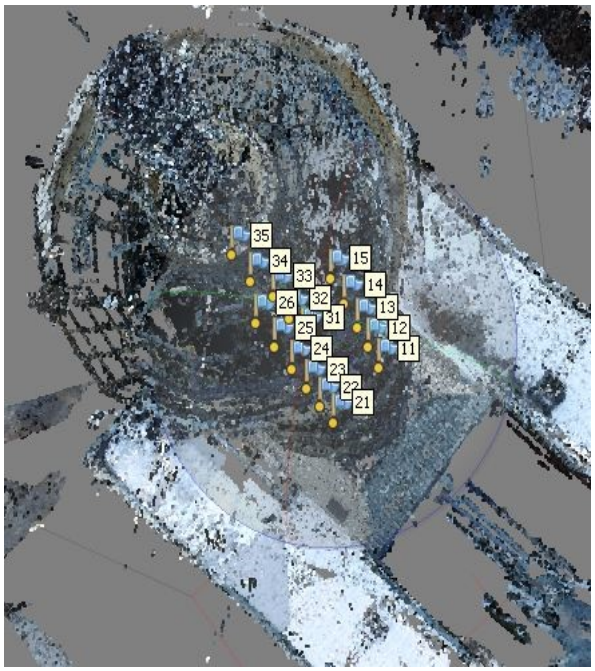

Figure 3.3 GCPs localization on model, Agisoft Photoscan

Figure 3.4 GCPs localization on a photo, Agisoft Photoscan

Coordinates of the points were obtained with polar measurements from control points stabilized previously. Its position can be noted as

$$X = X_S + D_P * \cos(A),$$

$$Y = Y_S + D_P * \sin(A),$$

$$Z = Z_S + D * \cos(V)$$

Where

X, Y, Z- coordinates of cross-section point,

X_S, Y_S, Z_S- coordinates of station from which measurement was conducted,

D_P- horizontal distance from station to the point,

A – bearing from station to the point,

V – vertical angle measured from zenith to the point.

GCPs accuracy was considered it in adjustment process in photogrammetry software. Since coordinates of GCPs and cross-sections were calculated indirectly by making direct measurements of other quantities (distances and directions) - Gauss error propagation law was used to calculate its final accuracy. In order to study influence of how individual, indirect measurements are combined in the result

$$m_X = \pm\sqrt{\left(\frac{\delta X}{\delta X_S} * m_{X_S}\right)^2 + \left(\frac{\delta X}{\delta D_P} * m_{D_P}\right)^2 + \left(\frac{\delta X}{\delta A} * m_A\right)^2},$$

$$m_Y = \pm\sqrt{\left(\frac{\delta Y}{\delta X_S} * m_{Y_S}\right)^2 + \left(\frac{\delta Y}{\delta D_P} * m_{D_P}\right)^2 + \left(\frac{\delta Y}{\delta A} * m_A\right)^2},$$

$$m_Z = \pm\sqrt{\left(\frac{\delta Z}{\delta X_S} * m_{X_S}\right)^2 + \left(\frac{\delta Z}{\delta D} * m_D\right)^2 + \left(\frac{\delta Z}{\delta A} * m_V\right)^2},$$

3D accuracy of a point is calculated as:

$$m_Z = \sqrt{{m_X}^2 + {m_Y}^2 + {m_Z}^2}$$

Where

m_X, m_Y, m_Z - accuracy of the point in X, Y, Z direction,

$m_{X_S}, m_{Y_S}, m_{Z_S}$ - accuracy of control and centring,

m_{D_P}, m_D - accuracy of distance measurement,

m_A, m_V – accuracy of angular measurement and aiming.

Accuracy	Value
distance (RL)	2 mm + 2 ppm
direction	1” (0.3 mgon)
aiming	31” (9,5 mgon)*
centring	3 mm
station height	2 mm

Table 8 Components for accuracy calculation of total station measurements

While measuring GCPs, aiming accuracy value was calculated as small-angle approximation for value of 15 mm measured from 100 m, caused by unambiguity of target (corner of the maintenance doors)

$$\alpha = \frac{\rho * t}{d} = \frac{63661{,}98\ mgon * 15\ mm}{100\ m} = 9{,}54\ mgon$$

Where:

α – angular value of aiming uncertainty,

ρ – full angle value,

t – aiming uncertainty,

d – mean distance to target,

Because some of the GCPs were measured from two adjacent stations, their coordinates were calculated as weighted mean with weights correlated with its determination accuracy.

$$\bar{X} = \frac{w_{XstA} * X_A + w_{XstB} * X_B}{w_{XstA} + w_{XstB}}, \qquad \sigma_{\bar{X}} = \frac{1}{\sqrt{w_{XstA} + w_{XstB}}}$$

$$\bar{Y} = \frac{w_{YstA} * Y_A + w_{YstB} * Y_B}{w_{YstA} + w_{YstB}}, \qquad \sigma_{\bar{Y}} = \frac{1}{\sqrt{w_{YstA} + w_{YstB}}}$$

$$\bar{Z} = \frac{w_{ZstA} * Z_A + w_{ZstB} * Z_B}{w_{ZstA} + w_{ZstB}}, \qquad \sigma_{\bar{Z}} = \frac{1}{\sqrt{w_{ZstA} + w_{ZstB}}}$$

Where

$w_{X,Y,Z} = \frac{1}{\sigma_{X,Y,Z}{}^2}$ – weight,

stA, stB –station A, station B,

GCP	X [m]	Y [m]	Z [m]	mX [m]	mY [m]	mp [m]	mZ [m]
11	1604180,446	96597,664	137,560	0,014	0,005	0,015	0,015
12	1604180,301	96597,697	145,501	0,014	0,005	0,015	0,015
13	1604180,329	96597,696	153,545	0,014	0,005	0,015	0,015
14	1604180,326	96597,711	161,511	0,014	0,005	0,015	0,015
15	1604180,317	96597,759	169,510	0,014	0,005	0,015	0,015
21	1604185,040	96600,343	137,584	0,004	0,006	0,007	0,007
22	1604185,073	96600,361	145,534	0,005	0,014	0,015	0,015
23	1604185,066	96600,364	153,536	0,005	0,014	0,015	0,015
24	1604185,072	96600,392	161,552	0,005	0,014	0,015	0,015
25	1604185,072	96600,405	169,537	0,005	0,014	0,015	0,015
26	1604185,058	96600,393	177,525	0,005	0,014	0,015	0,015
31	1604179,502	96604,062	137,571	0,007	0,004	0,008	0,010
32	1604179,604	96604,062	145,593	0,007	0,004	0,008	0,010
33	1604179,577	96604,087	153,563	0,007	0,004	0,008	0,010
34	1604180,246	96604,457	161,549	0,007	0,004	0,008	0,009
35	1604180,271	96604,504	169,547	0,014	0,004	0,015	0,012

Table 9 Ground Control Points coordinates with accuracy

Cross-section points were calculated the same way, with use of polar coordinates. Their accuracy was acquired with use of polar measurements quality assessment formula, and values from instrument's specification Table 1. Because points were selected arbitrary, aiming accuracy was not considered. For point 100 m distant from station, accuracy equals 4mm horizontal, 3mm vertical.

3.3. Laser scanning

Topcon ScanMaster was used in the task. It is Topcon GLS-1000 laser scanner integrated processing software with capability of remote controlling the device and its properties. It allows viewing, manipulating, registering and modelling acquired data.

Right after importing scanning data, scans appear as collected from one station. This is a look of the scanner internal polar coordinate system. That is why registration process is necessary.

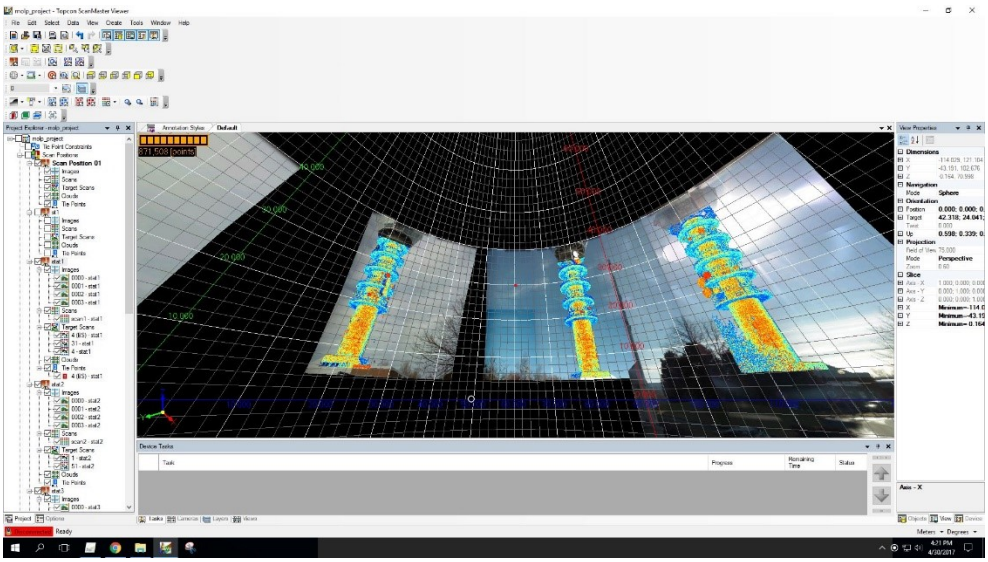

Figure 3.5 View of obtained scans in scanner's internal, polar, coordinate system, ScanMaster

Registration is the process of integrating scans obtained from different stations together into a desired coordinate system. In the ScanMaster software it can be done by defining certain constraints:

- *Registering Tie Points*: Registration based on multiple, constant target points scanned from subsequent stations.
- *Georeferencing*: Reorienting entire dataset to correspond the coordinates of the tie points.
- *Automated Tie Point Registration*: Automatic registration of points based on similar geometry or description attribute.
- *Occupation and Backsight Registration*: Alignment of scans based on placing station and backsight over known points.

The device is only compatible with special designated target sheets, and was delivered with only four of them. Only one of them was designated to be mounted on tripod, others were stuck Plexiglas plate, with no possibility of rotation without its centre position change. That was too few for such developed and busy environment for tie points registration.

Figure 3.6 Topcon GLS-1000 Target on a tribrach

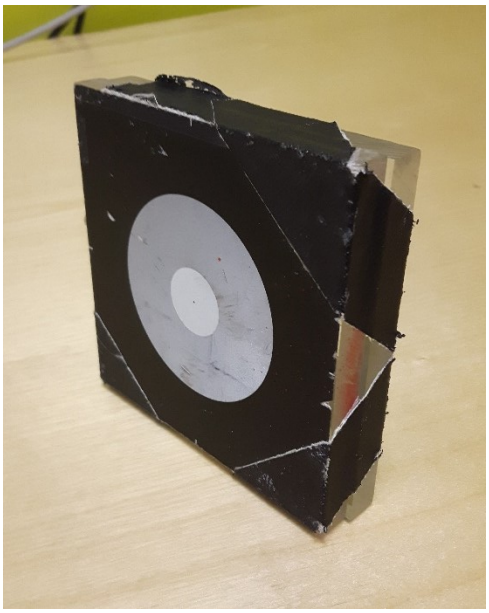

Figure 3.7 Topcon GLS-1000 Target stuck on a Plexiglas plate

Because of that and insufficient scans overlap from adjacent station "*Occupation and Backsight Registration*" method was used. Because of registering method, it is impossible to generate accuracy report from the software. For the purpose of quality assessment points' accuracy were calculated with use of accuracies of distance and direction measurement and station placement.

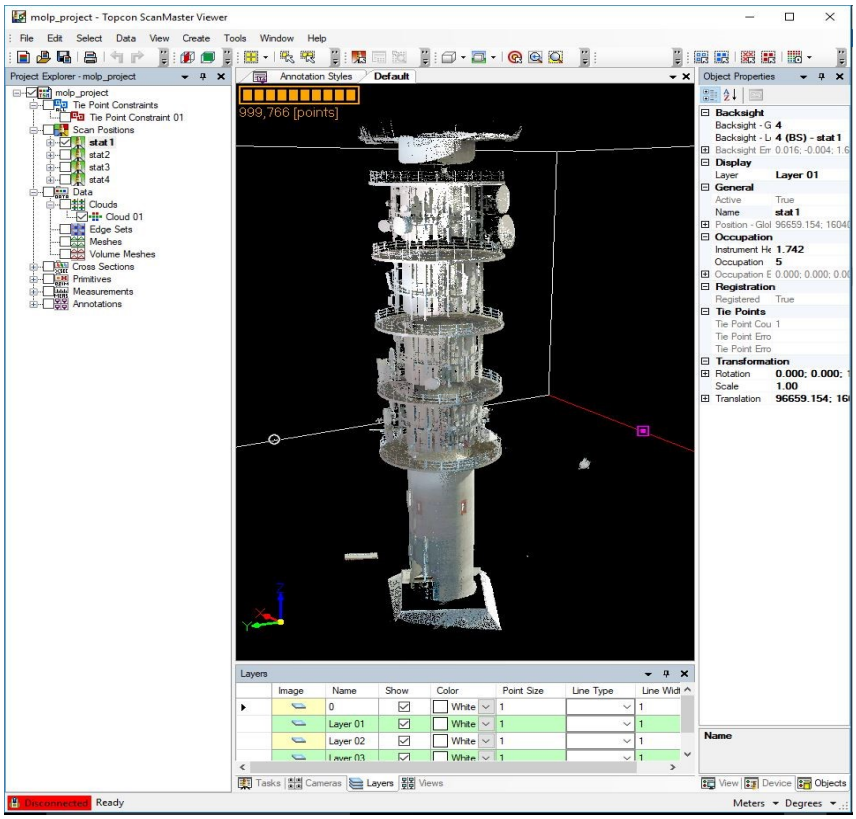

Figure 3.8 Merged scans, ScanMaster

To this end laser scanner specs Table 3 and formula for polar measurements uncertainty was used. Mean distance from station to tower was set as 100m. Accuracy calculated this way gave result of accuracy: 6 mm horizontal and 4mm vertical. For future references, value of 3D accuracy (7mm) is used.

Considering used device, stations placement and object type it seems reasonable.

When viewing obtained model, certain inconsistency was noticed. When looking at parts of point cloud consisting of scans from neighbouring stations, overlying parts of them is slightly divergent.

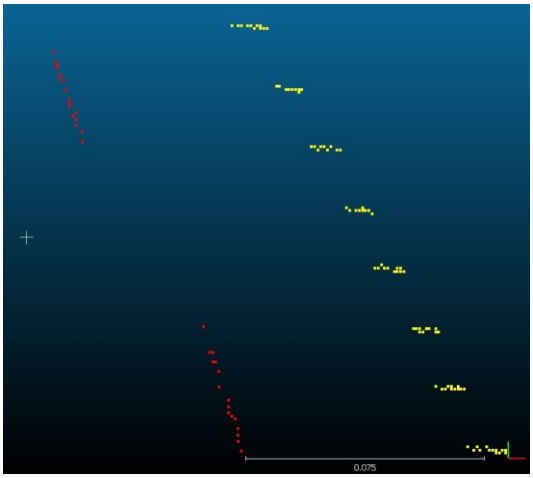

Figure 3.9 Noticed inconsistency

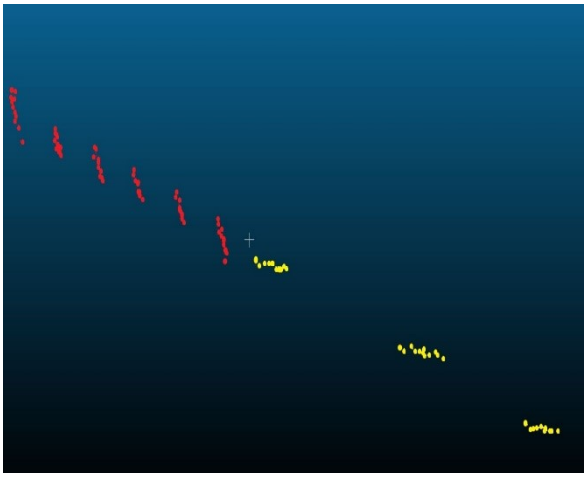

Figure 3.10 Cleared scans' join

Phenomenon is occurring on every junction; therefore, it seems to be due to the tower's cylindrical shape. Sides of the scanned region seems to be scanned with significantly inferior quality. Distance between two scans reaches even 7,5 cm. It might be caused by ray slippage on almost tangent to station part of the cylinder.

Geo-referenced scans were exported in .las format, and imported into CloudCompare.

In order to minimalize the effect the clouds were trimmed manually in such way to consist as much of points created with most perpendicular rays as possible. After the process, clouds were merged into one.

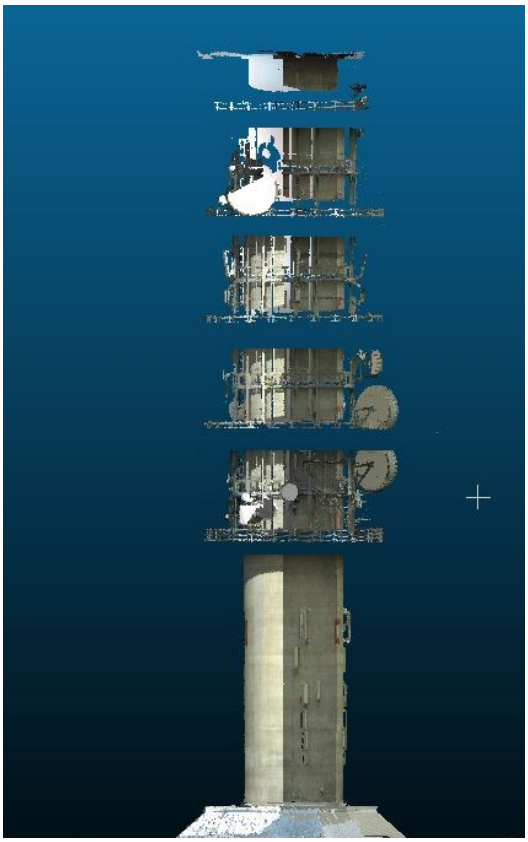

Figure 3.11 Obtained Point Cloud

Obtained results seems to be satisfying, yet difference in insolation between stations is clearly visible, especially scan from station 4 that was obtained as last one.

3.4. Photogrammetry software

There is many software available for stereoscopy, close-range, aerial and satellite photogrammetry, yet recently with rapid growth of UAS application, some of the producers created software concentrated on UAS-based photo processing. This software enables generation of most of the demanded products:

- point cloud,
- mesh,
- Digital Elevation Model (DEM)
- orthomosaic,

These can serve many application e.g. area, volume calculations, displacements detection, defects monitoring, etc. For the comparison, three software were used: Pix4D mapper Pro, AgiSoft professional, Bentley ContextCapture.

The software have high hardware and software requirements. In order to easily process-demanding projects the most important components are:

- CPU - Central Processing Unit, recommended – quad/hexa core
- RAM – Random-access memory, recommended – 16 GB
- Hard Drive – recommended SSD, free space demanding on the project :15-120 GB
- GPU – Graphics processing unit, compatible with OpenGL, recommended 2 GB

Computer used for the processing enabled highest performance and allowed the highest quality options to be used.

3.4.1. Pix4Dmapper Pro

The software was developed by Swiss company Pix4D and was initially released in 2011. The company aims to develop complete system for UAS-based mapping uses. Pix4D developed variety of tools for flight-planning, data acquisition, post-processing making it complete system for spatial data acquisition. It finds application in many industries e.g. Surveying, Constructions, Agriculture and Real Estate. Pix4D mapper allows processing, editing and analysing data.

First step in work with the program is to establish a project and assign images that will be used in process of model making. The software not only enables photos to be used but also allows time-sampled video-based captures for the processing. Photos obtained with use of the DJI UAS, thanks to integrated GPS receiver, are geolocated and thank to compass's and gimbal's features, are orientated in space (angles of rotation are known). Each photo's information is stored in EXIF metadata while performing image capture.

After that, it is possible to see position of photos visualized in Map View for initial control.

Data processing workflow in Pix4D is presented in three steps:

1. Initial Processing
2. Point Cloud and Mesh
3. DSM, Orthomosaic and Index

1. Initial Processing

Initial Processing is a process of finding common points on adjacent photos (matches) and performing Automatic Aerial Triangulation and Bundle Block Adjustment. These are processes of reconstructing rays creating each point and calculating position of photos.

Keypoints Image Scale tab allows defining image size for extracting keypoints; it is important to adjust the parameter with regard to used camera and used processing hardware. It was launched with "*Full*" Keypoint Image Scale for precise results.

Matching setup allows us to adjust the pair matching with regard to performed flight pattern. In this case, "*Freeflight or Terrestrial*" option was used due to that kind of flight-plan and verified best results.

While processing Geometrically Verified Matching strategy was used. This option uses not only image content to find matches but also relative camera positions are used to discard geometrically unrealistic matches. The procedure takes more time but provides results that are more robust.

In calibration tab, Number of Keypoint was not limited in any way and set as *Automatic*.

After that step, visualization of photos position and point cloud consisting of match points was possible in "*rayCloud*" view. It turned out that model based on photos' geolocation was shifted, investigating the problem revealed that it is common, unsolved issue among DJI Phantom 3 users, yet thanks to use of Ground Control Points it does not influence final results.

To generate accurately referenced models, GCPs with their accuracy were imported and marked on the photos. Marking of the GCPs on the photos was the longest process of the workflow in Pix4D, the software allow Automatic matching, nonetheless marks needed to be readjusted.

The software provides quite convenient and straightforward procedure of points marking. Provided layout allows for viewing many projections of certain point at once what definitely helps and speeds up marking process.

Even though the GCPs' location (corners of the doors) was rather unambiguous and visible, sometimes due to photos' uneven insolation and angular position on the photos some of them were little blurry and not perfectly pinpointed.

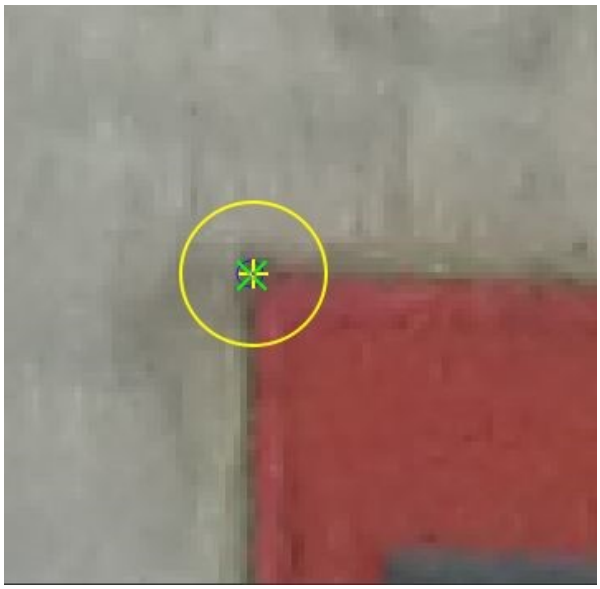

Figure 3.12 Distinct GCP, Agisoft Photoscan

Figure 3.13 Indistinct GCPs, Agisoft Photoscan

In order to get independent quality check of global accuracy of the adjustment, some of the GCPs were used as checkpoints. They were chosen in a way to have a checkpoint on different levels and on different sides of the tower.

	Label	Type	X [m]	Y [m]	Z [m]	Accuracy Horz [m]	Accuracy Vert [m]
21	11	3D GCP	96597.664	1604180.446	137.560	0.015	0.015
13	12	Check Point	96597.697	1604180.301	145.501		
16	13	3D GCP	96597.696	1604180.329	153.545	0.015	0.015
15	14	Check Point	96597.721	1604180.334	161.513		
14	15	3D GCP	96597.759	1604180.317	169.510	0.015	0.015
16	21	Check Point	96600.343	1604185.040	137.584		
16	22	3D GCP	96600.361	1604185.073	145.534	0.015	0.015
20	23	Check Point	96600.364	1604185.066	153.536		
20	24	3D GCP	96600.392	1604185.072	161.552	0.015	0.015
15	25	3D GCP	96600.405	1604185.072	169.537	0.015	0.015
20	26	3D GCP	96600.393	1604185.058	177.525	0.015	0.015
24	31	3D GCP	96604.062	1604179.502	137.571	0.008	0.010
9	32	3D GCP	96604.062	1604179.604	145.593	0.008	0.010
19	33	Check Point	96604.087	1604179.577	153.563		
18	34	3D GCP	96604.457	1604180.246	161.549	0.008	0.009
20	35	Check Point	96604.504	1604180.271	169.547		

Table 10 GCPs and Check Points table, Pix4Dmapper Pro

After completing marking, reoptimize process was started to recalculate internal and external camera parameters after adding GCP's.

GCP Name	Accuracy XY/Z [m]	Error X [m]	Error Y [m]	Error Z [m]	Projection Error [pixel]	Verified/Marked
11 (3D)	0.015/0.015	-0.008	0.003	0.007	0.502	21/21
13 (3D)	0.015/0.015	-0.006	-0.009	0.002	0.382	16/16
15 (3D)	0.015/0.015	-0.009	-0.013	-0.007	0.352	14/14
22 (3D)	0.015/0.015	0.008	0.007	-0.010	0.469	16/16
24 (3D)	0.015/0.015	0.006	0.009	0.001	0.432	20/20
25 (3D)	0.015/0.015	-0.005	0.003	-0.004	0.409	15/15
26 (3D)	0.015/0.015	0.003	-0.002	0.000	0.498	20/20
31 (3D)	0.008/0.010	-0.000	-0.002	0.002	0.421	24/24
32 (3D)	0.008/0.010	0.002	-0.002	-0.002	0.407	9/9
34 (3D)	0.008/0.009	0.003	0.004	0.003	0.407	18/18
Mean [m]		-0.000596	-0.000227	-0.000611		
Sigma [m]		0.005687	0.006566	0.004784		
RMS Error [m]		0.005718	0.006570	0.004823		

0 out of 6 check points have been labeled as inaccurate.

Check Point Name	Accuracy XY/Z [m]	Error X [m]	Error Y [m]	Error Z [m]	Projection Error [pixel]	Verified/Marked
12	0.0150/0.0150	-0.0154	0.0030	0.0113	0.5009	13/13
14	0.0150/0.0150	-0.0023	0.0036	0.0014	0.3321	15/15
21	0.0070/0.0070	0.0046	0.0155	-0.0099	0.3379	16/16
23	0.0150/0.0150	0.0052	0.0059	-0.0258	0.3415	20/20
33	0.0080/0.0100	-0.0160	-0.0108	0.0026	0.4489	19/19
35	0.0150/0.0120	0.0291	0.0127	0.0110	0.3646	20/20
Mean [m]		0.000857	0.004988	-0.001575		
Sigma [m]		0.015225	0.008426	0.012952		
RMS Error [m]		0.015250	0.009791	0.013047		

Localisation accuracy per GCP and mean errors in the three coordinate directions. The last column counts the number of calibrated images where the GCP has been automatically verified vs. manually marked.

Table 11 Quality report, GCPs and Check Points, Pix4Dmapper Pro

Root Mean Square Error values of the Check Points has all values on a similar level as GCPs, meaning that model creation was performed correctly and accuracy is preserved. Full report containing Initial Processing and Model Creating is in Appendix B.

2. Point Cloud and Mesh

This section allows defining parameters of point cloud densification and mesh creating.

Point cloud densification is a process of projecting points depicted on photographs. It provides increased number of 3D points what leads to higher accuracy both DSM and Orthomosaic. Provided options allow changing desired outputs. In order to do that it is possible to define:

- Image scale,

  This parameter determines the scale of the images at which 3D points are computed. For the processing *1* (Original image size) option was used. Other are: *2* (double image) $^1/_2$ (half image size), $^1/_4$ (quarter image size) and $^1/_8$ (eighth image size). The bigger the scale the more points are calculated and the longer processing time.

- Point Density,

Allows user to define density of final densified point cloud. For the computations $High$ (Slow) option was used, what effects 3D point calculation for every Image Scale pixel. Other options are $Optimal$ (Default) and Low (Fast). Every density step down reduces number of points by 4, making processing faster yet effects in less dense point cloud generation.

- Minimum Number of Matches,

  The option allows selecting number of valid re-projections of each 3D point. Available options: *2, 3, 4, 5, 6*. Default option is *4*, meaning that 3D point has to be correctly re-projected in at least 4 images. For the project *4* was used. Higher numbers reduce noise and improve quality of the point cloud, but might compute less 3D points in the final point cloud. The highest numbers of Minimum Matches are recommended for imagery projects with very high overlap.

To reduce processing of unnecessary area located around the tower and significantly reduce processing time Processing Area was set to cover the tower structure and few meter margin.

This stage of post processing takes the longest time and requires high hardware resources. For selected options, process of densification took 1,5 hour.

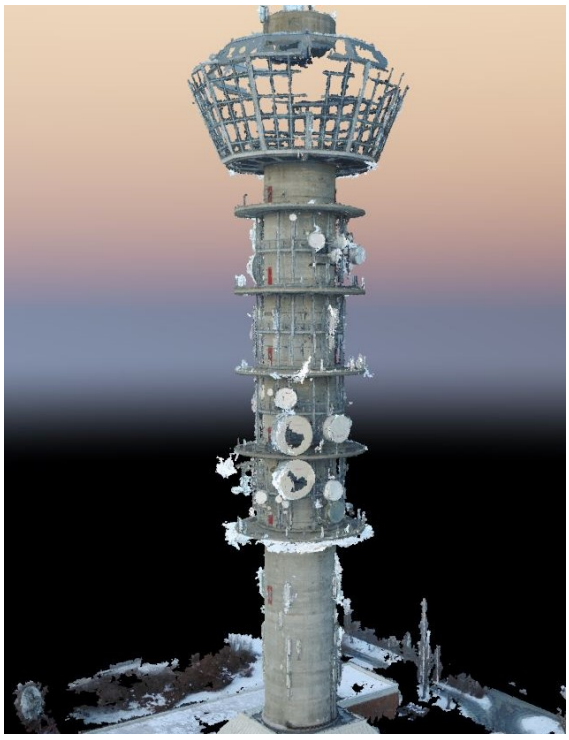

Figure 3.14 Generated Dense Point Cloud, Pix4Dmapper Pro

Due to considerable number of small, protruding elements like aerials' power cables, chains and rods, obtained point cloud contains a lot of noises or outliers – faulty positioned points detached from any surface around, not representing any real-life structure.

After changing minimum number of Minimum Number of Matches to *5*, point cloud was considerably sparser and even though part of outliers remained. Because of that, Point cloud with *4* matches was chosen.

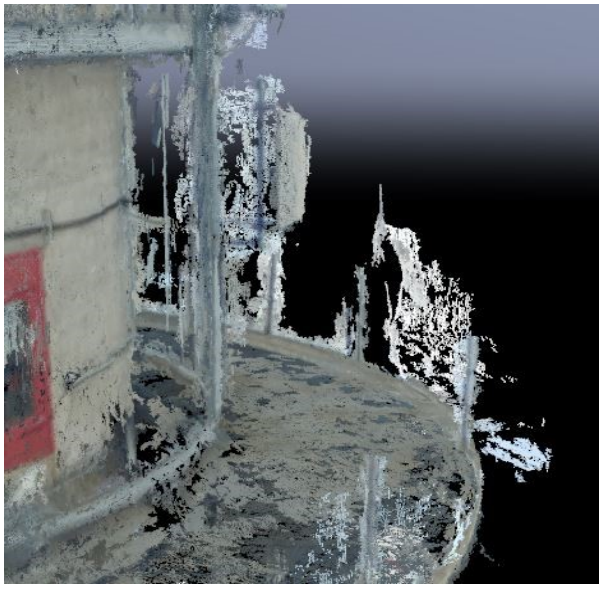

Figure 3.15 Point cloud outliers, Minimum 4 Matches

Figure 3.16 Point cloud outliers, Minimum 5 Matches

It is possible to edit obtained point cloud in Pix4D by manual editing but it seems very basic, therefore point cloud was processed in external software. For the purpose CloudCompare, software was used.

Because the point cloud contained a lot of outliers and discontinuities in obstructed by aerials places, results needed to be edited and therefore step 3 DSM, Orthomosaic and Index was not proceeded.

While working with the software it was clearly visible that the software is designated for processing UAV-obtained data. Processing options included many features helping adjust producing process concerning used hardware, object type, required accuracy. The software is very intuitive and transparent. Total work with the software took 1,5 hours of operator time and total 2 hours of computer processing.

Worth mentioning, is also a fact that the producer provides support section that contains Pix4D mapper Pro manual, users' forum and many legible and complete articles, that help users

serving the software. That significantly reduces time spent on processing and gives possibility for the best model producing.

3.4.2. Agisoft PhotoScan Professional

The software developed by Agisoft LCC, Research Company founded in 2006 in Russia. It provides tools for 3D reconstruction, visualization, surveying and mapping tasks. With the software, it is possible to generate point cloud, orthomosaic, DEM with georeference.

First thing done in the software was importing the photos and loading camera position from EXIF meta-data. Because camera positions were stored in WGS 84 coordinate system and output coordinate system was set as NTM, coordinates of the photos were transformed with use of one of the provided tools.

After importing camera coordinates, roughly analyse of their position is possible.

Next step of processing is photo alignment; this is a process of analysing photos content, finding matches and creating sparse point cloud. Available options allow setting:

- Accuracy:

  Accuracy level of obtaining camera position estimators. Levels are correlated with scaling of photo for tie points localization. *Highest* was chosen, it corresponds with upscaling the photos by 4 and thus prolonged processing. Other options are: *High* (Original size), *Medium* (Downscaled by 4), *Low* (Downscaled by 16), *Lowest* (Downscaled by 64). The lower the level the lower the accuracy of finding tip-points and faster processing.

- Pair preselection:

  Process of selection subsets of image pairs to be processed in order to speed up the process, is realised with use of the options:

  Generic – method of selecting overlapping pairs of photos based on matching photos with lower accuracy setting first.

  Reference – overlapping pairs of photos are selected basing on camera locations meta-data.

Key point and tie point limit are responsible for amount of points on every image, taken into account during processing and number of matching points for every image. Inappropriate limit

value of tie points can cause lacks in dense point cloud coverage. Values were set as recommended.

It is possible to initially check the position of photos and make corrections if necessary after the process.

Control points RMSE.

Count	X error (cm)	Y error (cm)	Z error (cm)	XY error (cm)	Total (cm)
10	0.589847	1.76451	2	1.86049	2.73156

Check points RMSE.

Count	X error (cm)	Y error (cm)	Z error (cm)	XY error (cm)	Total (cm)
6	1.17856	1.6341	2.36411	2.01477	3.10617

Table 12 Quality report, GCPs and Check Points, Agisoft Photoscan Pro

Check Points' RMSE values correspond with GCPs' values reaffirming model creating accuracy. Complete report of aerotriangulation is provided in Appendix C.

Once the photos alignment is finished process of georefencing can be started. It requires placing markers (pointing GCPs on the photos) and importing coordinates of the points. Even though, preliminary position of GCPs was known, thanks to photos alignment, marking process required much attention and labour. Automatically projected preliminary points location not always were in correct position and there was necessity for reviewing photos and editing.

GCPs and checkpoints were selected the same way as in Pix4D for comparison purposes.

For better accuracy results camera optimization was performed. This step provides better internal orientation, external orientation and distortion parameters.

To reduce unnecessary processing bounding box was set. As with processing in Pix4D, it was set to include the tower and its vicinity.

Next step in data processing was creating dense point cloud.

While setting the dense point cloud generation, Quality and Depth filtering factors can be adjusted.

Quality factor is correlated with size of photo taken in the processing stage, *Ultra high* option corresponds with processing of original photos and each subsequent level is downscaled by 4 (each side of the photo by 2). *Ultra high* setting provides the most accurate and detailed geometry but requires long time of processing. The parameter was set as *Ultra High*.

Depth filtering allows sorting out the outliers, badly reprojected points, caused by noise or badly focused photos. The software provides 3 modes of filtering: *Aggressive, Moderate, Mild*.

Each mode is provided for different projects. *Mild* if for objects with number of meaningful details and edges.

Aggressive mode is for projects without spatially distinguishable small detail. *Moderate* mode brings results in between *Mild* and *Aggressive* modes. Quality of the process was set as *Ultra High* and Depth filtering as *Mild*. Obtained point cloud was revised, and exported for future analyses.

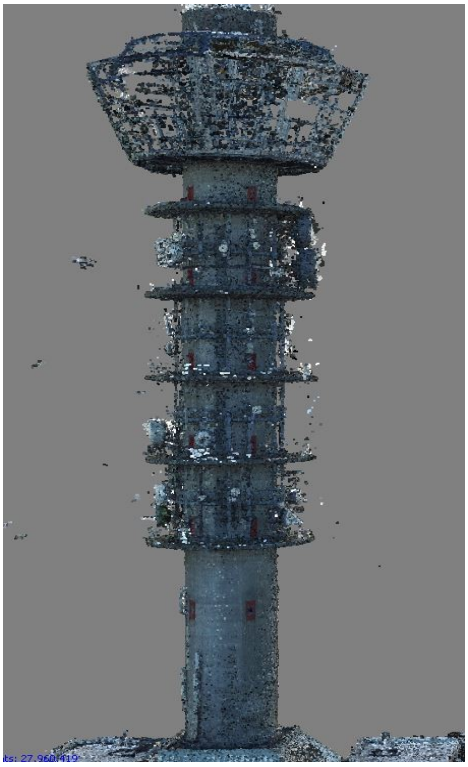

Figure 3.17 Generated Dense Point Cloud, Agisoft PhotoScan Professional

Whole work with the software took 2 hours of work hours and 2 hours of computer processing.

3.4.3. Bentley ContextCapture

It is a software developed in 2011 by Bentley Systems Inc. The company develops set of products for broad spectrum of infrastructure roles e.g. engineers, contractors, architects, inspectors etc. ContextCapture is a photogrammetry-based reality modelling software for all types of infrastructure projects. It allows processing, editing and presenting obtained results.

For the processing ConextCapture Desktop edition, v4.4.5.33 was used.

Workflow in the programme can be described as three-step process:

- Data block management
- Reconstruction
- Production

Each project is presented as block of data related with processed project. It manages collection of photos and their properties, point clouds, survey data (GCPs) and additional data. Photos by default are imported with their preliminary position thanks to attached EXIF metadata. GCPs coordinates were also imported. It is possible to view imported block of photos and initially check its arrangement in 3D view window.

In order to calculate photos' mutual relations and camera calibration, aerotriangulation process was started. It is possible to control aerotriangulation process with setting method of placing and orienting the block. Depending on available data and its properties, following methods of geolocation are available:

- *Arbitrary*: Arbitrary block position and orientation,

- *Automatic vertical*: Vertical direction is set with use of photo orientation. Scale and heading remain arbitrary.

- *Use positioning constraints on user tie points*: Rigid orientation is available thanks to user-defined constraints.

- *Use photo-positioning metadata for adjustment*: Accurate adjustment with use of accurate photos position data.

- *Use photo-positioning metadata for rigid registration*: Rigid adjustment with use of inaccurate photos position data.

- *Use control points for adjustment*: Accurate adjustment with use of accurate control points,

- *Use control points for rigid registration*: Rigid adjustment with use of inaccurate control points.

The software allows defining aerotriangulation setting such as: Keypoints density, Pair selection mode (method of computing tie points pairs), Component construction mode, Camera calibration parameters.

Unfortunately software wasn't able to reconstruct model basing on camera positions so initial orientation for easing marking process aerotriangulation with use of poses of the photos and camera calibration was not possible.

Aerotriangulation was performed with use of marked accurate GCPs and *High* variant of Key points density. Once all GCPs were marked on all visible photos, six of them were used as checkpoints and were chosen the same as before for results comparing. Camera calibration was set in *OnePass* estimation mode and every parameter of distortion was set to be adjusted. Full report of aerotriangulation is provided in Appendix D.

No.	Cat.	Check Point	Hor. acc. [m]	Vert. acc [m]	No of photos	RMS of reprojection errors [px]	RMS of distances to rays [m]	RMS of 3D errors [m]	RMS of horizontal errors [m]
11	Full		0.015	0.015	18	1,88	0.048	0.027	0.022
12	Full	x	0.015	0.015	12	3,55	0.056	0.027	0.015
13	Full		0.015	0.015	17	1,89	0.047	0.024	0.014
14	Full	x	0.015	0.015	15	1,82	0.048	0.020	0.016
15	Full		0.015	0.015	14	0,99	0.032	0.014	0.014
21	Full	x	0.007	0.007	18	2,53	0.034	0.023	0.015
22	Full		0.015	0.015	13	1,72	0.028	0.022	0.016
23	Full	x	0.015	0.015	16	3,46	0.030	0.038	0.022
24	Full		0.015	0.015	17	1,18	0.034	0.015	0.015
25	Full		0.015	0.015	13	0,89	0.026	0.009	0.005
26	Full		0.015	0.015	13	0,44	0.028	0.005	0.004
31	Full		0.008	0.010	18	0,39	0.034	0.004	0.003
32	Full		0.008	0.010	9	0,95	0.022	0.013	0.013
33	Full	x	0.008	0.010	13	1,7	0.030	0.016	0.015
34	Full		0.008	0.009	15	0,55	0.028	0.009	0.008
35	Full	x	0.015	0.012	15	2,45	0.047	0.029	0.023
							RMS Mean [m]		
							GCPs	**0.0142**	**0.0114**
							Check P.	**0.0255**	**0.0176**

Figure 3.18 Quality report, GCPs and Check Points, Bentley ContextCapture

The software did good job in model creating, and Check Points values of RMS seems to acknowledge that.

Once that was made Reconstruction menu could be entered. It allows setting boundaries of processing area what was done as in previous programmes. In processing settings Geometric

precision was set to *Ultra* what provided the most detailed point cloud. 3D point cloud producing options does not allow skipping Geometric simplification and holes filling what results in 3D point cloud surface being significantly smoothened. Because user manual provided by creator does not give comprehensive information about settings properties and influence on result, they had to be tested and manipulated with regard to observed results.

After setting all parameters, production process can be stared. It allows generating: 3D mesh, 3D point cloud, Orthophoto/DSM, 3D mesh for retouching, Reference 3D model only.

For purposes of the project, 3D point cloud was used. The software processed data for 3 hours, and generated very dense point cloud without outliers. However, created model was is good either. Its surface is considerably smoothened what causes major misinterpretation of the model.

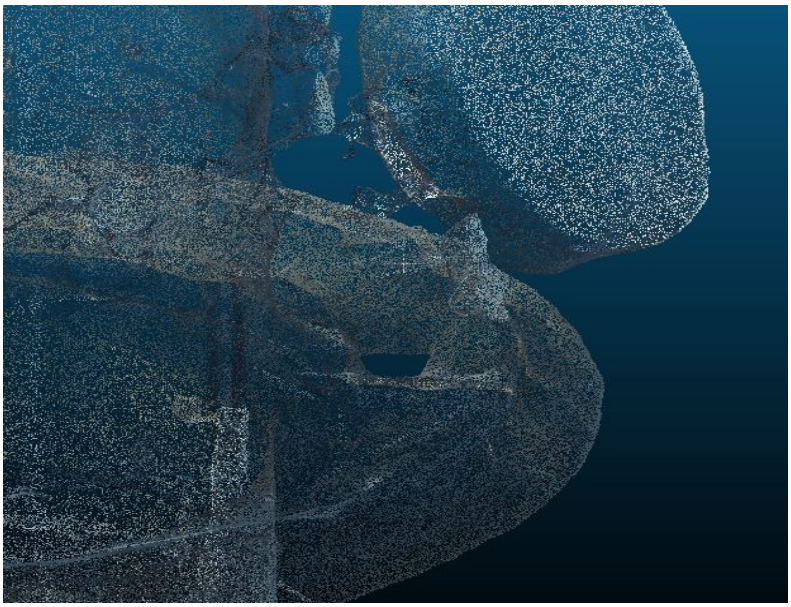

Figure 3.19 Deformed surrounding of holes in point cloud surface, ContextCapture

The software's holes filling option, which could not be disabled, created smoothened surface with high degree of displacements and glitches. Many details seems to be omitted.

Provided user guide does not provide comprehensive information about parameters of the reconstruction and used algorithms.

4. Results

As an outcome of the study, five data sets were obtained. Each one of them represents one method of spatial data acquisition or different software used for the processing. In the process, following sets of points were collected:

1. Total station positioning cross-sections,
2. Laser scanning point cloud,

Point clouds, obtained with use of:

3. Pix4Dmapper Pro,
4. Agisoft Photoscan Professional,
5. Bentley ContextCapture.

Each method of data collection has its specifics that needs to be considered when planning data collection. While planning data collection it is necessary to take into consideration factors like:

- Type of structure to be measured,
- Desired accuracy of data,
- Surroundings of the object,
- Weather conditions,
- Cost of the methods,
- Delivery time,

Etc…

All these factors influence choice of method to be used, and workflow.

4.1. Total station measurements

Classical land surveying instruments are well-developed structures. Nowadays, theirs precision performance can be much higher than humans' perception abilities, making it major cause of measurement errors. When properly prepared and executed this method provides the most accurate results.

In order to perform polar and distance measurements, visual sight line from a station to desired point is required. This condition demands appropriate planning of stations, which entails establishing control network, and performing preparation works. In order to measure complicated shape object many station are required. Performing long, complicated

measurement stages, requires experience and focus of an observer. These reasons and necessity of manual manipulation of measuring device makes it very time consuming method.

The method is the least depending on the weather condition compared to two others. Precipitation marginally influences the device, but it is necessary to notice that wet surface of measured object changes its reflectivity properties and can cause significant aberrations. Insolation also does not influence the measuring method, but high warming of objects in vicinity of line of sight causing refractions. This needs to be taken into account when measuring in developed areas with objects generating or emitting heat.

Nevertheless, when executed properly produces robust data set, consisting of only necessary features for future analyses. For successive process, it is necessary to know objectives of the analysis, and which elements need to be measured, to meet its goals.

For this project, total station measured points were distributed as horizontal cross-sections of the tower's body. Points were measured ~10 cm below edges of the balconies to avoid distance miss-measurements caused by size of measuring dot. 210 points were measured, providing test-field of enough quantity. The points' localization provides demanding check of accuracy for other methods.

The dataset is considered as the most accurate and its accuracy is o the same level as GCPs' (horizontal: 4mm, vertical: 3mm). 3D accuracy is calculated with use of formula for polar measurements uncertainty. Cross sections' points were obtained with 5mm accuracy.

Measured cross-section points could serve tower inclination measurement, as-built installation documentation and

Measuring process took 2 hours.

4.2. Laser scanning

Laser scanning is based on total station method yet its properties significantly differs it from progenitor. The method is about performing autonomous dense polar measurements, within chosen measuring window.

Depending on sort of used device, results vary. Accuracy of obtained data depends on device grade, method of measurement and weather conditions. For small objects with use of designated scanners, results can be on a millimetre level. For engineering structures which scanning requires many stations and registering process, results are usually on low centimetre level.

When scheming a measurement, most important is to adjust scanning stations to objects type and its neighbourhood. Performed badly, results in holes in coverage and even impossibility of registering scans.

Whole measuring process took 4 hours, which was considerably longer than any other method. It was caused by multiple repeating “Backsight” measurement due to errors prompted by the device.

Whole software seems obsolete and required rather complicated setting up procedure what lead to conclusion that the hardware is not the best available for engineering scans especially in crowded, active environment like building site, city centre.

Before any analyses was performed, cloud was cleared with noses, such as aerials, pendant rods and outliers.

Obtained distances, significantly exceed combined 3D accuracies of Total Station and Laser Scanning points, respectively 5mm and 7mm. Situation could be caused by improper registration process for high structures, due to lack of tying points at higher levels of the structure. With no constraints above, scans are prone to tilting. It is caused by imperfections of scanner’s levelling device.

4.3. UAS-based photogrammetry

This is very developing and gaining popularity method due to its versatility and quality of obtained data.

Thanks to ability of placing camera in desired location, it is possible to obtain high point cloud coverage of complex objects. With proper overlaps of photos, appropriate placement and accuracy of GCPs, it is possible to obtain satisfying model generation. Generally, models obtained using this method cover the most of measured object and are the densest data sets.

For quality assessment, one set of photos, Ground Control Points and Check Points was used in model generation process. For comparison purposes, some of Ground Control Points were chosen as Check Points. Setting some GCPs as Check Points provided information about real difference of coordinates between automatic process of reproduction, and manually indicated points reconstruction.

The technology allows significantly shortening measuring time and creating various number of products. A computer runs post-processing of the dataset, making operator working time shortened noticeably.

4.3.1. Pix4Dmapper Pro

Work with the software was rather effortless; the producer provides staged guidelines for processing in order to obtain desired results. While working it was noticed that the software provides for modelling of spatial engineering structures, not only terrestrial structures like mapping piles, open cut mines etc. It was especially visible when initial processing was done. Created model was correct and propositions of photos for marking GCPs spot-on.

Initial processing gave good results what enabled straightforward GCPs marking process, and further productions. Quality report is generated. Global accuracy of points is on 30 mm level. While inspecting obtained point cloud, high coverage of the object is visible, but there are some places with noticeable holes. Coverage of created model contain many noises and outliers. They mostly represent rods sticking out at rims of the balconies, and frames used for aerials attachment. Core structure of the object is precisely mapped, details are very accurately modelled and smoothing is not noticeable.

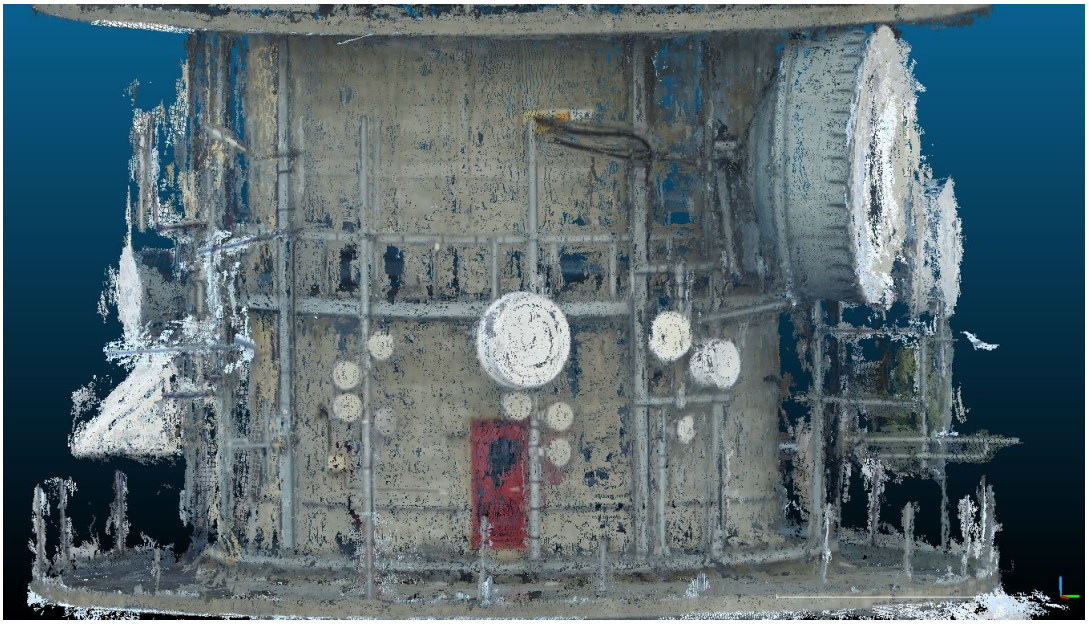

Figure 4.1 Good reconstruction of high-detailed scene, Pix4Dmapper Pro

These elements are not purpose of the study so they were deleted. Cleaning was performed manually using CloudCompare software. It required manipulating point cloud and selecting unwanted regions of points. Process of cleaning whole point cloud took 30 minutes. Results are

very satisfying, final model consist of only body of the tower and balconies. This was the dataset that was tested.

4.3.2. Agisoft Photoscan Professional

The software provides all necessary tools for spatial data creation. All necessary information, such as used photos, GCPs, marks are displayed in a main window. Processing workflow needs to be followed and it is not such straight forward as in Pix4D. Processing settings are explained in provided manual and online forum.

When processing the data, Agisoft had some problems with interpreting the model. It was particularly noticed when marking process was conducted. Because of the model misinterpretation, in order to mark GCPs, photos had to be revised manually. Furthermore provided marking system of placing flags, representing GCPs on a photos, took a lot of time.

According to quality report generated with use of the software, global results are on 30 mm level.

Generated point cloud is good quality. Outliers are visible and there is a lot of them even far away from the object itself. The core of the tower is mapped well, but smoothing effect shows up. It influences negatively sharp edges and places where small details are. Edges of the model are slightly rounded, and electricity boxes (located usually above doors) are modelled as small bulges.

Due to number of noises and unwanted objects, point cloud was cleared manually and forwarded for analysis.

4.3.3. Bentley ContextCapture

The software has modular structure and its usage requires following specified workflow. The software is not well described and maintenance requires awareness of settings influence on obtained model. Due to this poor description of settings, there is a necessity of taking multiple attempts at the beginning, to learn how the software is dealing with particular dataset.

The software also encountered problems with analysing shape of the object and anticipating GCPs position. Marking process had to be done entirely manually, what took a lot of time.

Model reconstruction process provided results with global accuracy of

Obtained point cloud is the densest. It is mostly caused by hole-filling procedure that is not possible to be disabled. Even though it was set to fill only small holes, whole dataset is much smoothened.

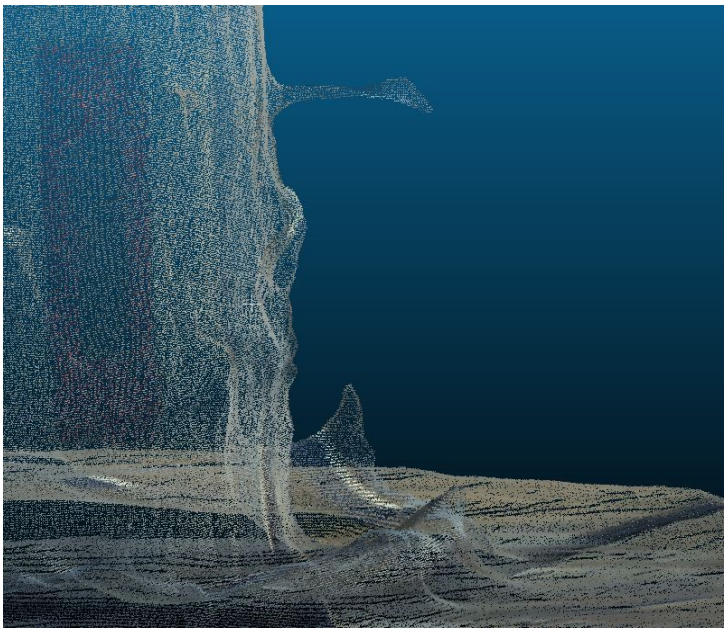

Figure 4.2 Deformed details of the tower's body, ContextCapture

This feature might be useful for ground or continuous surfaces modelling, but causes major problems when producing engineering structure model.

For the analysis purposes, the cloud needed to be cleared and recreated using photos. This process took over an hour.

4.4. Results comparison

In this part of the project, clouds are compared. Quality of producing every models was presented in previous chapter; this part revolves around comparing geometry of the datasets and its internal relations.

For comparison purposes, CloudCompare v2.8 software was used. It is an open source software for 3D point cloud processing and analyses. It allows projecting, geometric features estimation, distance calculation, filtering, mesh creating and many others.

Accuracy was checked using "*Compute Cloud/Cloud distance*". Its standard setting is calculation distance using "*Nearest Neighbour distance*", which tends to exaggerate distances due to differences in clouds' points distribution. Instead "*Local modelling*" option was used

with the most robust "*2D1/2 Triangulation"*. Other two functions "*Least Square Plane*" and "*Height function*" approximates respectively plane (for minimizing noises) and quadric (for complex shapes interpolation).

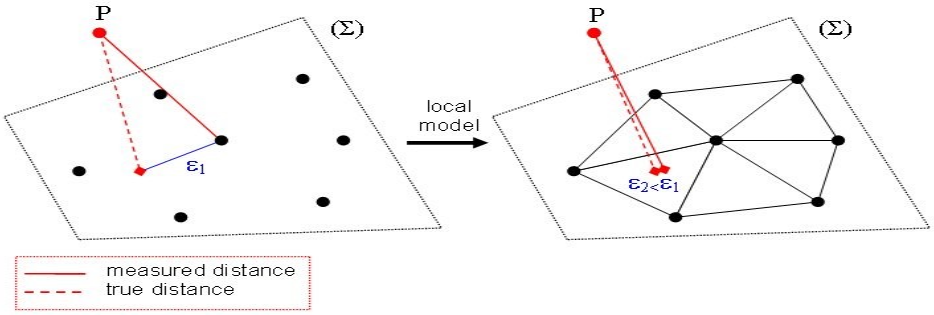

Figure 4.3 Distance calculation. Nearest Neighbour distance (left), Local modelling, 2D1/2 Triangulation (right), CloudCompare

This method gives more precise results due to more realistic projection of measured distance.

For future reference, datasets forwarded to analysis were named in following manner:

Total station cross-sections points – TS

Laser scanning point cloud – LS

Pix4D mapper Pro point cloud – P4

Agisoft Photoscan Pro point cloud – AG

Bentley ContextCapture point cloud – CC

First step of distance analysis is comparing point clouds to TS dataset.

CloudCompare manual advices use of *Compared* data set as the least quantity dataset, and others as was used, and others use as *Reference*. As a result mean distance between measured points and its' standard deviation is prompted. It is presented below.

Compared	**TS**	**Mean distance [m]**	**St. dev [m]**
Reference	LS	0.064	0.026
	P4	0.010	0.010
	AG	0.024	0.018
	CC	0.056	0.030

Table 13 Datasets comparison, distances between TS and point clouds

Results are very satisfying; they show that quality of point cloud obtaining methods are very accurate and steady. The analysis presents mainly horizontal coordinates accuracy of the point clouds because cross-section points were only distributed at the tower's cylinder body.

Unexpectedly LS gave worse results in reference to the most accurate TS. Analysing the device specification and processing workflow, this results could be caused by inadequate method of scans registering. Because "Occupation and backsight" method was used, no other than the two points were used for registering. These points were low on the ground, causing no tying point high above. Even though tilt compensation mode was turned on, some inconsistencies could appear due to instrument tilt.

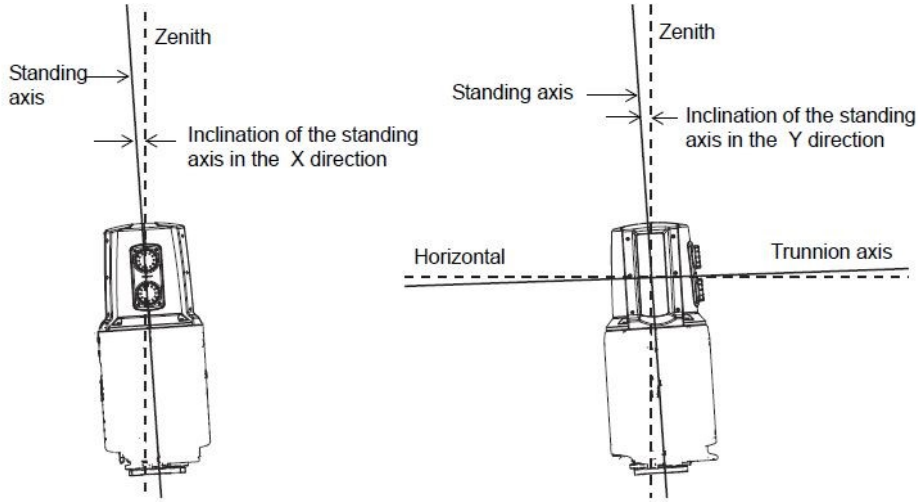

Figure 4.4 Sketch of instrument inclination

This effect could be caused by subsidence of tripod legs. Tall structures scanning is especially vulnerable for that kind of inconsistency propagation.

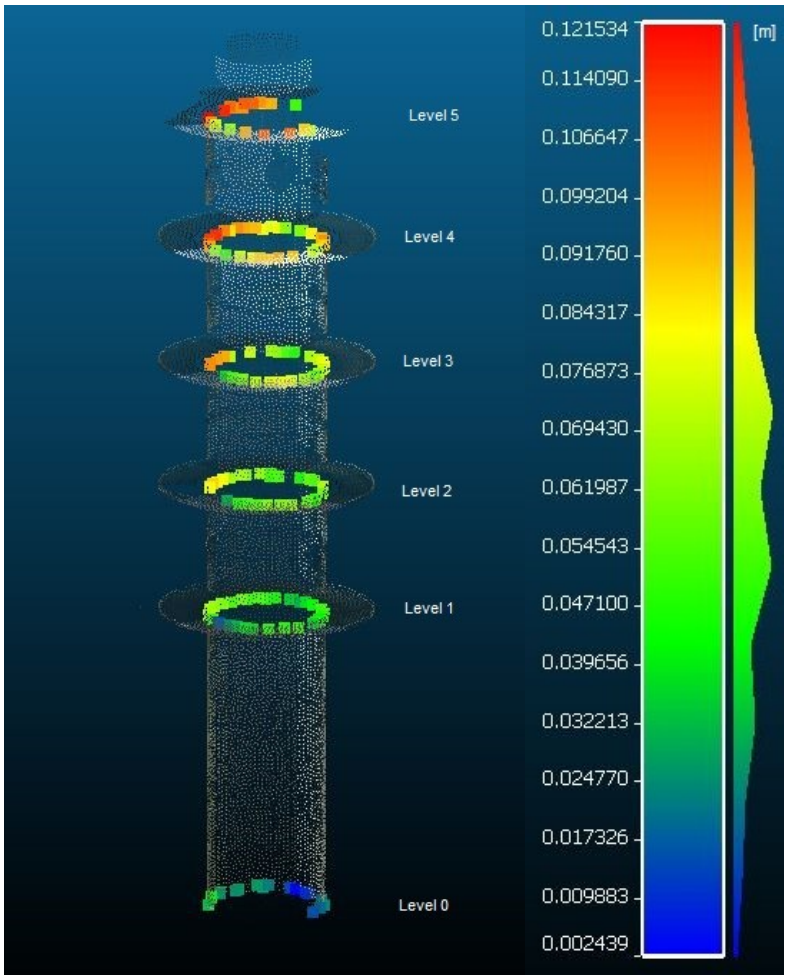

Figure 4.5 Illustration of distances calculation between TS and LS datasets

In order to examine size of the inclination distances between TS and LS point cloud were calculated separately on every level.

Level	Mean distance [m]	St. dev [m]
5	0.094	0.016
4	0.086	0.016
3	0.071	0.015
2	0.061	0.015
1	0.046	0.014
0	0.022	0.009

Table 14 Datasets comparison, distances between TS cross-sections and LS on each of the levels.

Looking at presented values of mean distances and theirs standard deviations some conclusions can be drawn. The higher the altitude the bigger the divergence. Standard deviations values are evidence of decreasing coherence of the data. The table proves that cause of such inaccurate LS dataset.

To avoid that effect, scans tying points should be placed on various heights or scanning station placed above. None of the options was possible due to used device's set and the object neighbourhood.

Photogrammetry software analysis confirms superiority of Pix4D. The software is prepared for orientated for UAS-based photographs and is compatible with many devices. Obtained results not only are the most accurate, detailed but obtaining process is well described and straightforward.

Whereas, LS provides many points on lower surface of balconies, due to small coverage of photogrammetry software, accurate calculation of distances cannot be performed.

For comparison purposes LS cloud was chosen as reference and all photogrammetry-based point clouds were compared with it. LS dataset presenting bottom surface of balconies is smooth and well formed, and its edges are firmly visible. These reasons make it good reference model for inspecting photogrammetry models. For the comparison purposes balcony with the best cover was chosen.

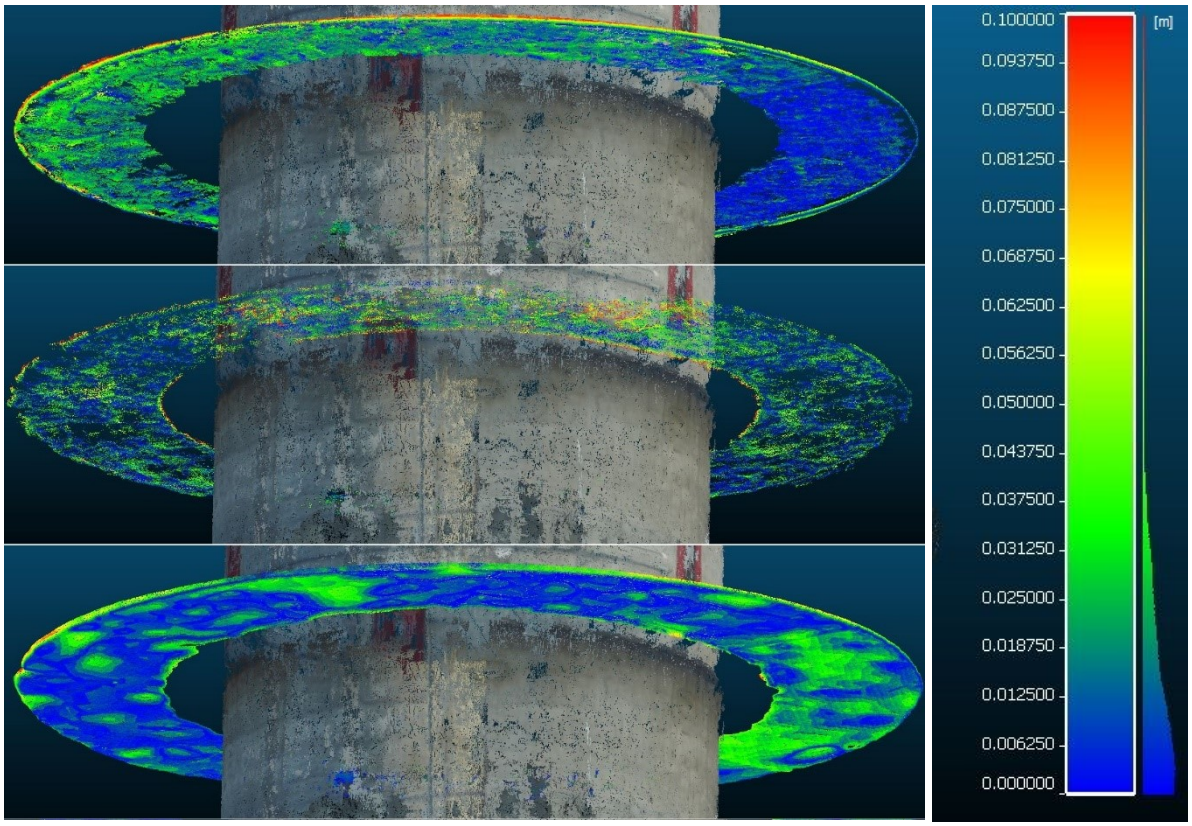

Figure 4.6 P4 (up), AG (middle), CC (bottom) cloud-to-cloud distance calculation in reference to LS, CloudCompare

Those photos confirm previously noticed phenomenon. P4 dataset presents steady and detailed surface, AG presents more bulgy model, and CC model is considerably smoothened and consist of many bulges, what is clearly visible on the photo. Distance calculation provided very similar results among all datasets. Mean distances between clouds are presented in the table below.

Compared	**LS**	**Mean distance [m]**	**St. dev [m]**
	P4	0.035	0.043
	AG	0.026	0.024
	CC	0.015	0.012

Table 15 Datasets comparison, distances between TS and point clouds

4.5. Final thoughts

When planning spatial data collection it is necessary to take into consideration many factors like: object type, desired accuracy, needed point coverage, available timeframe, etc.

Methods presented in the thesis, describe different approach for the task of engineering structures spatial data acquisition.

Total station positioning method is the most accurate and gives capability of measuring only features that need to be surveyed. However, this method is very time consuming and requires proper preparations. The method is not particularly weather dependant, but temperature, air pressure and humidity are taken in consideration in atmospheric correction calculation. Moreover, some conditions like avoidance of air refraction and dry measured surface need to be preserved for achieving high quality data.

Obtained results affirm assumptions.

Generally, laser scanning method is very useful for engineering structures modelling. It delivers a lot of information, but time of scanning is also significant. When project requires many features to be measured, this method is much more proficient than total station positioning.

It provides dense and low noise data set. However, in order to obtain high quality data, some conditions need to be fulfilled. Stations and targets need to be spread considering object type and desired coverage. It is important so place stations on a firm ground because of weight of the device and its technique of data collection.

Results seems to be corresponding with the assumptions. Unsuitable method of scans registering caused some inconsistencies, but even though scans are valuable because their internal relations are preserved.

Another aspect is consideration of size of the object. Higher buildings would not be possible to measure with use of terrestrial scanning due to high error propagation with increasing distance and elevation of object and necessity of getting away from the object.

UAS-based photogrammetry allows obtaining data with quality dependant on used sensor, flight-plan and processing software. When planning flight for engineering structure spatial data collection, it is necessary to perform field inspection. Flight arrangement requires inspecting object neighbourhood in terms of flight clearance and obstructions. Obtained results highly depend on used camera.

This method is also highly dependent on weather and environment conditions. High wind, precipitation, unstable solar activity, magnetic field variance cause impediments and even make

flight impossible to conduct. Very important is also even insolation of measured object. Due to circular characteristic of the tower, there was no possibility to avoid taking pictures against the sun. That is why for flight moment overcast sky was anticipated. This provided almost even insolation of whole object and very good reconstruction accuracy. Worth mentioning is that dimension of high structures does not influence quality of obtained results, in a way that influences other methods.

Pix4Dmapper Pro, Agisoft Professional, Bentley ContextCapture were checked on the same dataset to check its abilities of data processing.

Pix4Dmapper Pro software has proven its superiority over other ones in any consideration. It is the most comprehensive data processing tool, which provides the most accurate data when it comes to engineering structures' spatial data collection. It provided the most accurate, detailed data that covered most of the object. The software maintenance is well defined; every step and option is properly described, what makes work seamless.

Agisoft Photoscan Pro also provided high quality data, with small number of noises. Maintenance of the software requires following specific workflow and a little experience, however it is well explained and described. Final thought on the software is that it is not dedicated for structural objects.

Last tested software was ContextCapture. Processing options lacks of explanation and that is why the software requires adjusting settings with regards to obtained results. It provided correct results, but smoothing effect and low accuracy proves that it is not good software for demanding engineering structures.

4.6. Future recommendations

After completing whole process of spatial data acquisition, some concussions can be drawn.

In order to provide comprehensive accuracy check, total station measurements should be also spread on balconies to provide vertical accuracy.

Main problem with obtained terrestrial laser scanning data was caused with the registration method used. Other methods with higher number of targets would provide better results. Another way of getting better accuracy would be using cloud-to-cloud registration process. However if that was to be used, there would be necessity of increasing number of stations to provide higher scans overlaps.

For the thesis pre-installed, user-grade camera was used. In order to use higher quality camera, change of the UAV would be necessary because of low capabilities of the used DJI Phantom. This step would considerable improved quality and reduced noise.

Other way of obtaining data that are more detailed would be changing flight-plan to be located closer to measured object. Increasing overlaps would also improve quality, but it would prolong measuring time.

Bibliography

Abd. Manan Samad, N. K. (2013). The Potential of Unmanned Aerial Vehicle (UAV) for Civilian and Mapping Application.

Agisoft. (n). Agisoft Photoscan Support [http://www.agisoft.com/support/tutorials/beginner-level/].

Baltsavias, E. (1998). A comparison between photogrammetry and laser scanning.

CloudCompare User documentation [http://www.cloudcompare.org/doc/wiki/index.php?title=Main_Page]. (Accessed 02.06.2017).

F. Chiabrando, F. N. (2010). UAV and RPV systems for photogrammetric surveys in archaelogical areas: two tests in the Piedmont region (Italy).

G.Bitelli, M. D. (2004). Terrestrial laser scanning and digital photogrammetry techniques to minitor landslide bodies.

Statens kartverket, Geodesi. *Satellittbasert posisjonsbestemmelse, Versjon 2.1* Desember 2009.

Henry Eisenbeiss, M. S. (2010). Investigation of UAV systems and flight modes for photogrammetric applications.

J. Unger, M. R. (2014). UAV-based photogrammetry: monitoring of a building zone.

J.A. Gonçalves, R. H. (2013). UAV photogrammetry for topographic monitoring of coastal areas.

Kraus, K. (2007). *Photogrammetry.*

M. Sauerbier, E. S. (2011). The practical application of UAV-based photogrammetry under economic aspects.

Pix4D Support [https://support.pix4d.com/hc/en-us]. (Accessed 20.05.2017).

Rossana Gini, D. P. (2013). UAV photogrammetry: block triangulation comparisons.

Santiago Martinez, J. O. (2013). Recording complex structures using close range photogrammetry: The cathedral of Santiago de Compostela.

Sebastian Siebert, J. T. (2014). Mobile 3D mapping for surveying earthwork projects using an Unmanned Aerial Vehicle (UAV) system.

Systems, B. (2017). Bentley ContextCapture User Manual.

Zheng-Zong Tang, J. L.-X. (2012). Photogrammetry-based two-dimensional digital image correlation with nonperpendicular camera alignment.

WYRÓWNANIE ŚCISŁE PRZESTRZENNE

Wykaz punktów nawiązania

NR	X [m]	Y [m]	H [m]	mx [m]	my [m]	mp [m]	mh [m]
5	1604095.853	96659.154	108.828	0.000	0.000	0.000	0.000

Obserwacje azymutalne

Stanowisko	Cel	Azymut [g]	mAz [g]
5	4	317.1326	0.0010

Obserwacje przewyższeń niwelacyjnych

Od	Do	dH [m]	Dług. ciągu [km]	L. stan.	mdH [m]
5	4	4.587			0.005
5	7	2.279			0.005
5	3	0.332			0.005
4	6	0.550			0.005
4	2	0.254			0.005
4	1	0.378			0.005
4	5	-4.579			0.005
6	2	-0.294			0.005
6	1	-0.167			0.005
6	4	-0.545			0.005
2	1	0.127			0.005
2	4	-0.251			0.005
2	6	0.296			0.005
1	2	-0.124			0.005
1	6	0.168			0.005
1	4	-0.382			0.005
1	7	-2.681			0.005
1	3	-4.629			0.005
7	1	2.682			0.005
7	3	-1.948			0.005
7	5	-2.283			0.005
3	5	-0.335			0.005
3	7	1.944			0.005
3	1	4.622			0.005

Obserwacje pęki kierunków

Stanowisko	Cel	Kierunek [g]	mKie [g]
5	4	22.8754	0.0019
5	7	88.7845	0.0023
5	3	134.7655	0.0029
4	6	350.8562	0.0034
4	2	391.5707	0.0017
4	1	399.0553	0.0024
4	5	91.2356	0.0019
6	2	34.9303	0.0024
6	1	64.5677	0.0035
6	4	166.0344	0.0034
2	1	391.7454	0.0049
2	4	7.2418	0.0017
2	6	35.4203	0.0024
1	2	398.4499	0.0049
1	6	271.7740	0.0035
1	4	221.4417	0.0024
1	7	121.6103	0.0039
1	3	121.7903	0.0018
7	1	271.7486	0.0039
7	3	72.0851	0.0034
7	5	129.6654	0.0023
3	5	138.8685	0.0029

3	7	235.3108	0.0034
3	1	235.1541	0.0018

Obserwacje odległości zredukowanych

Stanowisko	Cel	Odległość [m]	mOdl [m]
5	4	129.248	0.006
5	7	108.333	0.006
5	3	85.292	0.006
4	6	72.305	0.006
4	2	149.057	0.006
4	1	101.698	0.006
4	5	129.246	0.006
6	2	100.756	0.006
6	1	69.874	0.006
6	4	72.306	0.006
2	1	49.518	0.006
2	4	149.056	0.006
2	6	100.750	0.006
1	2	49.523	0.006
1	6	69.876	0.006
1	4	101.699	0.006
1	7	62.008	0.006
1	3	133.717	0.006
7	1	62.005	0.006
7	3	71.721	0.006
7	5	108.328	0.006
3	5	85.298	0.006
3	7	71.724	0.006
3	1	133.716	0.006

Liczebność obserwacji

Rodzaj obserwacji	Ilość
Azymuty topograficzne	1
Kąty poziome	0
Odległości poziome	24
Przewyższenia niwelacyjne	24
Wektory GNSS	0
Kierunki poziome	24
Kąty pionowe	0
Odległości skośne	0
Ilość obserwacji nadliczbowych	48

Liczebność niewiadomych

Rodzaj	Ilość
Punktów sytuacyjnych	6
Punktów wysokościowych	6
Stałych orientacji pęku	7

Charakterystyka procesu iteracyjnego

Nr iteracji	Średnia (DX)	Max (DX)	[pll]	[pvv]	m0
1	10,257	41,641	563,3901	18,5707	0,6220046
2	0,002	0,010	18,9285	18,5688	0,6219719

Globalny test statystyczny poprawności przyjęcia błędów średnich

Poziom istotności testu	Dolna wartość krytyczna	Statystyka testowa	Górna wartość testu
95.0	30.75	18.57	69.02

! Na poziomie istotności 95.0% hipoteza m0=1 odrzucona. 0.621972<<1 !

Wykaz współrzędnych punktów po wyrównaniu

NR	X [m]	Y [m]	H [m]	mx	my	mp	mh	Elipsa	Elipsa	Elipsa

								A	B	Fi
5	1604095.853	96659.154	108.828	0.000	0.000	0.000	0.000			
4	1604130.218	96534.556	113.410	0.001	0.002	0.002	0.002	0.0021	0.0013	317.1326
3	1604172.436	96696.703	109.163	0.002	0.002	0.003	0.002	0.0022	0.0017	369.1484
2	1604273.699	96574.942	113.663	0.002	0.003	0.004	0.002	0.0034	0.0020	96.5083
1	1604224.203	96573.409	113.789	0.002	0.003	0.003	0.002	0.0026	0.0016	87.0615
7	1604200.363	96630.642	111.109	0.002	0.002	0.003	0.002	0.0022	0.0017	310.2418
6	1604197.755	96508.734	113.958	0.002	0.003	0.004	0.002	0.0027	0.0022	52.2205

Najgorzej wyznaczony punkt sytuacyjnie: 2 mp=0.004
Najgorzej wyznaczony punkt wysokościowo: 2 mh=0.002
Średniokwadratowy błąd położenia punktu: 0.0031
Średniokwadratowy błąd wysokości: 0.0018

Obserwacje azymutalne

Stanowisko	Cel	Azymut [g]	v	Az wyr	mAz wyr	mv	v/mv
5	4	317.1326	0.0000	317.1326	0.0006	0.0000	0.0

Obserwacje przewyższeń niwelacyjnych

Od	Do	dH [m]	v	dHwyr	mdHwyr	mv	v/m
5	4	4.587	-0.005	4.582	0.002	0.003	1.799
5	7	2.279	0.002	2.281	0.002	0.003	0.574
5	3	0.332	0.003	0.335	0.002	0.003	0.993
4	6	0.550	-0.003	0.547	0.002	0.003	0.981
4	2	0.254	-0.001	0.253	0.002	0.003	0.431
4	1	0.378	0.001	0.379	0.001	0.003	0.412
4	5	-4.579	-0.003	-4.582	0.002	0.003	1.263
6	2	-0.294	0.000	-0.294	0.002	0.003	0.185
6	1	-0.167	-0.001	-0.168	0.002	0.003	0.431
6	4	-0.545	-0.002	-0.547	0.002	0.003	0.853
2	1	0.127	-0.001	0.126	0.002	0.003	0.248
2	4	-0.251	-0.002	-0.253	0.002	0.003	0.670
2	6	0.296	-0.002	0.294	0.002	0.003	0.555
1	2	-0.124	-0.002	-0.126	0.002	0.003	0.853
1	6	0.168	0.000	0.168	0.002	0.003	0.064
1	4	-0.382	0.003	-0.379	0.001	0.003	1.021
1	7	-2.681	0.000	-2.681	0.002	0.003	0.033
1	3	-4.629	0.002	-4.627	0.002	0.003	0.825
7	1	2.682	-0.001	2.681	0.002	0.003	0.406
7	3	-1.948	0.002	-1.946	0.002	0.003	0.786
7	5	-2.283	0.002	-2.281	0.002	0.003	0.919
3	5	-0.335	0.000	-0.335	0.002	0.003	0.126
3	7	1.944	0.002	1.946	0.002	0.003	0.694
3	1	4.622	0.005	4.627	0.002	0.003	1.786

Obserwacje kierunkowe

Stanowisko	Cel	Kierunek [g]	v	Hz wyr	mHzwyr	mv	v/mv
5	4	22.8754	-0.0004	22.8750	0.0010	0.0007	0.7
5	7	88.7845	0.0025	88.7870	0.0010	0.0010	2.6
5	3	134.7655	-0.0021	134.7634	0.0013	0.0013	1.6
4	6	350.8562	-0.0019	350.8543	0.0013	0.0017	1.2
4	2	391.5707	-0.0009	391.5698	0.0008	0.0007	1.4
4	1	399.0553	0.0030	399.0583	0.0009	0.0012	2.5
4	5	91.2356	-0.0001	91.2355	0.0010	0.0006	0.2
6	2	34.9303	-0.0016	34.9287	0.0012	0.0009	1.8
6	1	64.5677	0.0021	64.5698	0.0014	0.0016	1.3
6	4	166.0344	-0.0006	166.0338	0.0016	0.0014	0.4
2	1	391.7454	-0.0003	391.7451	0.0016	0.0026	0.1
2	4	7.2418	-0.0003	7.2415	0.0009	0.0005	0.5
2	6	35.4203	0.0006	35.4209	0.0010	0.0011	0.5
1	2	398.4499	0.0046	398.4545	0.0021	0.0022	2.1
1	6	271.7740	-0.0026	271.7714	0.0015	0.0016	1.7
1	4	221.4417	-0.0022	221.4395	0.0011	0.0010	2.2

1	7	121.6103	0.0001	121.6104	0.0014	0.0020	0.1
1	3	121.7903	0.0001	121.7904	0.0009	0.0006	0.2
7	1	271.7486	-0.0002	271.7484	0.0018	0.0016	0.1
7	3	72.0851	-0.0011	72.0840	0.0015	0.0015	0.7
7	5	129.6654	0.0013	129.6667	0.0012	0.0008	1.7
3	5	138.8685	0.0005	138.8690	0.0013	0.0012	0.5
3	7	235.3108	-0.0008	235.3100	0.0013	0.0017	0.5
3	1	235.1541	0.0003	235.1544	0.0009	0.0006	0.4

Obserwacje odległości zredukowanych

Stanowisko	Cel	Odległość [m]	v	HD wyr	mHD wyr	mv	v/mv
5	4	129.248	0.002	129.250	0.002	0.003	0.6
5	7	108.333	-0.003	108.330	0.002	0.003	1.0
5	3	85.292	0.001	85.293	0.002	0.003	0.4
4	6	72.305	0.000	72.305	0.002	0.003	0.1
4	2	149.057	-0.001	149.056	0.002	0.003	0.2
4	1	101.698	0.001	101.699	0.002	0.004	0.3
4	5	129.246	0.004	129.250	0.002	0.003	1.2
6	2	100.756	-0.004	100.752	0.002	0.003	1.2
6	1	69.874	0.000	69.874	0.002	0.004	0.1
6	4	72.306	-0.001	72.305	0.002	0.003	0.2
2	1	49.518	0.002	49.520	0.002	0.003	0.6
2	4	149.056	0.000	149.056	0.002	0.003	0.1
2	6	100.750	0.002	100.752	0.002	0.003	0.5
1	2	49.523	-0.003	49.520	0.002	0.003	0.9
1	6	69.876	-0.002	69.874	0.002	0.004	0.7
1	4	101.699	0.000	101.699	0.002	0.004	0.0
1	7	62.008	-0.008	62.000	0.002	0.003	2.5
1	3	133.717	0.004	133.721	0.002	0.003	1.1
7	1	62.005	-0.005	62.000	0.002	0.003	1.6
7	3	71.721	0.001	71.722	0.002	0.003	0.2
7	5	108.328	0.002	108.330	0.002	0.003	0.5
3	5	85.298	-0.005	85.293	0.002	0.003	1.4
3	7	71.724	-0.002	71.722	0.002	0.003	0.7
3	1	133.716	0.005	133.721	0.002	0.003	1.4

Quality Report

Important: Click on the different icons for:

Help to analyze the results in the Quality Report

Additional information about the sections

Click here for additional tips to analyze the Quality Report

Summary

Project	molp_project_2_free_min4_check6
Processed	2017-05-23 14:38:27
Camera Model Name(s)	FC300X_3.6_4000x3000 (RGB)
Average Ground Sampling Distance (GSD)	31.12 cm / 12.25 in
Time for Initial Processing (without report)	46m:10s

Quality Check

Images	median of 23353 keypoints per image	✓
Dataset	150 out of 150 images calibrated (100%), all images enabled	✓
Camera Optimization	1.23% relative difference between initial and optimized internal camera parameters	✓
Matching	median of 11359.7 matches per calibrated image	✓
Georeferencing	yes, 10 GCPs (10 3D), mean RMS error = 0.005 m	✓

Calibration Details

Number of Calibrated Images	150 out of 150
Number of Geolocated Images	150 out of 150

Initial Image Positions

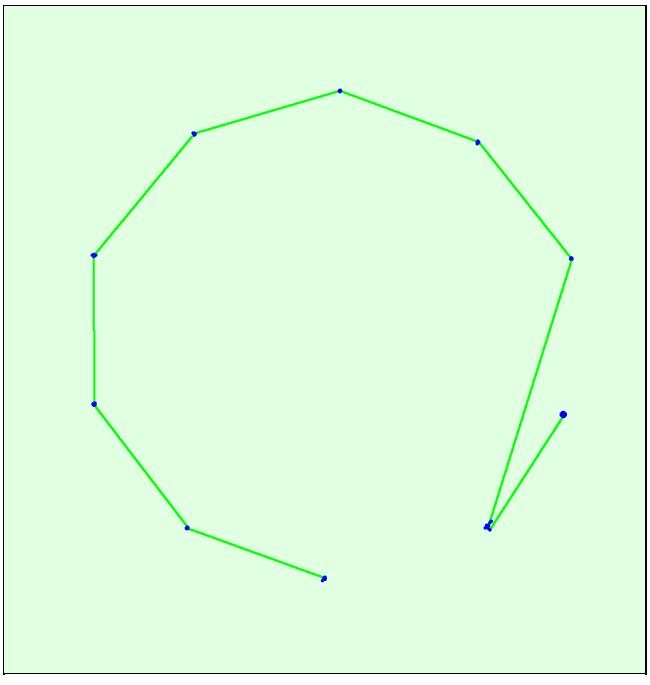

Figure 2: Top view of the initial image position. The green line follows the position of the images in time starting from the large blue dot.

Computed Image/GCPs/Manual Tie Points Positions

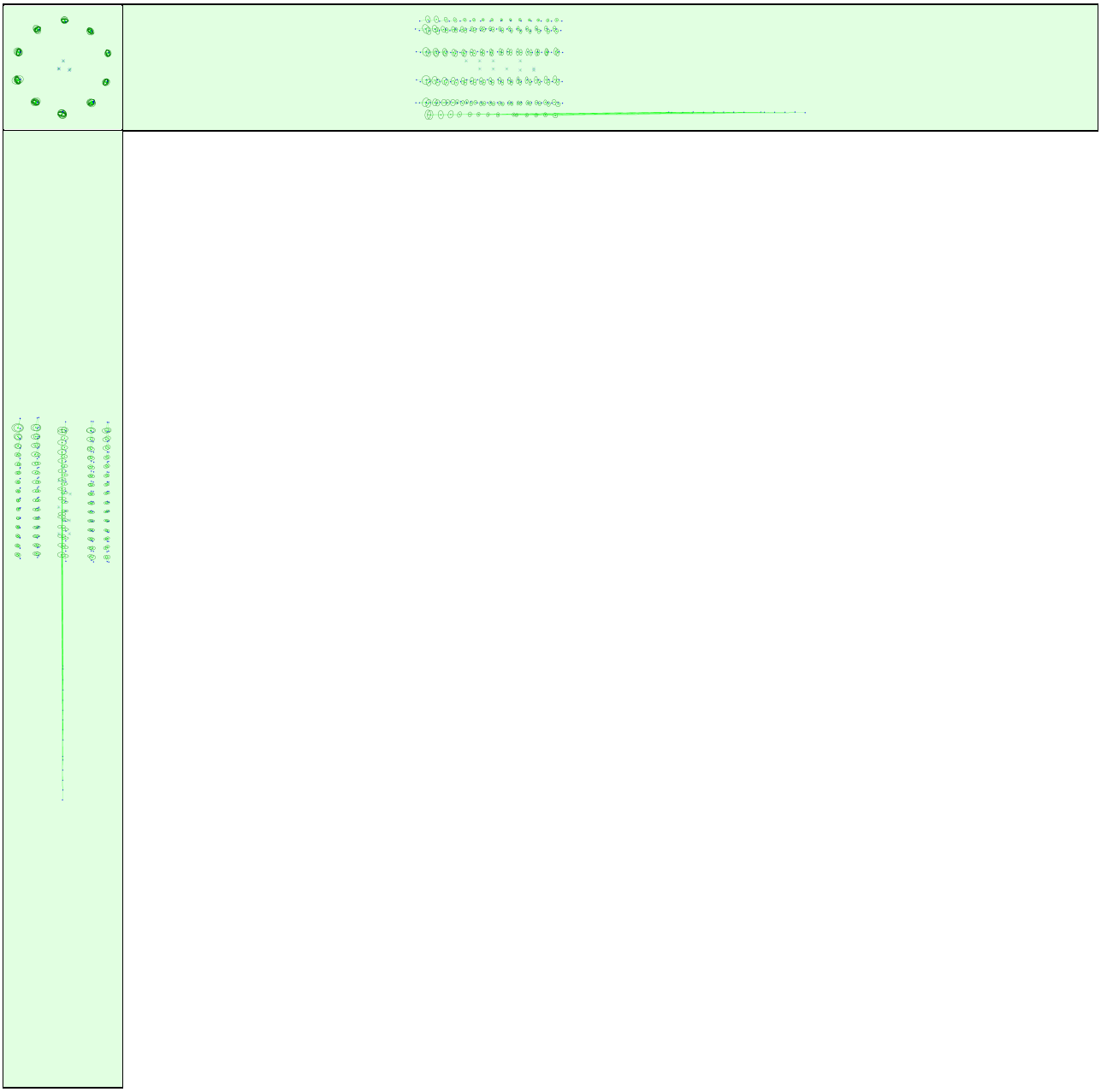

Uncertainty ellipses 100x magnified

Figure 3: Offset between initial (blue dots) and computed (green dots) image positions as well as the offset between the GCPs initial positions (blue crosses) and their computed positions (green crosses) in the top-view (XY plane), front-view (XZ plane), and side-view (YZ plane). Dark green ellipses indicate the absolute position uncertainty of the bundle block adjustment result.

Absolute camera position and orientation uncertainties

	X [m]	Y [m]	Z [m]	Omega [degree]	Phi [degree]	Kappa [degree]
Mean	0.017	0.017	0.010	0.081	0.046	0.011
Sigma	0.005	0.004	0.003	0.062	0.002	0.002

Bundle Block Adjustment Details

Number of 2D Keypoint Observations for Bundle Block Adjustment	1466982
Number of 3D Points for Bundle Block Adjustment	418077
Mean Reprojection Error [pixels]	0.262

Internal Camera Parameters

FC300X_3.6_4000x3000 (RGB). Sensor Dimensions: 6.317 [mm] x 4.738 [mm]

EXIF ID: FC300X_3.6_4000x3000

	Focal Length	Principal Point x	Principal Point y	R1	R2	R3	T1	T2
Initial Values	2285.722 [pixel] 3.610 [mm]	2000.006 [pixel] 3.159 [mm]	1500.003 [pixel] 2.369 [mm]	-0.014	0.013	-0.000	0.001	0.000
Optimized Values	2313.859 [pixel] 3.654 [mm]	2002.915 [pixel] 3.163 [mm]	1529.326 [pixel] 2.415 [mm]	-0.010	0.009	0.004	0.002	0.000
Uncertainties (Sigma)	0.417 [pixel] 0.001 [mm]	0.318 [pixel] 0.001 [mm]	1.165 [pixel] 0.002 [mm]	0.000	0.001	0.001	0.000	0.000

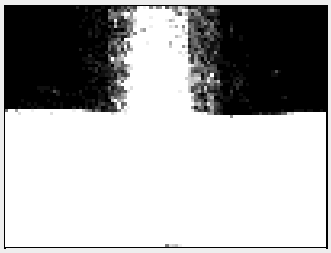

The number of Automatic Tie Points (ATPs) per pixel, averaged over all images of the camera model, is color coded between black and white. White indicates that, on average, more than 16 ATPs have been extracted at the pixel location. Black indicates that, on average, 0 ATPs have been extracted at the pixel location. Click on the image to the see the average direction and magnitude of the re-projection error for each pixel. Note that the vectors are scaled for better visualization.

2D Keypoints Table

	Number of 2D Keypoints per Image	Number of Matched 2D Keypoints per Image
Median	23353	11360
Min	16441	1407
Max	34465	15225
Mean	23735	9780

3D Points from 2D Keypoint Matches

	Number of 3D Points Observed
In 2 Images	232079
In 3 Images	66626
In 4 Images	36385
In 5 Images	23088
In 6 Images	15597
In 7 Images	11044
In 8 Images	8320
In 9 Images	6200
In 10 Images	4559
In 11 Images	3437
In 12 Images	2652
In 13 Images	1873
In 14 Images	1240
In 15 Images	971
In 16 Images	753
In 17 Images	632
In 18 Images	566
In 19 Images	438
In 20 Images	419
In 21 Images	337
In 22 Images	270
In 23 Images	211

In 24 Images	144
In 25 Images	89
In 26 Images	62
In 27 Images	46
In 28 Images	18
In 29 Images	10
In 30 Images	6
In 31 Images	2
In 32 Images	2
In 34 Images	1

2D Keypoint Matches

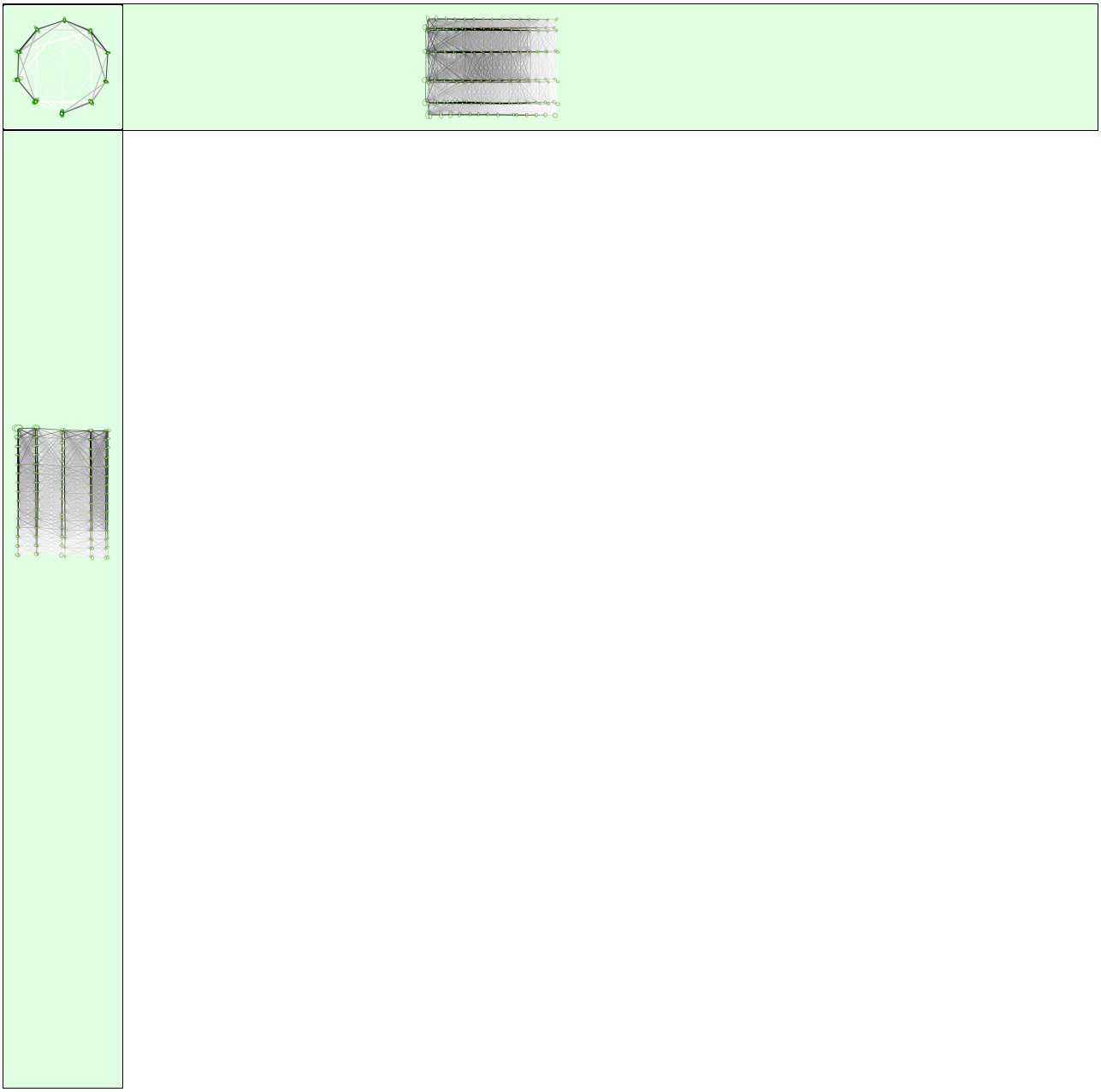

Figure 5: Computed image positions with links between matched images. The darkness of the links indicates the number of matched 2D keypoints between the images. Bright links indicate weak links and require manual tie points or more images. Dark green ellipses indicate the relative camera position uncertainty of the bundle block adjustment result.

Relative camera position and orientation uncertainties

	X [m]	Y [m]	Z [m]	Omega [degree]	Phi [degree]	Kappa [degree]
Mean	0.009	0.008	0.007	0.045	0.016	0.009
Sigma	0.004	0.004	0.003	0.028	0.005	0.003

Geolocation Details

Ground Control Points

GCP Name	Accuracy XY/Z [m]	Error X [m]	Error Y [m]	Error Z [m]	Projection Error [pixel]	Verified/Marked
11 (3D)	0.015/ 0.015	-0.008	0.003	0.007	0.502	21 / 21
13 (3D)	0.015/ 0.015	-0.006	-0.009	0.002	0.382	16 / 16
15 (3D)	0.015/ 0.015	-0.009	-0.013	-0.007	0.352	14 / 14
22 (3D)	0.015/ 0.015	0.008	0.007	-0.010	0.469	16 / 16
24 (3D)	0.015/ 0.015	0.006	0.009	0.001	0.432	20 / 20
25 (3D)	0.015/ 0.015	-0.005	0.003	-0.004	0.409	15 / 15
26 (3D)	0.015/ 0.015	0.003	-0.002	0.000	0.498	20 / 20
31 (3D)	0.008/ 0.010	-0.000	-0.002	0.002	0.421	24 / 24
32 (3D)	0.008/ 0.010	0.002	-0.002	-0.002	0.407	9 / 9
34 (3D)	0.008/ 0.009	0.003	0.004	0.003	0.407	18 / 18
Mean [m]		-0.000596	-0.000227	-0.000611		
Sigma [m]		0.005687	0.006566	0.004784		
RMS Error [m]		0.005718	0.006570	0.004823		

0 out of 6 check points have been labeled as inaccurate.

Check Point Name	Accuracy XY/Z [m]	Error X [m]	Error Y [m]	Error Z [m]	Projection Error [pixel]	Verified/Marked
12	0.0150/0.0150	-0.0154	0.0030	0.0113	0.5009	13 / 13
14	0.0150/0.0150	-0.0023	0.0036	0.0014	0.3321	15 / 15
21	0.0070/0.0070	0.0046	0.0155	-0.0099	0.3379	16 / 16
23	0.0150/0.0150	0.0052	0.0059	-0.0258	0.3415	20 / 20
33	0.0080/0.0100	-0.0160	-0.0108	0.0026	0.4489	19 / 19
35	0.0150/0.0120	0.0291	0.0127	0.0110	0.3646	20 / 20
Mean [m]		0.000857	0.004988	-0.001575		
Sigma [m]		0.015225	0.008426	0.012952		
RMS Error [m]		0.015250	0.009791	0.013047		

Localisation accuracy per GCP and mean errors in the three coordinate directions. The last column counts the number of calibrated images where the GCP has been automatically verified vs. manually marked.

Absolute Geolocation Variance

Min Error [m]	Max Error [m]	Geolocation Error X [%]	Geolocation Error Y [%]	Geolocation Error Z [%]
-	-15.00	0.00	0.00	0.00
-15.00	-12.00	0.00	0.00	0.00
-12.00	-9.00	0.00	0.00	0.00
-9.00	-6.00	0.00	0.00	0.00
-6.00	-3.00	0.00	0.00	12.59
-3.00	0.00	57.04	44.44	36.30
0.00	3.00	42.96	55.56	38.52
3.00	6.00	0.00	0.00	12.59
6.00	9.00	0.00	0.00	0.00
9.00	12.00	0.00	0.00	0.00
12.00	15.00	0.00	0.00	0.00
15.00	-	0.00	0.00	0.00
Mean [m]		0.842335	0.138404	1.576570

Sigma [m]	0.340985	0.426917	2.418802
RMS Error [m]	0.908735	0.448792	2.887244

Min Error and Max Error represent geolocation error intervalsbetween -1.5 and 1.5 times the maximum accuracy of all the images. Columns X, Y, Z show the percentage of images with geolocation errors within the predefined error intervals. The geolocation error is the difference between the intial and computed image positions. Note that the image geolocation errors do not correspond to the accuracy of the observed 3D points.

Geolocation Bias	X	Y	Z
Translation [m]	0.842219	0.138569	1.576510

Bias between image initial and computed geolocation given in output coordinate system.

Relative Geolocation Variance

Relative Geolocation Error	Images X [%]	Images Y [%]	Images Z [%]
[-1.00, 1.00]	100.00	100.00	100.00
[-2.00, 2.00]	100.00	100.00	100.00
[-3.00, 3.00]	100.00	100.00	100.00
Mean of Geolocation Accuracy [m]	5.000000	5.000000	10.000000
Sigma of Geolocation Accuracy [m]	0.000000	0.000000	0.000000

Images X, Y, Z represent the percentage of images with a relative geolocation error in X, Y, Z.

Geolocation Orientational Variance	RMS [degree]
Omega	0.529
Phi	6.811
Kappa	1.215

Geolocation RMS error of the orientation angles given by the difference between the initial and computed image orientation angles.

Initial Processing Details

System Information

Hardware	CPU: Intel(R) Xeon(R) CPU E5-2670 v2 @ 2.50GHz RAM: 32GB GPU: NVIDIA Quadro K5000 (Driver: 10.18.13.5362)
Operating System	Windows 10 Education, 64-bit

Coordinate Systems

Image Coordinate System	WGS84 (egm96)
Ground Control Point (GCP) Coordinate System	ETRS89 / NTM zone 10 (egm96)
Output Coordinate System	ETRS89 / NTM zone 10 (egm96)

Processing Options

Detected Template	No Template Available
Keypoints Image Scale	Full, Image Scale: 1
Advanced: Matching Image Pairs	Free Flight or Terrestrial
Advanced: Matching Strategy	Use Geometrically Verified Matching: yes
Advanced: Keypoint Extraction	Targeted Number of Keypoints: Automatic
Advanced: Calibration	Calibration Method: Standard Internal Parameters Optimization: All External Parameters Optimization: All Rematch: Auto, yes Bundle Adjustment: Classic

Point Cloud Densification details

Processing Options

Image Scale	multiscale, 1 (Original image size, Slow)
Point Density	High (Slow)
Minimum Number of Matches	4
3D Textured Mesh Generation	no
Advanced: Matching Window Size	9x9 pixels
Advanced: Image Groups	group1
Advanced: Use Processing Area	yes
Advanced: Use Annotations	yes
Advanced: Limit Camera Depth Automatically	yes
Time for Point Cloud Densification	01h:28m:54s

Results

Number of Processed Clusters	2
Number of Generated Tiles	1
Number of 3D Densified Points	30597403
Average Density (per m^3)	330.33

Appendix C

molp_report_6check_front

Processing Report

25 May 2017

Survey Data

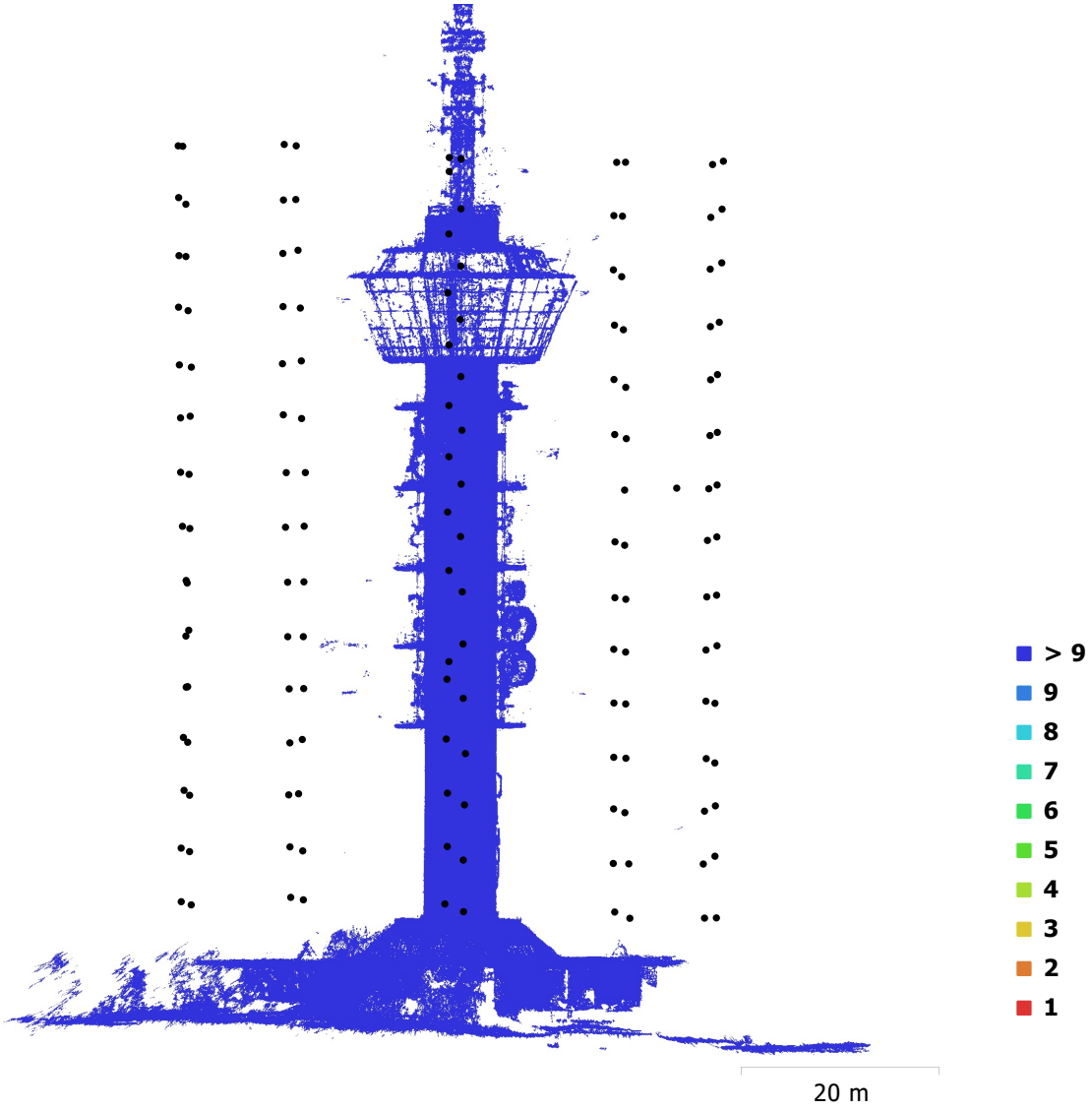

Fig. 1. Camera locations and image overlap.

Number of images:	150	Camera stations:	150
Flying altitude:	175 m	Tie points:	72,310
Ground resolution:	1.1 cm/pix	Projections:	183,236
Coverage area:	1.14e+03 m²	Reprojection error:	0.907 pix

Camera Model	Resolution	Focal Length	Pixel Size	Precalibrated
FC300X (3.61 mm)	4000 x 3000	3.61 mm	1.56 x 1.56 µm	No

Table 1. Cameras.

Camera Calibration

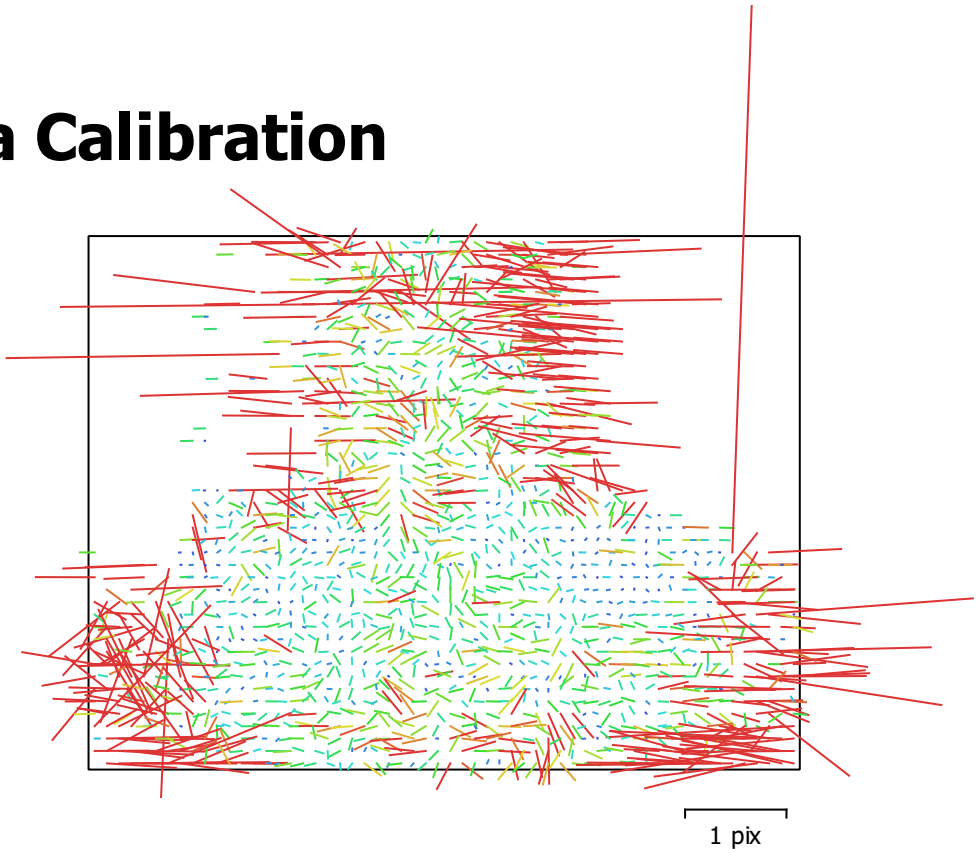

Fig. 2. Image residuals for FC300X (3.61 mm).

FC300X (3.61 mm)

150 images

Type	Resolution	Focal Length	Pixel Size
Frame	**4000 x 3000**	**3.61 mm**	**1.56 x 1.56 µm**

	Value	Error	F	K1	K2	P1	P2
F	**2325.37**	0.34	1.00	-0.03	0.22	0.15	0.45
K1	**-0.00672057**	7.8e-05		1.00	-0.87	0.04	0.06
K2	**0.00438677**	0.00018			1.00	0.01	-0.00
P1	**0.000948222**	1.3e-05				1.00	0.13
P2	**0.00127671**	2.4e-05					1.00

Table 2. Calibration coefficients and correlation matrix.

Ground Control Points

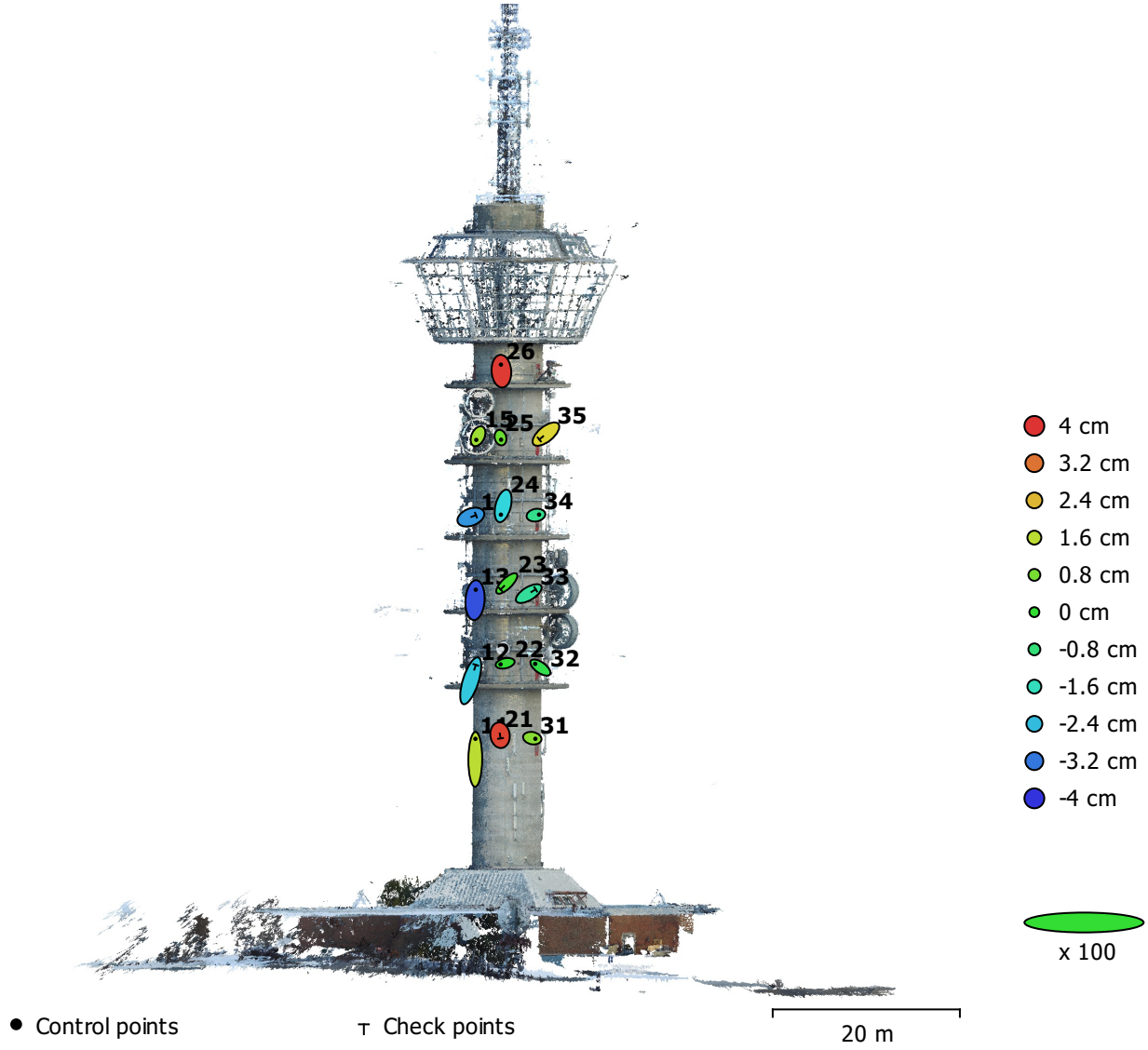

Fig. 3. GCP locations and error estimates.
Z error is represented by ellipse color. X,Y errors are represented by ellipse shape.
Estimated GCP locations are marked with a dot or crossing.

Count	X error (cm)	Y error (cm)	Z error (cm)	XY error (cm)	Total (cm)
10	0.589847	1.76451	2	1.86049	2.73156

Table 3. Control points RMSE.
X - Easting, Y - Northing, Z - Altitude.

Count	X error (cm)	Y error (cm)	Z error (cm)	XY error (cm)	Total (cm)
6	1.17856	1.6341	2.36411	2.01477	3.10617

Table 4. Check points RMSE.
X - Easting, Y - Northing, Z - Altitude.

Label	X error (cm)	Y error (cm)	Z error (cm)	Total (cm)	Image (pix)
11	0.0315559	4.38339	1.57169	4.65675	0.426 (22)
13	0.152811	2.2203	-3.68704	4.30666	0.487 (19)
15	-0.367776	-0.788989	1.24438	1.51863	0.271 (16)
26	-0.0930441	1.39897	3.89655	4.14112	0.287 (20)
25	0.127961	-0.441033	0.639689	0.787456	0.673 (17)
24	-0.480049	-1.87258	-2.14781	2.88965	0.621 (21)
22	-0.975551	-0.221489	-0.0101825	1.00043	0.322 (19)
31	0.658923	-0.131591	0.969704	1.17975	0.113 (24)
32	-1.11209	0.793901	-0.32376	1.40422	0.365 (10)
34	0.664452	0.117416	-1.06604	1.26163	0.369 (20)
Total	**0.589847**	**1.76451**	**2**	**2.73156**	**0.422**

Table 5. Control points.

X - Easting, Y - Northing, Z - Altitude.

Label	X error (cm)	Y error (cm)	Z error (cm)	Total (cm)	Image (pix)
12	1.0899	3.40342	-2.2582	4.22737	0.569 (17)
14	1.08932	0.423012	-2.88936	3.11672	0.409 (15)
23	-1.32466	-1.27933	0.178007	1.85017	0.459 (20)
21	0.098058	-0.685143	3.78116	3.84398	0.321 (18)
33	1.4785	0.909202	-1.21365	2.11791	0.324 (20)
35	-1.4175	-1.15185	2.06986	2.7605	0.160 (21)
Total	**1.17856**	**1.6341**	**2.36411**	**3.10617**	**0.388**

Table 6. Check points.

X - Easting, Y - Northing, Z - Altitude.

Digital Elevation Model

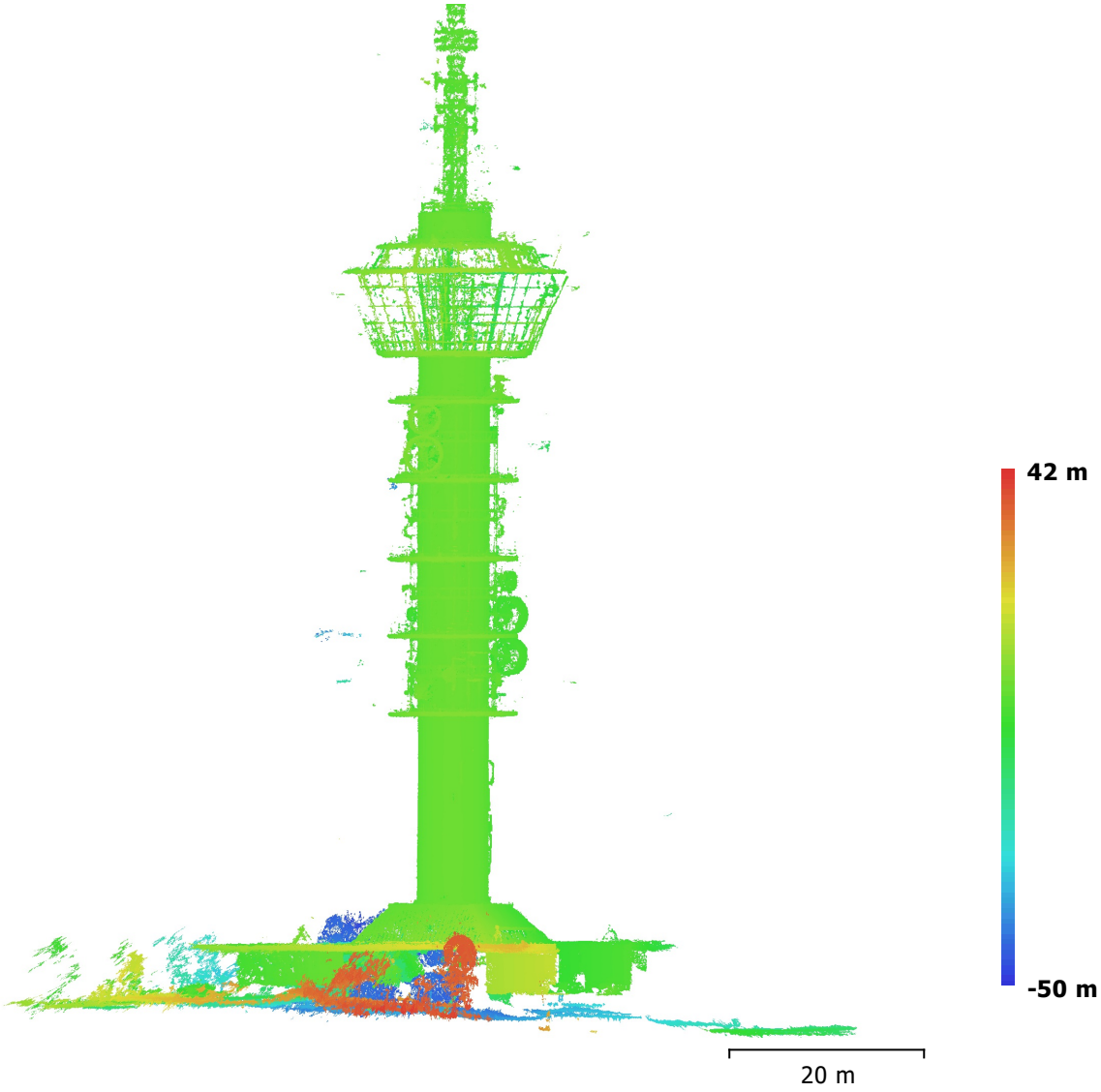

Fig. 4. Reconstructed digital elevation model.

Resolution:	unknown
Point density:	unknown

Processing Parameters

General	
Cameras	150
Aligned cameras	150
Markers	16
Coordinate system	ETRS89 / NTM zone 10 (EPSG::5110)
Rotation angles	Yaw, Pitch, Roll
Point Cloud	
Points	72,310 of 84,409
RMS reprojection error	0.3512 (0.906704 pix)
Max reprojection error	32.9289 (81.4895 pix)
Mean key point size	3.25673 pix
Effective overlap	2.56516
Alignment parameters	
Accuracy	Highest
Generic preselection	Yes
Reference preselection	Yes
Key point limit	40,000
Tie point limit	4,000
Constrain features by mask	Yes
Adaptive camera model fitting	Yes
Matching time	12 minutes 11 seconds
Alignment time	26 seconds
Optimization parameters	
Parameters	f, k1, k2, p1, p2
Fit rolling shutter	No
Optimization time	0 seconds
Dense Point Cloud	
Points	27,960,419
Reconstruction parameters	
Quality	Ultra High
Depth filtering	Mild
Depth maps generation time	2 hours 42 minutes
Dense cloud generation time	1 hours 34 minutes
Software	
Version	1.3.1 build 4030
Platform	Windows 64

Appendix D

I. Settings

A. Positioning/georeferencing:
- Positioning mode: Use control points for adjustment

B. Main settings:
- Key point density: Normal
- Pair selection mode: Default
- Component construction mode: OnePass

C. Estimation policies:
- Tie points: Compute
- Position: Compute
- Rotation: Compute
- Photogroup estimation mode: OnePass
- Focal length: Adjust
- Fisheye focal: Keep
- Principal point: Adjust
- Radial distortion: Adjust
- Tangential distortion: Adjust
- Aspect ratio: Adjust
- Skew: Adjust
- Fisheye distortion: Keep
- Estimation groups: PerPhotogroup

II. Results

A. Global:

- Errors

	Before aerotriangulation							After aerotriangulation					
Type	**Number of points**	**Median reprojection error [px]**	**RMS of reprojection errors [px]**	**RMS of distances to rays [m]**	**RMS of 3D errors [m]**	**RMS of horizontal errors [m]**	**RMS of vertical errors [m]**	**Number of points**	**Median reprojection error [px]**	**RMS of reprojection errors [px]**	**RMS of distances to rays [m]**	**RMS of 3D errors [m]**	**RMS o horizont errors [r**
Control_points	16	44754.99	44291.54	143.338	151.212	0.836	151.210	16	1.31	1.90	0.037	0.021	0.015
Automatic_tie_points	28079	0.39	0.60	0.266				31255	0.47	0.67	0.409		

NB: Horizontal and vertical errors are given according to the following spatial reference system: WGS84

- Connections

		Before aerotriangulation	After aerotriangulation
Number of tested pairs	**Median number of tested pairs per photo**	**Median number of connected photos per photo**	**Median number of connected photos per photo**
2262	30	71	72

B. Per photo:

- Control points

Photo		**Before aerotriangulation**			**After aerotriangulation**		
Photogroup	**File name**	**Number of points**	**RMS of reprojection errors [px]**	**RMS of distances to rays [m]**	**Number of points**	**RMS of reprojection errors [px]**	**RMS of distances to rays [m]**
Photogroup_1	DJI_10_1.JPG	1	41802.73	135.190	1	3.13	0.020
Photogroup_1	DJI_10_10.JPG	1	47356.97	150.531	1	0.37	0.005
Photogroup_1	DJI_10_11.JPG	1	49820.93	151.252	1	0.30	0.001
Photogroup_1	DJI_10_12.JPG	1	51403.72	144.829	1	0.24	0.019
Photogroup_1	DJI_10_13.JPG	1	53275.98	132.797	1	0.18	0.055
Photogroup_1	DJI_10_2.JPG	1	43018.98	144.653	1	1.70	0.004
Photogroup_1	DJI_10_3.JPG	1	43737.49	150.376	1	2.86	0.028
Photogroup_1	DJI_10_4.JPG	3	44356.35	144.676	3	3.24	0.019
Photogroup_1	DJI_10_5.JPG	4	44955.21	141.998	4	2.35	0.042
Photogroup_1	DJI_10_6.JPG	4	46401.74	142.001	4	2.50	0.044
Photogroup_1	DJI_10_7.JPG	3	47766.64	144.665	3	2.85	0.034
Photogroup_1	DJI_10_8.JPG	4	46523.30	142.578	4	1.99	0.035
Photogroup_1	DJI_10_9.JPG	3	47591.30	146.584	3	1.04	0.020
Photogroup_1	DJI_1_1.JPG	1	33938.24	131.696	1	3.50	0.046
Photogroup_1	DJI_1_10.JPG	3	35854.26	145.674	3	1.04	0.023

Photogroup_1	DJI_1_11.JPG	3	36552.12	140.089	3	0.90	0.039
Photogroup_1	DJI_1_12.JPG	2	36653.86	138.541	2	0.77	0.031
Photogroup_1	DJI_1_13.JPG	1	36631.85	136.456	1	0.40	0.033
Photogroup_1	DJI_1_2.JPG	1	34463.01	142.451	1	3.12	0.017
Photogroup_1	DJI_1_3.JPG	2	34939.41	144.085	2	1.83	0.027
Photogroup_1	DJI_1_4.JPG	3	34749.12	143.369	3	3.72	0.030
Photogroup_1	DJI_1_5.JPG	3	35154.65	145.950	3	2.74	0.021
Photogroup_1	DJI_1_6.JPG	4	35080.30	142.194	4	2.26	0.031
Photogroup_1	DJI_1_7.JPG	4	35019.09	142.597	4	2.65	0.041
Photogroup_1	DJI_1_8.JPG	4	35690.71	141.191	4	2.08	0.033
Photogroup_1	DJI_1_9.JPG	4	35743.28	142.692	4	1.87	0.026
Photogroup_1	DJI_2_10.JPG	2	45907.56	144.502	2	0.71	0.024
Photogroup_1	DJI_2_11.JPG	2	46154.13	147.589	2	0.78	0.011
Photogroup_1	DJI_2_12.JPG	2	46956.01	139.783	2	0.79	0.035
Photogroup_1	DJI_2_7.JPG	1	43442.20	147.646	1	0.65	0.017
Photogroup_1	DJI_2_8.JPG	1	43945.29	151.435	1	0.44	0.005
Photogroup_1	DJI_2_9.JPG	1	44785.71	147.776	1	0.41	0.010
Photogroup_1	DJI_3_1.JPG	1	41881.60	131.365	1	0.48	0.061
Photogroup_1	DJI_3_10.JPG	2	46650.12	144.213	2	0.84	0.032
Photogroup_1	DJI_3_11.JPG	1	47508.84	142.280	1	1.43	0.039
Photogroup_1	DJI_3_12.JPG	1	48240.23	130.891	1	1.31	0.070
Photogroup_1	DJI_3_2.JPG	1	43044.99	143.715	1	0.44	0.022
Photogroup_1	DJI_3_3.JPG	1	44230.86	149.716	1	0.41	0.003
Photogroup_1	DJI_3_4.JPG	1	45129.17	150.273	1	0.39	0.002
Photogroup_1	DJI_3_5.JPG	2	44268.01	143.729	2	1.19	0.021
Photogroup_1	DJI_3_6.JPG	3	44137.56	141.069	3	1.03	0.039
Photogroup_1	DJI_3_7.JPG	2	43888.12	149.145	2	1.53	0.018
Photogroup_1	DJI_3_8.JPG	2	45727.58	147.253	2	0.61	0.021
Photogroup_1	DJI_3_9.JPG	2	45647.52	149.185	2	1.27	0.020
Photogroup_1	DJI_4_1.JPG	1	48408.68	127.762	1	0.53	0.060
Photogroup_1	DJI_4_10.JPG	2	48086.83	143.884	2	0.74	0.031
Photogroup_1	DJI_4_11.JPG	1	48107.38	142.357	1	1.67	0.032
Photogroup_1	DJI_4_12.JPG	1	48807.00	129.971	1	1.96	0.066
Photogroup_1	DJI_4_2.JPG	1	49541.09	140.520	1	0.46	0.022
Photogroup_1	DJI_4_3.JPG	2	48680.72	142.293	2	0.52	0.031
Photogroup_1	DJI_4_4.JPG	2	49286.32	148.019	2	0.44	0.009
Photogroup_1	DJI_4_5.JPG	3	49151.81	145.301	3	0.63	0.017
Photogroup_1	DJI_4_6.JPG	4	49336.91	141.354	4	0.73	0.033
Photogroup_1	DJI_4_7.JPG	4	47900.43	141.547	4	1.41	0.039
Photogroup_1	DJI_4_8.JPG	3	48061.01	145.832	3	2.14	0.032
Photogroup_1	DJI_4_9.JPG	3	48407.11	143.107	3	2.25	0.042
Photogroup_1	DJI_5_1.JPG	1	43140.56	129.930	1	0.47	0.057
Photogroup_1	DJI_5_10.JPG	2	49488.96	144.692	2	2.14	0.036
Photogroup_1	DJI_5_11.JPG	1	50030.41	144.086	1	2.71	0.042
Photogroup_1	DJI_5_12.JPG	1	51665.86	131.171	1	2.87	0.075
Photogroup_1	DJI_5_2.JPG	1	44868.81	141.608	1	0.45	0.022
Photogroup_1	DJI_5_3.JPG	1	46622.82	148.966	1	0.37	0.004
Photogroup_1	DJI_5_4.JPG	2	46959.45	148.239	2	0.82	0.009
Photogroup_1	DJI_5_5.JPG	2	48053.17	147.154	2	0.79	0.014
Photogroup_1	DJI_5_6.JPG	4	47374.88	142.159	4	1.27	0.036
Photogroup_1	DJI_5_7.JPG	3	46966.79	145.663	3	1.29	0.023
Photogroup_1	DJI_5_8.JPG	3	46907.22	146.305	3	2.40	0.031
Photogroup_1	DJI_5_9.JPG	3	48588.04	143.700	3	2.34	0.038
Photogroup_1	DJI_7_1.JPG	1	43545.20	134.896	1	2.81	0.073
Photogroup_1	DJI_7_10.JPG	2	47432.42	141.568	2	0.79	0.033
Photogroup_1	DJI_7_11.JPG	1	47570.73	140.383	1	0.86	0.023

Photogroup_1	DJI_7_2.JPG	2	44129.10	137.197	2	2.50	0.070
Photogroup_1	DJI_7_3.JPG	2	45113.86	145.563	2	2.05	0.036
Photogroup_1	DJI_7_4.JPG	3	45716.22	144.444	3	2.55	0.048
Photogroup_1	DJI_7_5.JPG	4	45626.93	142.027	4	2.41	0.055
Photogroup_1	DJI_7_6.JPG	4	46820.84	142.033	4	2.39	0.051
Photogroup_1	DJI_7_7.JPG	4	45866.00	142.810	4	2.47	0.050
Photogroup_1	DJI_7_8.JPG	3	45672.81	146.320	3	0.82	0.026
Photogroup_1	DJI_7_9.JPG	2	47599.45	137.246	2	0.83	0.055
Photogroup_1	DJI_8_1.JPG	1	39346.78	135.728	1	2.42	0.071
Photogroup_1	DJI_8_10.JPG	2	45242.19	142.629	2	1.20	0.043
Photogroup_1	DJI_8_11.JPG	1	45159.99	141.455	1	1.08	0.023
Photogroup_1	DJI_8_12.JPG	1	46129.26	129.320	1	1.24	0.060
Photogroup_1	DJI_8_2.JPG	1	40574.14	145.382	1	2.02	0.037
Photogroup_1	DJI_8_3.JPG	1	42084.69	150.479	1	1.59	0.018
Photogroup_1	DJI_8_4.JPG	3	41865.60	145.253	3	2.52	0.046
Photogroup_1	DJI_8_5.JPG	4	43065.47	142.513	4	1.84	0.048
Photogroup_1	DJI_8_6.JPG	4	43982.98	142.487	4	1.40	0.042
Photogroup_1	DJI_8_7.JPG	4	43984.23	143.160	4	1.79	0.039
Photogroup_1	DJI_8_8.JPG	3	43975.87	146.624	3	1.03	0.027
Photogroup_1	DJI_8_9.JPG	3	44403.09	142.751	3	1.03	0.046
Photogroup_1	DJI_9_1.JPG	2	39283.66	135.960	2	3.25	0.072
Photogroup_1	DJI_9_10.JPG	1	43607.53	149.392	1	0.83	0.002
Photogroup_1	DJI_9_11.JPG	2	45774.98	142.230	2	1.10	0.025
Photogroup_1	DJI_9_12.JPG	1	46909.25	130.247	1	1.31	0.062
Photogroup_1	DJI_9_2.JPG	3	39733.53	140.642	3	2.58	0.035
Photogroup_1	DJI_9_3.JPG	2	40915.56	150.357	2	1.36	0.016
Photogroup_1	DJI_9_4.JPG	3	41016.65	145.290	3	1.80	0.041
Photogroup_1	DJI_9_5.JPG	7	41513.76	144.655	7	3.52	0.050
Photogroup_1	DJI_9_6.JPG	6	42719.21	142.460	6	1.73	0.044
Photogroup_1	DJI_9_7.JPG	4	42499.15	146.858	4	1.68	0.025
Photogroup_1	DJI_9_8.JPG	4	43156.35	145.829	4	1.34	0.026
Photogroup_1	DJI_9_9.JPG	3	43561.82	143.781	3	1.77	0.025

- Automatic tie points

Photo			Before aerotriangulation			After aerotriangulation		
Photogroup	**File name**	**Number of key points**	**Number of points**	**RMS of reprojection errors [px]**	**RMS of distances to rays [m]**	**Number of points**	**RMS of reprojection errors [px]**	**RMS of distances to rays [m]**
Photogroup_1	DJI_10_1.JPG	6940	318	0.39	0.481	200	0.32	0.537
Photogroup_1	DJI_10_10.JPG	19820	1326	0.58	0.380	1381	0.64	0.533
Photogroup_1	DJI_10_11.JPG	20894	1396	0.58	0.402	1443	0.62	0.570
Photogroup_1	DJI_10_12.JPG	17500	1429	0.58	0.417	1566	0.63	0.596
Photogroup_1	DJI_10_13.JPG	14408	1298	0.58	0.484	1471	0.63	0.631
Photogroup_1	DJI_10_14.JPG	16141	1315	0.63	0.532	1382	0.63	0.677
Photogroup_1	DJI_10_15.JPG	17802	1361	0.72	0.490	1393	0.76	0.669
Photogroup_1	DJI_10_2.JPG	9731	578	0.55	0.417	428	0.54	0.460
Photogroup_1	DJI_10_3.JPG	12538	854	0.60	0.372	745	0.63	0.379
Photogroup_1	DJI_10_4.JPG	13959	1094	0.64	0.364	1011	0.72	0.397
Photogroup_1	DJI_10_5.JPG	13550	1218	0.65	0.343	1149	0.82	0.391
Photogroup_1	DJI_10_6.JPG	13832	1291	0.64	0.367	1222	0.77	0.415
Photogroup_1	DJI_10_7.JPG	14299	1325	0.62	0.392	1241	0.68	0.471
Photogroup_1	DJI_10_8.JPG	14633	1453	0.66	0.370	1359	0.89	0.456
Photogroup_1	DJI_10_9.JPG	16145	1502	0.64	0.386	1460	0.77	0.485
Photogroup_1	DJI_1_1.JPG	8395	378	0.44	0.657	275	0.38	0.565
Photogroup_1	DJI_1_10.JPG	20781	1279	0.60	0.435	1000	0.88	0.385
Photogroup_1	DJI_1_11.JPG	23818	1220	0.62	0.393	991	0.82	0.492
Photogroup_1	DJI_1_12.JPG	20422	1245	0.58	0.408	1154	0.67	0.506

Photogroup_1	DJI_1_13.JPG	17947	1112	0.57	0.460	1105	0.61	0.523
Photogroup_1	DJI_1_14.JPG	18518	1042	0.57	0.542	953	0.53	0.562
Photogroup_1	DJI_1_15.JPG	19333	1053	0.62	0.503	952	0.64	0.536
Photogroup_1	DJI_1_2.JPG	11223	683	0.61	0.528	556	0.63	0.383
Photogroup_1	DJI_1_3.JPG	14094	857	0.64	0.460	755	0.69	0.357
Photogroup_1	DJI_1_4.JPG	15662	1022	0.64	0.440	936	0.71	0.323
Photogroup_1	DJI_1_5.JPG	15933	1094	0.61	0.451	994	0.67	0.355
Photogroup_1	DJI_1_6.JPG	16149	1120	0.59	0.454	1020	0.71	0.403
Photogroup_1	DJI_1_7.JPG	17060	1165	0.61	0.428	1018	0.70	0.394
Photogroup_1	DJI_1_8.JPG	17426	1230	0.61	0.445	1046	0.70	0.472
Photogroup_1	DJI_1_9.JPG	17524	1291	0.64	0.482	1045	0.79	0.507
Photogroup_1	DJI_2_1.JPG	8306	344	0.42	0.079	313	0.46	0.140
Photogroup_1	DJI_2_10.JPG	18855	1220	0.60	0.246	1360	0.68	0.418
Photogroup_1	DJI_2_11.JPG	21808	1086	0.58	0.276	1197	0.82	0.482
Photogroup_1	DJI_2_12.JPG	19275	1118	0.53	0.288	1336	0.84	0.478
Photogroup_1	DJI_2_13.JPG	16175	964	0.50	0.337	1237	0.55	0.535
Photogroup_1	DJI_2_14.JPG	16578	832	0.47	0.349	1109	0.55	0.561
Photogroup_1	DJI_2_15.JPG	17014	893	0.59	0.352	1118	0.66	0.566
Photogroup_1	DJI_2_2.JPG	11298	571	0.59	0.090	554	0.63	0.150
Photogroup_1	DJI_2_3.JPG	12674	723	0.62	0.122	708	0.66	0.205
Photogroup_1	DJI_2_4.JPG	13754	859	0.64	0.142	867	0.69	0.237
Photogroup_1	DJI_2_5.JPG	13649	1000	0.64	0.158	1023	0.69	0.269
Photogroup_1	DJI_2_6.JPG	14390	1108	0.63	0.186	1165	0.68	0.306
Photogroup_1	DJI_2_7.JPG	14611	1139	0.64	0.198	1237	0.71	0.335
Photogroup_1	DJI_2_8.JPG	15477	1225	0.64	0.214	1335	0.69	0.360
Photogroup_1	DJI_2_9.JPG	16582	1304	0.65	0.236	1400	0.69	0.398
Photogroup_1	DJI_3_1.JPG	10033	196	0.32	0.056	156	0.26	0.091
Photogroup_1	DJI_3_10.JPG	20170	1191	0.62	0.227	1254	0.66	0.396
Photogroup_1	DJI_3_11.JPG	21280	1129	0.62	0.252	1241	0.63	0.438
Photogroup_1	DJI_3_12.JPG	20743	1100	0.61	0.278	1311	0.62	0.469
Photogroup_1	DJI_3_13.JPG	16521	919	0.55	0.313	1194	0.57	0.518
Photogroup_1	DJI_3_14.JPG	16505	775	0.49	0.332	1043	0.53	0.556
Photogroup_1	DJI_3_15.JPG	17505	845	0.61	0.334	1042	0.64	0.566
Photogroup_1	DJI_3_2.JPG	10972	477	0.54	0.077	432	0.59	0.113
Photogroup_1	DJI_3_3.JPG	13902	716	0.60	0.082	675	0.70	0.134
Photogroup_1	DJI_3_4.JPG	15562	844	0.65	0.099	819	0.71	0.162
Photogroup_1	DJI_3_5.JPG	15630	996	0.65	0.118	996	0.72	0.197
Photogroup_1	DJI_3_6.JPG	16506	1044	0.64	0.141	1080	0.75	0.237
Photogroup_1	DJI_3_7.JPG	17757	1103	0.61	0.161	1117	0.64	0.264
Photogroup_1	DJI_3_8.JPG	17668	1249	0.62	0.187	1239	0.69	0.314
Photogroup_1	DJI_3_9.JPG	18289	1319	0.63	0.201	1349	0.69	0.340
Photogroup_1	DJI_4_1.JPG	10966	103	0.20	0.047	88	0.17	0.108
Photogroup_1	DJI_4_10.JPG	17854	1343	0.63	0.214	1437	0.68	0.371
Photogroup_1	DJI_4_11.JPG	22298	1131	0.57	0.238	1216	0.59	0.404
Photogroup_1	DJI_4_12.JPG	19306	1146	0.58	0.256	1298	0.61	0.434
Photogroup_1	DJI_4_13.JPG	15422	936	0.51	0.282	1134	0.56	0.484
Photogroup_1	DJI_4_14.JPG	14752	699	0.44	0.321	853	0.47	0.534
Photogroup_1	DJI_4_15.JPG	16853	832	0.54	0.322	933	0.54	0.535
Photogroup_1	DJI_4_2.JPG	9585	338	0.48	0.075	335	0.54	0.129
Photogroup_1	DJI_4_3.JPG	12291	590	0.59	0.093	566	0.69	0.149
Photogroup_1	DJI_4_4.JPG	14450	808	0.64	0.113	730	0.80	0.177
Photogroup_1	DJI_4_5.JPG	14801	986	0.66	0.128	872	0.91	0.210
Photogroup_1	DJI_4_6.JPG	15567	1077	0.63	0.143	996	0.87	0.261
Photogroup_1	DJI_4_7.JPG	15881	1251	0.65	0.163	1226	0.89	0.276
Photogroup_1	DJI_4_8.JPG	16475	1353	0.65	0.182	1391	0.74	0.299
Photogroup_1	DJI_4_9.JPG	16678	1384	0.63	0.198	1435	0.69	0.332

Photogroup_1	DJI_5_1.JPG	10868	146	0.31	0.047	134	0.31	0.093
Photogroup_1	DJI_5_10.JPG	18762	1178	0.63	0.236	1238	0.68	0.413
Photogroup_1	DJI_5_11.JPG	21446	1105	0.63	0.264	1165	0.63	0.454
Photogroup_1	DJI_5_12.JPG	19863	1144	0.58	0.279	1282	0.63	0.477
Photogroup_1	DJI_5_13.JPG	17285	956	0.53	0.306	1220	0.60	0.531
Photogroup_1	DJI_5_14.JPG	15427	704	0.47	0.354	958	0.53	0.594
Photogroup_1	DJI_5_15.JPG	16608	859	0.57	0.336	1043	0.64	0.593
Photogroup_1	DJI_5_2.JPG	9625	321	0.47	0.069	271	0.51	0.145
Photogroup_1	DJI_5_3.JPG	12104	522	0.58	0.099	423	0.73	0.185
Photogroup_1	DJI_5_4.JPG	14203	735	0.64	0.128	587	0.72	0.196
Photogroup_1	DJI_5_5.JPG	14627	877	0.64	0.137	693	0.86	0.207
Photogroup_1	DJI_5_6.JPG	15189	991	0.68	0.162	811	0.86	0.258
Photogroup_1	DJI_5_7.JPG	15723	1063	0.68	0.181	911	0.91	0.336
Photogroup_1	DJI_5_8.JPG	16386	1135	0.64	0.197	1051	0.76	0.334
Photogroup_1	DJI_5_9.JPG	17280	1240	0.64	0.213	1183	0.72	0.369
Photogroup_1	DJI_6_1.JPG	12626	140	0.23	0.077	147	0.24	0.145
Photogroup_1	DJI_6_10.JPG	22348	1198	0.60	0.224	1390	0.61	0.383
Photogroup_1	DJI_6_11.JPG	21214	1267	0.59	0.239	1546	0.62	0.409
Photogroup_1	DJI_6_12.JPG	18779	1207	0.58	0.253	1596	0.63	0.433
Photogroup_1	DJI_6_13.JPG	17124	965	0.52	0.278	1342	0.58	0.469
Photogroup_1	DJI_6_14.JPG	17623	853	0.50	0.290	1187	0.55	0.491
Photogroup_1	DJI_6_15.JPG	17669	880	0.53	0.293	1189	0.56	0.495
Photogroup_1	DJI_6_2.JPG	13380	368	0.51	0.091	400	0.48	0.169
Photogroup_1	DJI_6_3.JPG	14300	590	0.57	0.101	676	0.61	0.184
Photogroup_1	DJI_6_4.JPG	16445	817	0.66	0.109	902	0.69	0.189
Photogroup_1	DJI_6_5.JPG	17709	936	0.66	0.126	1013	0.72	0.219
Photogroup_1	DJI_6_6.JPG	17761	921	0.63	0.135	934	0.65	0.254
Photogroup_1	DJI_6_7.JPG	18463	1105	0.66	0.173	1134	0.66	0.312
Photogroup_1	DJI_6_8.JPG	18580	1206	0.66	0.188	1308	0.64	0.341
Photogroup_1	DJI_6_9.JPG	19656	1272	0.62	0.199	1415	0.63	0.363
Photogroup_1	DJI_7_1.JPG	15707	250	0.25	0.192	254	0.29	0.190
Photogroup_1	DJI_7_10.JPG	19702	1305	0.61	0.371	1414	0.65	0.562
Photogroup_1	DJI_7_11.JPG	20080	1233	0.57	0.363	1348	0.63	0.563
Photogroup_1	DJI_7_12.JPG	17895	1130	0.57	0.406	1309	0.65	0.607
Photogroup_1	DJI_7_13.JPG	15204	974	0.52	0.442	1194	0.59	0.637
Photogroup_1	DJI_7_14.JPG	15548	894	0.51	0.485	1058	0.54	0.710
Photogroup_1	DJI_7_15.JPG	16442	914	0.61	0.456	1036	0.63	0.686
Photogroup_1	DJI_7_2.JPG	11233	588	0.52	0.258	612	0.60	0.287
Photogroup_1	DJI_7_3.JPG	12831	862	0.58	0.248	927	0.66	0.297
Photogroup_1	DJI_7_4.JPG	14887	1093	0.62	0.254	1146	0.69	0.317
Photogroup_1	DJI_7_5.JPG	15236	1197	0.63	0.302	1285	0.78	0.391
Photogroup_1	DJI_7_6.JPG	15507	1300	0.63	0.306	1345	0.84	0.444
Photogroup_1	DJI_7_7.JPG	16645	1252	0.63	0.346	1319	0.80	0.435
Photogroup_1	DJI_7_8.JPG	16682	1369	0.65	0.335	1449	0.72	0.506
Photogroup_1	DJI_7_9.JPG	16955	1436	0.63	0.357	1508	0.68	0.520
Photogroup_1	DJI_8_1.JPG	10645	159	0.23	0.537	108	0.20	0.418
Photogroup_1	DJI_8_10.JPG	18395	1410	0.62	0.381	1453	0.66	0.524
Photogroup_1	DJI_8_11.JPG	18806	1374	0.59	0.418	1480	0.63	0.573
Photogroup_1	DJI_8_12.JPG	16670	1375	0.57	0.436	1553	0.62	0.592
Photogroup_1	DJI_8_13.JPG	14508	1220	0.55	0.474	1427	0.58	0.629
Photogroup_1	DJI_8_14.JPG	14920	1138	0.56	0.498	1284	0.58	0.673
Photogroup_1	DJI_8_15.JPG	15409	1116	0.62	0.510	1229	0.64	0.678
Photogroup_1	DJI_8_2.JPG	9670	441	0.46	0.380	374	0.46	0.355
Photogroup_1	DJI_8_3.JPG	11794	829	0.57	0.343	792	0.64	0.312
Photogroup_1	DJI_8_4.JPG	13047	1109	0.65	0.331	1116	0.83	0.302
Photogroup_1	DJI_8_5.JPG	13446	1303	0.67	0.334	1288	0.78	0.387

Photogroup_1	DJI_8_6.JPG	13665	1376	0.69	0.361	1341	0.79	0.451
Photogroup_1	DJI_8_7.JPG	14755	1441	0.65	0.371	1399	0.77	0.490
Photogroup_1	DJI_8_8.JPG	14868	1512	0.63	0.390	1475	0.68	0.493
Photogroup_1	DJI_8_9.JPG	16260	1572	0.66	0.382	1568	0.79	0.492
Photogroup_1	DJI_9_1.JPG	6704	250	0.36	0.649	155	0.34	0.707
Photogroup_1	DJI_9_10.JPG	19230	1425	0.58	0.449	1422	0.63	0.572
Photogroup_1	DJI_9_11.JPG	20215	1368	0.58	0.455	1398	0.69	0.584
Photogroup_1	DJI_9_12.JPG	16739	1423	0.60	0.461	1501	0.65	0.601
Photogroup_1	DJI_9_13.JPG	13583	1263	0.58	0.564	1357	0.62	0.709
Photogroup_1	DJI_9_14.JPG	14659	1214	0.61	0.557	1252	0.61	0.719
Photogroup_1	DJI_9_15.JPG	16353	1288	0.70	0.548	1327	0.72	0.724
Photogroup_1	DJI_9_2.JPG	10333	529	0.46	0.534	411	0.52	0.574
Photogroup_1	DJI_9_3.JPG	12761	838	0.54	0.464	696	0.58	0.483
Photogroup_1	DJI_9_4.JPG	14122	1101	0.59	0.442	993	0.67	0.459
Photogroup_1	DJI_9_5.JPG	14368	1311	0.65	0.400	1223	0.86	0.440
Photogroup_1	DJI_9_6.JPG	13832	1461	0.63	0.429	1371	0.74	0.490
Photogroup_1	DJI_9_7.JPG	14176	1499	0.66	0.447	1438	0.83	0.533
Photogroup_1	DJI_9_8.JPG	15155	1543	0.64	0.419	1517	0.76	0.517
Photogroup_1	DJI_9_9.JPG	16405	1565	0.63	0.443	1513	0.70	0.554

- Connections

Photo			Before aerotriangulation	After aerotriangulation
Photogroup	**File name**	**Number of tested pairs**	**Number of connected photos**	**Number of connected photos**
Photogroup_1	DJI_10_1.JPG	30	74	60
Photogroup_1	DJI_10_10.JPG	28	74	73
Photogroup_1	DJI_10_11.JPG	29	74	73
Photogroup_1	DJI_10_12.JPG	30	74	73
Photogroup_1	DJI_10_13.JPG	28	74	72
Photogroup_1	DJI_10_14.JPG	20	74	74
Photogroup_1	DJI_10_15.JPG	21	74	74
Photogroup_1	DJI_10_2.JPG	23	75	79
Photogroup_1	DJI_10_3.JPG	23	75	79
Photogroup_1	DJI_10_4.JPG	31	74	82
Photogroup_1	DJI_10_5.JPG	38	74	79
Photogroup_1	DJI_10_6.JPG	35	74	74
Photogroup_1	DJI_10_7.JPG	31	74	73
Photogroup_1	DJI_10_8.JPG	35	74	73
Photogroup_1	DJI_10_9.JPG	33	74	73
Photogroup_1	DJI_1_1.JPG	34	63	49
Photogroup_1	DJI_1_10.JPG	34	74	73
Photogroup_1	DJI_1_11.JPG	37	73	70
Photogroup_1	DJI_1_12.JPG	31	75	74
Photogroup_1	DJI_1_13.JPG	32	74	74
Photogroup_1	DJI_1_14.JPG	26	73	72
Photogroup_1	DJI_1_15.JPG	20	74	74
Photogroup_1	DJI_1_2.JPG	29	72	66
Photogroup_1	DJI_1_3.JPG	33	73	73
Photogroup_1	DJI_1_4.JPG	39	73	77
Photogroup_1	DJI_1_5.JPG	39	74	79
Photogroup_1	DJI_1_6.JPG	40	74	77
Photogroup_1	DJI_1_7.JPG	38	74	76
Photogroup_1	DJI_1_8.JPG	38	74	75
Photogroup_1	DJI_1_9.JPG	38	74	73
Photogroup_1	DJI_2_1.JPG	28	68	62
Photogroup_1	DJI_2_10.JPG	39	79	75
Photogroup_1	DJI_2_11.JPG	35	75	74

Photogroup_1	DJI_2_12.JPG	37	75	74
Photogroup_1	DJI_2_13.JPG	23	72	71
Photogroup_1	DJI_2_14.JPG	25	70	71
Photogroup_1	DJI_2_15.JPG	21	71	72
Photogroup_1	DJI_2_2.JPG	20	74	73
Photogroup_1	DJI_2_3.JPG	23	74	74
Photogroup_1	DJI_2_4.JPG	24	75	75
Photogroup_1	DJI_2_5.JPG	25	74	74
Photogroup_1	DJI_2_6.JPG	24	74	72
Photogroup_1	DJI_2_7.JPG	35	75	74
Photogroup_1	DJI_2_8.JPG	34	75	77
Photogroup_1	DJI_2_9.JPG	35	75	76
Photogroup_1	DJI_3_1.JPG	32	66	60
Photogroup_1	DJI_3_10.JPG	34	74	73
Photogroup_1	DJI_3_11.JPG	35	75	70
Photogroup_1	DJI_3_12.JPG	31	73	69
Photogroup_1	DJI_3_13.JPG	24	77	66
Photogroup_1	DJI_3_14.JPG	22	72	60
Photogroup_1	DJI_3_15.JPG	21	73	64
Photogroup_1	DJI_3_2.JPG	33	72	64
Photogroup_1	DJI_3_3.JPG	34	76	72
Photogroup_1	DJI_3_4.JPG	32	74	70
Photogroup_1	DJI_3_5.JPG	36	74	75
Photogroup_1	DJI_3_6.JPG	38	74	74
Photogroup_1	DJI_3_7.JPG	30	74	74
Photogroup_1	DJI_3_8.JPG	30	73	72
Photogroup_1	DJI_3_9.JPG	35	73	72
Photogroup_1	DJI_4_1.JPG	28	47	47
Photogroup_1	DJI_4_10.JPG	28	71	71
Photogroup_1	DJI_4_11.JPG	27	70	68
Photogroup_1	DJI_4_12.JPG	26	71	70
Photogroup_1	DJI_4_13.JPG	24	67	62
Photogroup_1	DJI_4_14.JPG	18	66	59
Photogroup_1	DJI_4_15.JPG	20	70	65
Photogroup_1	DJI_4_2.JPG	25	71	66
Photogroup_1	DJI_4_3.JPG	28	74	70
Photogroup_1	DJI_4_4.JPG	28	74	76
Photogroup_1	DJI_4_5.JPG	27	72	75
Photogroup_1	DJI_4_6.JPG	32	71	69
Photogroup_1	DJI_4_7.JPG	33	69	69
Photogroup_1	DJI_4_8.JPG	29	70	70
Photogroup_1	DJI_4_9.JPG	30	70	70
Photogroup_1	DJI_5_1.JPG	32	41	44
Photogroup_1	DJI_5_10.JPG	35	56	65
Photogroup_1	DJI_5_11.JPG	30	57	65
Photogroup_1	DJI_5_12.JPG	38	57	64
Photogroup_1	DJI_5_13.JPG	27	54	61
Photogroup_1	DJI_5_14.JPG	19	43	55
Photogroup_1	DJI_5_15.JPG	23	55	64
Photogroup_1	DJI_5_2.JPG	27	50	50
Photogroup_1	DJI_5_3.JPG	29	58	70
Photogroup_1	DJI_5_4.JPG	34	59	69
Photogroup_1	DJI_5_5.JPG	34	59	75
Photogroup_1	DJI_5_6.JPG	38	61	70
Photogroup_1	DJI_5_7.JPG	33	58	59
Photogroup_1	DJI_5_8.JPG	33	56	67

Photogroup_1	DJI_5_9.JPG	34	58	65
Photogroup_1	DJI_6_1.JPG	25	28	40
Photogroup_1	DJI_6_10.JPG	27	42	69
Photogroup_1	DJI_6_11.JPG	29	43	71
Photogroup_1	DJI_6_12.JPG	24	43	69
Photogroup_1	DJI_6_13.JPG	23	42	66
Photogroup_1	DJI_6_14.JPG	21	43	70
Photogroup_1	DJI_6_15.JPG	21	42	69
Photogroup_1	DJI_6_2.JPG	21	40	61
Photogroup_1	DJI_6_3.JPG	24	46	66
Photogroup_1	DJI_6_4.JPG	27	45	71
Photogroup_1	DJI_6_5.JPG	25	44	70
Photogroup_1	DJI_6_6.JPG	28	45	70
Photogroup_1	DJI_6_7.JPG	27	45	70
Photogroup_1	DJI_6_8.JPG	28	42	71
Photogroup_1	DJI_6_9.JPG	27	42	71
Photogroup_1	DJI_7_1.JPG	33	44	48
Photogroup_1	DJI_7_10.JPG	35	44	69
Photogroup_1	DJI_7_11.JPG	31	44	71
Photogroup_1	DJI_7_12.JPG	31	44	71
Photogroup_1	DJI_7_13.JPG	26	42	63
Photogroup_1	DJI_7_14.JPG	24	46	67
Photogroup_1	DJI_7_15.JPG	22	46	71
Photogroup_1	DJI_7_2.JPG	32	44	61
Photogroup_1	DJI_7_3.JPG	30	46	78
Photogroup_1	DJI_7_4.JPG	36	48	76
Photogroup_1	DJI_7_5.JPG	40	46	74
Photogroup_1	DJI_7_6.JPG	37	46	72
Photogroup_1	DJI_7_7.JPG	37	45	73
Photogroup_1	DJI_7_8.JPG	34	44	72
Photogroup_1	DJI_7_9.JPG	32	44	71
Photogroup_1	DJI_8_1.JPG	29	56	71
Photogroup_1	DJI_8_10.JPG	30	60	73
Photogroup_1	DJI_8_11.JPG	28	59	72
Photogroup_1	DJI_8_12.JPG	31	59	71
Photogroup_1	DJI_8_13.JPG	24	62	74
Photogroup_1	DJI_8_14.JPG	20	62	74
Photogroup_1	DJI_8_15.JPG	20	62	74
Photogroup_1	DJI_8_2.JPG	27	57	73
Photogroup_1	DJI_8_3.JPG	23	59	81
Photogroup_1	DJI_8_4.JPG	32	59	80
Photogroup_1	DJI_8_5.JPG	34	59	77
Photogroup_1	DJI_8_6.JPG	30	59	73
Photogroup_1	DJI_8_7.JPG	31	59	73
Photogroup_1	DJI_8_8.JPG	29	59	73
Photogroup_1	DJI_8_9.JPG	29	60	73
Photogroup_1	DJI_9_1.JPG	38	74	74
Photogroup_1	DJI_9_10.JPG	36	78	77
Photogroup_1	DJI_9_11.JPG	39	78	77
Photogroup_1	DJI_9_12.JPG	32	73	74
Photogroup_1	DJI_9_13.JPG	27	72	72
Photogroup_1	DJI_9_14.JPG	19	77	73
Photogroup_1	DJI_9_15.JPG	19	77	74
Photogroup_1	DJI_9_2.JPG	36	74	74
Photogroup_1	DJI_9_3.JPG	33	74	74
Photogroup_1	DJI_9_4.JPG	42	74	74

Photogroup_1	DJI_9_5.JPG	50	74	74
Photogroup_1	DJI_9_6.JPG	48	74	74
Photogroup_1	DJI_9_7.JPG	37	74	74
Photogroup_1	DJI_9_8.JPG	46	78	78
Photogroup_1	DJI_9_9.JPG	41	78	78

C. Per point:

- Control points:

					Before aerotriangulation						After aerotriangulation				
Name	**Category**	**Check point**	**Horizontal accuracy [m]**	**Vertical accuracy [m]**	**Number of photos**	**RMS of reprojection errors [px]**	**RMS of distances to rays [m]**	**RMS of 3D errors [m]**	**RMS of horizontal errors [m]**	**RMS of vertical errors [m]**	**Number of photos**	**RMS of reprojection errors [px]**	**RMS of distances to rays [m]**	**RMS of 3D errors [m]**	**RMS of horizonta errors [m**
11	Full		0.015	0.015	18	43930.15	141.956	150.624	0.602	150.623	18	1.88	0.048	0.027	0.022
12	Full	x	0.015	0.015	12	44584.12	142.875	150.891	0.667	150.890	12	3.55	0.056	0.027	0.015
13	Full		0.015	0.015	17	44156.55	143.230	151.174	0.719	151.173	17	1.89	0.047	0.024	0.014
14	Full	x	0.015	0.015	15	43703.35	142.442	151.454	0.788	151.452	15	1.82	0.048	0.020	0.016
15	Full		0.015	0.015	14	44448.87	143.107	151.751	0.842	151.749	14	0.99	0.032	0.014	0.014
21	Full	x	0.007	0.007	18	40736.04	141.953	150.626	0.669	150.625	18	2.53	0.034	0.023	0.015
22	Full		0.015	0.015	13	40854.38	143.258	150.892	0.726	150.891	13	1.72	0.028	0.022	0.016
23	Full	x	0.015	0.015	16	41038.23	143.639	151.186	0.778	151.184	16	3.46	0.030	0.038	0.022
24	Full		0.015	0.015	17	41875.04	144.187	151.431	0.844	151.429	17	1.18	0.034	0.015	0.015
25	Full		0.015	0.015	13	41515.25	143.960	151.714	0.914	151.712	13	0.89	0.026	0.009	0.005
26	Full		0.015	0.015	13	43647.60	144.630	151.988	0.966	151.985	13	0.44	0.028	0.005	0.004
31	Full		0.008	0.010	18	47316.18	141.251	150.585	0.824	150.583	18	0.39	0.034	0.004	0.003
32	Full		0.008	0.010	9	48431.06	144.621	150.859	0.878	150.857	9	0.95	0.022	0.013	0.013
33	Full	x	0.008	0.010	13	47311.29	144.651	151.134	0.953	151.131	13	1.70	0.030	0.016	0.015
34	Full		0.008	0.009	15	46589.79	144.500	151.405	1.013	151.401	15	0.55	0.028	0.009	0.008
35	Full	x	0.015	0.012	15	47398.47	143.095	151.670	1.041	151.667	15	2.45	0.047	0.029	0.023

NB: Horizontal and vertical errors are given according to each control point respective spatial reference system

- Automatic tie points:

	Before aerotriangulation					After aerotriangulation				
Median number of key points per photo	**Number of points**	**Median number of photos per point**	**Median number of points per photo**	**RMS of reprojection errors [px]**	**RMS of distances to rays [m]**	**Number of points**	**Median number of photos per point**	**Median number of points per photo**	**RMS of reprojection errors [px]**	**RMS of distances to rays [m]**
15933	28079	4	1108	0.60	0.266	31255	4	1154	0.67	0.409